Czech Technical University in Prague
Faculty of Biomedical Engineering
Department of Health Care Disciplines and Population Protection

EFFICIENT BIOREMEDIATION OF TOXIC WASTE BY NEW NITRILASES

Doctoral Thesis

Mgr. Anastasia Sedova

Kladno, February 2024

Ph.D. Programme: P1032 Civil Emergency Preparedness

Supervisor: doc. RNDr. Pavla Bojarová, Ph.D.
Academic advisor: Ing. Ludmila Martínková, DSc.

Statement of originality

I hereby declare that the thesis: “Efficient bioremediation of toxic waste by new nitrilases” submitted at the Faculty of Biomedical Engineering, CTU in Prague has been composed and written by myself. The research, to which it refers, represents my own work. All information sources and literature used are referenced in the thesis.

_____ _____

Anastasia Sedova Date

Acknowledgement

Supported by grants:

no. 18-00184S (Czech Science Foundation)

no. GA22-06785S (Czech Science Foundation)

SGS 21/181/OHK4/3T/17 (Czech Technical University in Prague)

I express my deep gratitude to the Department of Health Care Disciplines and Population Protection, Faculty of Biomedical Engineering, Czech Technical University in Prague, especially to my supervisor doc. RNDr. Pavla Bojarová, Ph.D., for her professional guidance and patience throughout the doctoral studies, and to the Laboratory of Biotransformation, Institute of Microbiology of the Czech Academy of Sciences, especially to my academic advisor, Ing. Ludmila Martínková, DSc.

I also thank the Laboratory of Modulation of Gene Expression, Institute of Microbiology of the Czech Academy of Sciences, especially Ing. Lenka Rucká, Ph.D., and Laboratory of Photosynthesis, Algatech Centre, Institute of Microbiology of the Czech Academy of Sciences – Ing. Natalia Kulik, Ph.D., for computational research (molecular modeling, assistance with database searches).

Finally, the steadfast support of my sister, Dr. Ksenia Sedova, was indispensable for the successful completion of my academic journey.

Abstract

Wastewater from certain industrial processes (gold and silver mining, electroplating with Cu, Ag and other metals, coal coking) contains high concentrations of free cyanide (hydrogen cyanide and cyanide ions; fCN) and can pose a threat to environmental safety. Modern approaches to wastewater treatment are primarily based on (physico)chemical methods and a final biological treatment with mixed microbial cultures. Enzymatic removal of fCN represents an environmentally promising approach.

This work focuses on the remediation potential of enzymes from the nitrilase superfamily. In fungi, hypothetical nitrilases and cyanide hydratases were found through database searches. Selected enzymes were overproduced in *Escherichia coli*, purified and characterized, and their remediation potential was evaluated based on these results.

Two of the enzymes belonged to the NIT4-type nitrilases (EC 3.5.5.4) according to their amino acid sequences: the NitTv1 enzyme from *Trametes versicolor* (protein XP_008032838.1) and the NitAb enzyme from *Agaricus bisporus* (protein XP_006462086.1). NIT4-type nitrilases are widespread plant enzymes that transform β-cyano-L-alanine (AlaCN), an intermediate of fCN scavenging. AlaCN is converted to utilizable amino acids by NIT4. In this work, these enzymes were described for the first time in fungi. The fungal enzymes NitTv1 and NitAb exhibited high specific activities with AlaCN − approximately 132 and 40 U/mg of protein, respectively. In addition, the substrate specificity of these enzymes went beyond plant NIT4, as they could also transform other nitriles (phenylpropionitrile, cinnamonitrile, fumaronitrile). The stability properties were better for NitTv1 than NitAb. Presumably, these nitrilases play a role in plant-fungus interactions, allowing fungi to detoxify plant nitriles.

Cyanide hydratases (CynHs) (EC 4.2.1.66) convert fCN into the much less toxic formamide and have been therefore considered for the decontamination of cyanide effluents. The purified CynH from *Exidia glandulosa* (protein KZV92691.1, enzyme NitEg) showed

high activity towards fCN with 784 U/mg of protein, k_{cat} (turnover number) of 927/s, and k_{cat}/K_M (catalytic efficiency) of 42 l/s/mmol. pH and temperature optimum were 6–9 and 40–45 °C, respectively. Thus, the catalytic properties of NitEg surpassed those of the second CynH studied, which was from the fungus *Stereum hirsutum* (protein XP_007307917.1, enzyme NitSh). High concentrations of silver and copper (1 mM) reduced the activity of NitEg by 30–40%, whereas phenol, thiocyanate, sulfide, and ammonia, at levels typical for industrial effluents, did not lead to a significant reduction in fCN conversion. The enzyme was also functional at high fCN concentrations (100 mM), which is relevant to the remediation of wastewater from metal electroplating.

NitEg is thus a promising biocatalyst for direct fCN detoxification, and NIT4 was shown to likely play an important role in fCN detoxification by fungi. Both enzymes are thus prospective for the detection and determination of fCN. Nevertheless, the potential of the enzymes is just emerging and requires further intensive research to improve and scale up their production and application.

Keywords: cokemaking; cyanide hydratase; cyanide waste; electroplating; free cyanide; formamide; industrial effluent; wastewater treatment; nitrilase.

Abstrakt

Odpadní vody z některých průmyslových procesů (těžba zlata a stříbra, galvanické pokovování Cu, Ag a dalšími kovy, koksování uhlí) obsahují vysoké koncentrace volného kyanidu (kyanovodík a kyanidové ionty) a mohou představovat hrozbu pro bezpečnost životního prostředí. Moderní přístupy k čištění odpadních vod jsou založeny především na (fyzikálně)-chemických metodách a konečném biologickém čištění pomocí směsných mikrobiálních kultur. Enzymatické odstraňování volného kyanidu představuje přístup šetrný k životnímu prostředí.

Tato práce se zaměřuje na remediační potenciál enzymů z nadrodiny nitrilas. U hub byly pomocí vyhledávání v databázích identifikovány hypotetické nitrilasy a kyanidhydratasy. Vybrané enzymy byly nadprodukovány v heterologním hostiteli (*Escherichia coli*), purifikovány a charakterizovány a na základě těchto výsledků byl vyhodnocen jejich remediační potenciál.

Dva z enzymů patřily podle aminokyselinových sekvencí k nitrilasám typu NIT4 (EC 3.5.5.4): enzym NitTv1 z houby *Trametes versicolor* (protein XP_008032838.1) a enzym NitAb z houby *Agaricus bisporus* (protein XP_006462086.1). Nitrilasy typu NIT4 jsou široce rozšířené rostlinné enzymy, které přeměňují β-kyano-L-alanin (AlaCN), meziprodukt detoxifikace a utilizace volného kyanidu. AlaCN je pomocí nitrilasy NIT4 přeměňován na využitelné aminokyseliny. V této práci byly tyto enzymy poprvé popsány u hub. Fungální enzymy NitTv1 a NitAb vykazovaly vysoké specifické aktivity pro AlaCN - přibližně 132, resp. 40 U/mg proteinu. Substrátová specifita těchto enzymů byla navíc širší ve srovnání s rostlinnou nitrilasou NIT4. Fungální enzymy přeměňovaly i jiné nitrily (fenylpropionitril, nitril kyseliny skořicové, fumaronitril). Stabilita byla lepší u NitTv1 než u NitAb. Pravděpodobně tyto nitrilasy hrají roli v interakcích mezi rostlinami a houbami a umožňují houbám detoxikovat rostlinné nitrily.

Kyanidhydratasy (EC 4.2.1.66) přeměňují volný kyanid na mnohem méně toxický formamid, a proto se o nich uvažuje jako o enzymu pro dekontaminaci kyanidových odpadních vod. Purifikovaná CynH z houby *Exidia glandulosa* (protein KZV92691.1, enzym NitEg) vykazovala vysokou aktivitu pro volný kyanid (asi 784 U/mg proteinu), k_{cat} (číslo přeměny) 927/s a k_{cat}/K_M (katalytická účinnost) 42 l/s/mmol. pH a teplotní optimum byly 6-9 a 40-45 °C. Katalytické vlastnosti NitEg tak předčily vlastnosti druhého studovaného enzyme, CynH, který pocházel z houby *Stereum hirsutum* (protein XP_007307917.1, enzym NitSh). Vysoké koncentrace stříbra a mědi (1 mM) snížily aktivitu NitEg o 30-40 %, zatímco fenol, thiokyanát, sulfid a amoniak v koncentracích typických pro průmyslové odpadní vody nevedly k významnému snížení konverze fCN. Enzym byl funkční i při vysokých koncentracích fCN (100 mM), což je důležité pro sanaci odpadních vod z galvanického pokovování.

NitEg je tedy slibným biokatalyzátorem pro přímou detoxikaci fCN a ukázalo se, že NIT4 pravděpodobně hraje důležitou roli při detoxikaci fCN houbami. Oba enzymy jsou také perspektivní pro detekci a stanovení fCN. Nicméně potenciál těchto enzymů se teprve objevuje a vyžaduje další intenzivní výzkum ke zlepšení a rozšíření jejich výroby a použití.

Klíčová slova: čištění odpadních vod; elektrolytické pokovování; formamid; kyanidhydratasa; kyanidový odpad; koksování; nitrilasa; průmyslové odpadní vody; volný kyanid.

Contents

List of abbreviations:

AlaCN – β-cyano-L-alanine

Asn – L-asparagine

Asp – L-aspartic acid

B-R - Britton–Robinson (buffer)

CiN – cinnamonitrile

CN-WAD - weak-acid dissociable cyanides

2CP – 2-cyanopyridine

3CP – 3-cyanopyridine

4CP – 4-cyanopyridine

CynD – cyanide dihydratase

CynH – cyanide hydratase

IAN – indole-3-acetonitrile

IMAC – immobilized metal affinity chromatography

fCN – free cyanide

HPLC - High-Performance Liquid Chromatography

FN – fumaronitrile

NIT4 – type 4 nitrilase

NHase – nitrile hydratase

NLase - nitrilase

PAN – phenylacetonitrile

PPN - 3-phenylpropionitrile

PTAN – phenylthioacetonitrile

SAB - Simultaneous Adsorption and Bioremediation

TCN – total cyanide

1. Introduction

HCN and simple cyanide (NaCN, KCN) are well known as very toxic compounds, highly lethal for most living organisms. The toxic effect of cyanide on the body is due to its high affinity to metals and especially due to the inhibition of the enzyme cytochrome c oxidase, which leads to the disruption of cellular respiration and, in consequence, to tissue hypoxia and acidosis, and to the disturbance of the nervous system.

Currently, there are a number of industries associated with the use of cyanide or the formation of cyanide as a by-product. Accordingly, cyanide and other hazardous substances are present in the effluents of these industries. Cyanides are used extensively in the mining of precious metals and in the manufacture of pharmaceuticals, chemicals, pesticides, and plastics. In the gold/ silver mining and jewelry industries, cyanides are used for the selective extraction of the precious metals from ores and for electroplating processes, respectively (Luque-Almagro et al., 2016). Wastewaters from agriculture may also contain cyanides due to the decomposition of plant cyanoglycosides and cyanolipids during the processing of some raw materials (cyanide-containing crops, such as cassava, millet, etc.). These factors, among others, cause cyanide contamination of soil, groundwater, and other environments.

The methods currently used to treat cyanide-containing waste (physicochemical, chemical) have disadvantages such as a high consumption of chemicals or energy and the generation of secondary waste. Bioremediation is an environmentally friendly alternative or complement to abiotic methods, and the search for new green methods and options for the bioremediation of cyanide waste is required (Anning et al., 2020). This work focuses on the search for enzymes that participate in the detoxification of HCN, on their function and their potential uses in cyanide decontamination and thus protection of population and environment.

The enzymes of interest largely belong to the nitrilase superfamily. This group includes 13 branches, and its known members catalyze the hydrolysis of non-peptide carbon-nitrogen

bonds. The branches differ in the amino acid sequence and the catalytic activity. The most studied and best characterized enzymes of the nitrilase superfamily are, e.g., nitrilase (NLase; EC 3.5.5.1), amino-terminal amidase (EC 3.5.1.-), aliphatic amidase (EC 3.5.1.4), biotinidase (EC 3.5.1.12), β-ureidopropionase (3.5.1.6), and D- and L-carbamoylase (EC 3.5.1.77; EC 3.5.1.87). Members of this superfamily are involved in the biosynthesis and modification of various natural compounds and are found in bacteria, fungi, plants, and animals (Pace and Brenner, 2001).

This work focuses on the enzymes of the first branch, the so-called "true NLases" (hereafter referred to as NLases), in particular their subtypes involved in the detoxification of HCN. Different subtypes of NLases are specific for certain bacteria, fungi, or plants. The functions of NLases in nature seem to mainly involve plant-microbe interactions. For example, microbial NLases may participate in the synthesis of some plant hormones or detoxify and metabolize plant nitriles. At the same time, microbial NLases may take part in some of the mechanisms that promote microbial parasitism in plants containing nitrile compounds (Howden et al., 2009; O'Reilly and Turner, 2003).

NLases catalyze nitrile hydrolysis and have a wide range of substrate specificities, so they are able to process nitriles of different structures as substrates: aliphatic nitriles (e.g., β-cyano-L-alanine (AlaCN), acrylonitrile), aromatic nitriles (e.g., cyanopyridine, benzonitrile), and arylaliphatic nitriles (e.g., 3-phenylpropionitrile) (Figure 1) (Brenner, 2002; O'Reilly and Turner, 2003). Cyanide hydratase (CynH) and cyanide dihydratase (CynD) catalyze the cyanide transformation into amide and acid products (formamide and formic acid), respectively (O'Reilly and Turner, 2003).

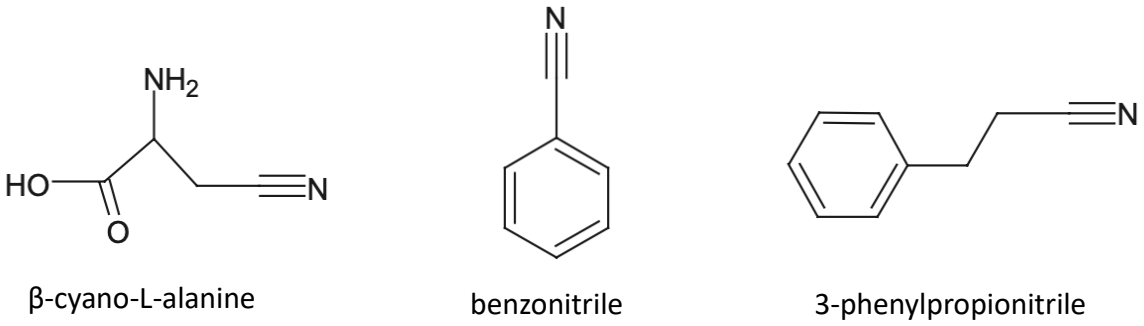

Figure 1. Examples of structurally different nitriles.

NLases have a wide range of potential applications in various fields. One reason for this is their environmental compatibility. The biotechnological importance of NLases is very high in the production of chemicals and in the degradation of waste materials. Biohydrolysis of nitriles and bioremediation of cyanides by NLases are promising routes due to the high catalytic activities and suitable substrate specificities of the enzymes. Since the discovery of microorganisms possessing nitrile-hydrolyzing enzymes, many papers have been published on the biochemical and genetic background of the nitrile transformation process, the enzyme structures, and the metabolic pathways, in which the enzymes are involved (Sharma et al., 2019; Kumar et al., 2017).

Here we discuss the potential of these enzymes in the context of the current state of cyanide remediation and up-to-date trends in alternative solutions. The source of the enzymes in this work was Basidiomycota fungi, a group of organisms known for their broad biodegradation potential. However, the potential of this group of fungi for the detoxification of cyanide has been poorly explored so far. Basidiomycota were found to be a rich source of plant NLase homologues (NIT4) involved in the hydrolysis of AlaCN, an intermediate of HCN scavenging. In addition, Basidiomycota were found to produce some CynHs which directly convert HCN. The biochemical and catalytic properties of the enzymes were studied after selected representatives of these enzymes were obtained by heterologous expression of synthetic genes (Rucká et al., 2020; Sedova et al., 2021).

In addition, the CynHs were used as purified enzymes to study their ability to work in media contaminated with cyanide. Future uses of the enzymes for environmental technologies and bioanalytics were discussed, comparing their properties with alternative chemical and biological tools.

Aims of the thesis

The primary aim of this thesis was the preparation of new biocatalysts for the biodegradation of free cyanide and the evaluation of their suitability for future uses such as the remediation of industrial wastewater or of contaminated environment, for the sake of population protection.

Specific aims were:

- investigate the cyanide detoxification potential of fungi focusing on Basidiomycota;
- express selected genes focusing on cyanide hydratase and nitrilase NIT4;
- determine the catalytic properties of the enzymes;
- investigate the enzyme operation in cyanide-contaminated media.

2. State of the art

The problem of cyanide discharge via industrial effluents and how to deal with it have been the subject of numerous reviews. The reviews published over the past approximately ten years have focused on the following topics: cyanide waste treatment solutions in gold mines (Kuyucak and Akcil, 2013; Mekuto et al., 2016; Anning et al., 2019), ability of microbes and plants to degrade and utilize cyanide (Kumar et al., 2017), cyanide detoxification by enzymes (Martínková et al., 2015; Park et al., 2017; Sharma et al. 2019), anaerobic degradation of cyanide (Luque-Almagro et al., 2018) and the cyanide degradation potential of an isolate of *Pseudomonas pseudoalcaligenes* (Luque-Almagro et al., 2016; Cabello et al., 2018). A wide range of topics including the chemical and biological properties of cyanide, its occurrence and biodegradation were reviewed by Anning et al. (2020). However, reviews of the full range of cyanide waste treatment processes (chemical, microbial, enzymatic, etc.) have been lacking, especially for the most recent period. Therefore, the literature review part of this work will address cyanide disposal options as a whole. It will summarize the recent promising solutions in this research area, considering chemical, physicochemical and biological methods. It will also address the types and sources of cyanides and collect data on cyanide levels in various industrial wastewaters. A separate subchapter will address the legal aspects of cyanide regulation. Finally, this part of the work will focus on enzymes suitable for the degradation of cyanide to less toxic or relatively harmless products, as well as enzymes involved in the turnover of cyanide in plants and some microorganisms.

2.1. Cyanides – origin, properties and regulatory directives

Sources of cyanides in the environment, foods or products may be natural or man-made. The frequently encountered anthropogenic sources of cyanide release into air and water include certain industrial facilities, forest and house fires, products of incomplete combustion

of nitrogen-containing organic polymers, cigarette smoke and vehicle emissions. In industry, cyanide is required for certain processes in metal plating facilities, petrochemical and organic chemical industries, or machine-building plants. In addition, cyanide is present in primary wastewaters from coke plants and iron-smelting plants. Agricultural plants containing cyanoglycosides can release HCN (Bolarinwa et al., 2014, Kuyucak and Akcil, 2013). Due to the highly toxic nature of the cyanide anion, as well as of HCN (released especially under acidic conditions), the cyanide content in wastewater, natural and drinking water is subject to strict standards (see below).

2.1.1. Types and chemical properties of cyanides

Simple cyanides are a cyanide anion (CN^-) and metal cation containing compounds. An important feature of cyanide solutions is the ratio of the undissociated hydrocyanic acid (HCN) and the cyanide ions; the sum of both is named free cyanide (fCN). In water, simple cyanides dissociate to form cyanide anions and metal cations or are present as undissociated HCN. In acidic environment, the ratio of HCN and cyanide anion increases. If pH is lower than about 8.5, HCN readily evaporates from the solution as very dangerous fumes. Therefore, it is recommended that the solutions of cyanide salts are kept at pH even higher, such as pH over 10. When cyanides are oxidized with hydrogen peroxide or other oxidants, cyanates (OCN^-) are formed. Cyanates are much less toxic than cyanides. Cyanide complexes (chelates) with, e.g., Cd, Ag, Cu, Zn, or Ni ions are designated weak-acid dissociable cyanides (CN-WAD). The sum of all cyanide types is referred to as total cyanide (TCN). It contains fCN, CN-WAD and hardly dissociable cyanide complexes with Fe ions (Kuyucak and Akcil, 2013).

2.1.2. Industrial sources

An important property of fCN is its complexation with metals and its electrolytic

properties, which are utilized in several industrial processes (Table 1). In the mining of precious metals such as gold and silver, the use of cyanide has been well known since ancient times. To extract gold from ore with cyanide, 0.1-0.5 g NaCN/L (pH > 10) is used, and the resulting $[Au(CN)_2]^-$ complexes are exposed to zinc, which reduces Au^+ to Au^0. Another option for the recovery of gold is the adsorption of the metal-cyanide complex on activated carbon, followed by elution of gold with a mixture of 0.1% NaCN and 1% NaOH. The process of preparing silver is similar, but either higher concentrations or a longer exposure to NaCN are used to produce the $[Ag(CN)_2]^-$ complex (Kuyucak and Akcil, 2013). The amount of gold mined in 2020 was approximately 3,200 tons (Gold mine production worldwide from 2005 to 2020, 2021; Global mine production of silver from 2005 to 2020, 2021). Each year, between 2001 and 2005, approximately 120 tons of NaCN were used at a single gold-silver mine (Akcil, 2006).

The complexation ability of cyanide is also useful for metal plating. The aim of this industrial field is to refine the surface of a range of products including jewellery. Cyanides are used in electroplating baths of silver, copper, cadmium and zinc. Typically, a cyanide solution contains NaCN and a metal salt or oxide, and its pH must be above 10 to avoid the formation of HCN vapors (Safe Work Australia, 2012).

The DuPont process for producing adiponitrile, a precursor for polyamide 6.6, involves the use of cyanide. The process consists of the Ni-catalyzed hydrocyanation of butadiene to adiponitrile. Adiponitrile can then be further processed to produce hexamethylene diamine, which is one of the monomers used in the production of polyamide 6.6, commonly known as nylon 6.6. Cyanation reactions like the one used in this process are important in the synthesis of various organic compounds and are widely employed in the chemical industry (Bini et al., 2010).

In the process of producing pharmaceutical chemicals, useful intermediate substances

are cyanohydrins, which are the products of cyanation of ketones or aldehydes. For instance, the production of mandelic acid (a chiral compound) uses mandelonitrile, which in turn is obtained by cyanation of benzaldehyde. To obtain the enantiopure (*R*)-mandelic acid, biocatalytic hydrolysis of racemic mandelonitrile is possible (Martínková and Křen, 2018). The precursor of clopidogrel (an antithrombotic drug) is (*R*)-2-chloromandelic acid, which is produced in a similar way (Zou et al., 2021). The product of cyanation of acetone is acetone cyanohydrin, from which methyl methacrylate is obtained, and used to produce polymethyl methacrylate (PMMA) - this is the well-known acrylic or "Plexiglas".

Cyanide can be a by-product in various industries. One example is the production of coke: during the pyrolysis of coal at temperatures reaching 1200 °C, HCN with other substances (H_2S, ammonia and other organics) is transferred into coke oven gas which is then cooled, thus forming "raw coke wastewater" (Kwiecińska-Mydlak et al., 2019). Annual coke production worldwide was approximately 650 tons in 2016 (Ghosh et al., 2022). One of the main uses of coke is in the metallurgical industry (Kwiecińska-Mydlak et al., 2019). In this technology field, coke is used in the iron production process in blast furnaces. It provides the fuel for achieving high temperatures needed to convert iron ore into "pig iron" (crude iron). At this stage, reactions between alkali metals, carbon and nitrogen lead to the formation of cyanide (Mondal et al., 2021).

The concentration of cyanide and the presence of other components in wastewater will vary significantly depending on the industry, processes and technologies used in that industry (Table 1). Data on the amount of cyanide in various wastewaters can differ by several orders of magnitude (Table 1) and are important for the decision on the further treatment of the wastewater.

Kwiecińska-Mydlak et al. (2019) used the term "raw coking wastewater" to refer to wastewater after ammonia removal and tar separation. This wastewater is usually heavily

polluted with multiple contaminants and is released in very large volumes. For example, in one day, 2000 m^3 was released in a coke plant that produced more than 3500 tons of coke per day (Yu et al., 2016). With a coke production capacity of approximately 11 500 tons per year, 2900-3600 m^3 per day were produced (Fan et al., 2021). The content of fCN in these wastewaters was largely between 3.5 and 18.2 mg/l. However, fCN was not found in two samples of the raw wastewater and the sample after biological treatment, whereas TCN was present in all of them at significant concentrations of 34-105 mg/l (Table 1).

Table 1. Content of free cyanide (fCN) and total cyanide (TCN) in cyanide-containing effluents from various industries

Industry	**TCN**	**fCN**	**Reference**
Gold mining	231	n.d.	Zheng et al., 2015
	7155	n.d.	Pan et al., 2021
	n.d.	13 760	Carmona Orozco et al., 2019
	1574	276	Chen et al., 2020
Coking	n.d.	4 - 15	Papadimitriou et al., 2009
(raw effluent)	46 ± 10	3.5 ± 2.1	Yu et al., 2016
	105	n.d.	Viña Mediavilla et al., 2019
	n.d.	5 - 20	Kwiecińska-Mydlak et al., 2019
	≈13	5.3 ± 1.6	Mondal et al., 2021
	78.2	n.d.	Fan et al., 2021
	n.d.	8.3	Martínková and Chmátal, 2016
	n.d.	18.6 ± 2.1	Ban et al., 2022
	n.d.	8 - 10	Ghosh et al., 2022
Coking (after biotreatment)	35.4 ± 1.5	n.d.	Liu et al., 2020
Petrochemical	n.d.	≤ 120	Jarrah and Mu´azu, 2016
Chemical	1280	n.d.	Yang et al., 2020
Iron smelting	≈10	4.8 ± 1.0	Mondal et al., 2021
Electroplating	n.d.	≈26 000	Basile et al., 2008
	n.d.	51 200 ± 420	Pérez-Cid et al., 2020
Jewelry	≈39 000	26 000	Ibáñez et al., 2017

fCN – free cyanide; TCN – total cyanide (sum of fCN and all metal-complexed cyanide); n.d. - no data available.

In addition, high concentrations of phenols were found in coke wastewater samples (400–2100 mg/l) (Papadimitriou et al., 2009; Martínková and Chmátal, 2016). After the

primary stage, phenols are reduced by 13%, which is insufficient (Ban et al., 2022). Coke wastewater also contains ammonia and thiocyanate (Papadimitriou et al., 2009; Pillai and Gupta, 2016; Yu et al., 2016; Viña Mediavilla et al., 2019).

Effluents from jewelry and electroplating industry have a high content of cyanide, such as 39 g TCN/l (Ibáñez et al., 2017) or 25 - 52 g fCN/l (Basile et al., 2008; Pérez-Cid et al., 2020), respectively. In addition, this wastewater contains metals, such as Fe, Cu, Ag, Zn, Al or Ni. Gold mine wastewater also contains a combination of a high concentration of cyanide with residues of metals (Carmona-Orozco and Pannay, 2019; Chen et al., 2020) (Table 1).

2.1.3. Toxicity

Lethal dose for adults is estimated at 50–200 mg of a simple cyanide such as NaCN or KCN. The toxic dose depends on the form of cyanide and the route of entry into the body; the most rapid manifestations of symptoms of cyanide poisoning occur following inhalation and intravenous penetration into the body (Bogucki and Weir, 2002). Exposure to airborne cyanide of 270 ppm is rapidly fatal.

A concentration of fCN of only 5 - 7 μg/l in aquatic habitats has a negative effect on fish, inhibiting their swimming functions and reproduction processes. A higher concentration of cyanide (over 20 μg/l) is lethal for most fish species (Eisler and Wiemeyer, 2004).

Chronic exposure to sub-lethal doses of fCN is also highly hazardous as it can damage the sensory system (visual and auditory nerves). This can result from frequent consumption of foods made from plants that naturally contain cyanides, unless the processing of the plant foods is done properly. A well-known plant of this type is cassava, which is regularly consumed in oriental countries.

According to Anning et al. (2020), contamination of aquatic ecosystems with cyanide due to excessive discharges to surface waters has detrimental effects on fish both chronically and acutely at cyanide concentrations from 5 μg/l and 50 μg/l, respectively.

Complexes of cyanides with metals such as nickel, copper, zinc or iron are less toxic than fCNas their solubility is limited. However, cyanide complexes such as ferro- and ferricyanides decompose under the action of light to form free HCN (Kuyucak and Akcil, 2013).

2.1.4. Legislative frameworks

Different cyanide-containing compounds have varying degrees of toxicity. Organic cyanides and hexacyanoferrates, in which the cyanide ions are tightly bound to the iron ions (ferrocyanide and ferricyanide), have low toxicity. In contrast, HCN and simple cyanides (e.g., KCN, NaCN) are the most toxic. There are also organic compounds that readily release cyanide ion/ hydrogen cyanide, such as trimethylsilyl cyanide upon contact with water, cyanoacrylates upon pyrolysis, or cyanohydrins (2-hydroxynitriles) in alkaline media (Rustler et al., 2008).

All civilized countries have legislation regulating the use of cyanide and its content in various environments.

The US Environmental Protection Agency (EPA) classifies cyanide as an inorganic contaminant of drinking water and surface water (National Primary Drinking Water Regulations), and wastewater (US Clean Water Act). EPA guidelines allow a maximum fCN level of 0.2 mg per liter of drinking water (Code of Federal Regulations, 2002). EPA cyanide discharge limits vary by industry and facility size (up to 38 000 and over 38 000 liters per day). The EPA sets cyanide standards as follows: 5.2 μg/l - total cyanide for continuous publicly owned treatment work discharges, 22 μg/l - maximum permissible amount of

discharge into fresh water, 1 μg/l - maximum permissible amount of discharge into salt water (Code of Federal Regulations, 2008).

The European drinking water standard allows a lower fCN limit than EPA: 0.05 mg/l (Directive 75/440/EEC).

In the Czech Republic, Law No. 254/2001 Coll., on water and on amendments to certain laws (Water Law), regulates activities in the field of regulation, management and protection of surface water or groundwater (ČR Zákon č. 254/2001 Sb.).

Directive 2006/21/EC of 15 March 2006 on the management of waste from extractive industries (Mining Waste Directive), article 13(6) of the Mining Waste Directive, defines the permissible concentration of fCN at the point of discharge of mining waste into a tailing pond as not exceeding 10 ppm. According to Article 14 of Directive 2006/21/EC, companies must also provide financial guarantees to ensure environmental remediation following mine closure. This could reduce the number of small companies seeking to develop gold mines in the EU due to a lack of financial resources to provide such guarantees (Directive 2006/21/EC).

Directive 2000/60/EC of 23 October 2000 (Water Framework Directive) sets standards for discharges into water and it considers cyanide as one of the main pollutants. According to the directive, direct discharges of pollutants into groundwater are prohibited without first achieving the ecological status of surface waters (An official website of the European Union).

Another aspect regulated at the legislative level is the problem of large-scale industrial accidents with a subsequent release of hazardous substances of a toxic, flammable or explosive nature, which can lead to serious consequences including damage to human health and life and material and financial losses, contamination of groundwater and the environment. This is addressed by the Directive 2012/18/EU of the European Parliament and of the Council of July 2012 on the control of the risk of serious accidents arising from the presence of hazardous substances and amending and subsequently repealing Council Directive 96/82/EC. The need

to implement the changes introduced by the Directive of July 2012 is contained in the law of the Czech Republic, which is discussed below.

The Ministry of the Environment of the Czech Republic is responsible for the prevention of accidents caused by certain hazardous chemicals, including cyanide. In the Czech Republic, Law No. 224/2015 Coll. on the Prevention of Serious Accidents is the legal regulatory document in this area. This law implements the SEVESO III directive (Directive 2012/18/EU) (https://www.zakonyprolidi.cz/cs/2015-224). According to this law, a major accident is defined as “an extraordinary, partially or completely uncontrollable event limited in time and space, in particular a serious release of a hazardous substance, fire or explosion, occurring or imminent in connection with the use of a facility, resulting in a serious threat or serious consequences for the life and health of people and animals, the environment or property and associated with one or more hazardous substances." This law regulates the prevention of serious accidents and was created after the well-known major cyanide accident in Baia Mare, Romania, in 2000.

2.2. Current state of the art in cyanide remediation

Nowadays, physicochemical and chemical methods are extensively used for wastewater treatment. The search for methods that are environmentally friendly and, moreover, allow to increase efficiency and reduce the cost of wastewater treatment, is a modern trend. The biological and enzymatic methods for wastewater treatment are promising and hopeful, although not the only possible solutions. Prospective methods have also emerged in the area of coagulation, oxidation, photocatalysis, electrolysis, and combined processes (Table 2). The advantages and drawbacks of various types of cyanide disposal processes are discussed in the following sections.

Table 2. Examples of recently reported processes of cyanide removal from wastewaters

Process	Chemical(s), (bio)catalyst(s)	Scale	Reference
Coagulation	Polyferric sulfate, organic polymer	75 m^3/h	Shen et al., 2014
	$FeSO_4$	200 ml	Yu et al., 2016
Adsorption	Activated carbon	100 ml	Liu et al., 2020
	Calcium alginate beads	20 ml	Pérez-Cid et al., 2020
	Metal-organic resin	50 ml	Chen et al., 2021
Oxidation	O_2	700 l	Oulego et al., 2014
	H_2O_2, $CuSO_4$	240 ml	Wang et al., 2017
	O_2, Cu-Mn-O	25,000/h[a]	Li et al., 2018
	O_3 + air (O_2) + H_2O_2	5 m^3/h	Acha et al., 2013
Cyanation	2-Methoxybenzaldehyde, CO_2	20 ml	Petersen et al., 2021
Electrooxidation	Pt-coated Ti electrode	16 ml	Valiuniene et al., 2013
	BDD electrode[b], Na_2SO_4	2 l	Jarrah and Mu´azu, 2016
	PbO_2 electrode	250 ml	Pillai and Gupta, 2016
	BDD electrode[b], $Na_2S_2O_8$	500 ml	Yang et al., 2020
	Ti electrode	100 ml	Chen et al., 2020
Electrodialysis	dialysis membrane, Na_2SO_4	15 l/h	Zheng et al., 2015
Photocatalysis	Pt/Ga_2O_3/SiO_2	300 ml	Baeissa and Mohamed, 2013
	ZnO	300 ml	Bagabas et al., 2013
	$K_2La_2Ti_3O_{10}$/CeO_2	25 ml	Pala et al., 2015
	TiO_2	50 ml	Pattanayak et al., 2021
Microbial remediation	*Pseudomonas*	10 l	Ibáñez et al., 2017
	Bacillus	0.26 l/d	Mekuto et al., 2015
		5.1 l	Burneo et al., 2020
	Bacterial consortia	0.14-1 l/d	Mekuto et al., 2017
		0.5 l/d	Shin et al., 2020
		≥120 m^3/h	Fan et al., 2021
	Tetraspora	100 ml	Rai et al., 2021
Biocatalysis	Cyanide hydratase	50 ml	Martínková and Chmátal, 2016
	Cyanide dihydratase	n.d.	Carmona-Orozco et al., 2019
Combined	Activated carbon, *Serratia odorifera*	100 ml	Singh et al., 2016
	H_2O_2, cyanase	10 l	Sáez et al., 2019

[a] gas flow rate/ catalyst volume, [b] BDD - boron-doped diamond; GHSV

Processes tested with real industrial effluents are marked in color: coke-oven plant effluents, gold mine wastewater, electroplating wastewater, jewelry wastewater, chemical plant effluent.

Other processes were tested with model solutions.

2.2.1. Industrial processes

Cyanides can be removed from various environments using a variety of methods, such as chemical, physicochemical, biological, or enzymatic. The choice of method depends on many factors, including the type of cyanide, its concentration, the nature of the contamination, available resources and clean-up requirements. However, not all methods are equally effective or safe. When choosing a method, it is important to consider the effectiveness, safety and economic feasibility of this method under specific conditions. There are not many methods known that are effective and have already been tested in practice. Such approaches include the chemical oxidation of cyanides, the reaction product of which is cyanate. Another method is the precipitation of metal complexes with cyanide. A combination of both approaches is also possible. As for the biological approach, bioremediation with activated sludge is known, but this method is only suitable for wastewaters with a low cyanide content; for example, the method is applicable for a pre-treated coking wastewater (Fan et al., 2021). Due to their cheapness and relative simplicity, passive methods of cyanide removal remain popular. These combine photodegradation, evaporation, complexation and precipitation, and biodegradation by plants and other organisms.

A method developed by Hemlo Gold Mines Inc. (Ontario, Canada) was based on a two-step complexation of cyanide with metals (Fe^{2+} and/or $Cu^{2+)}$ (Figure 2) followed by oxidation with hydrogen peroxide, and final remediation in "tailings ponds" (Kuyucak and Akcil 2013).

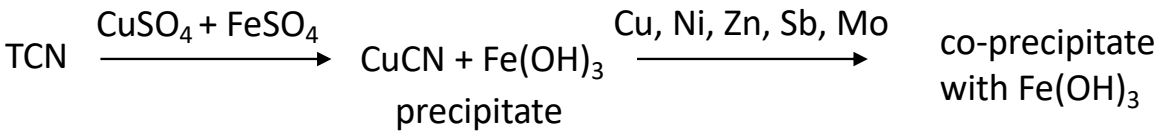

Figure 2. Precipitation of total cyanide (TCN) using copper (II) and iron (II) sulfate. Heavy metal co-precipitate with iron (III) hydroxide was formed.

Coke effluent may retain TCN at levels of 4 - 5 mg/l after sedimentation (Shen et al., 2014), which may be due to the presence of compounds that prevent the formation of cyanide complexes with metals (see below).

Chlorine, oxygen, air, hypochlorite, ozone, H_2O_2 or SO_2/ air, sometimes together with copper as a catalyst, were used as oxidizing agents for the conversion of cyanide to cyanate (Figure 3).

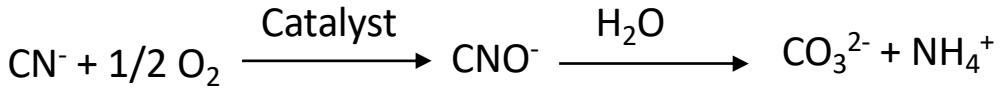

Figure 3. Degradation of free cyanide to the much less toxic cyanate (CNO^-). Hydrolysis of cyanate is optional.

The product of alkaline chlorination is cyanate in the one-step process, which may be sufficient for the detoxification of the waste treated. The products are N_2 and CO_2 if a two-step process is used (Figure 4).

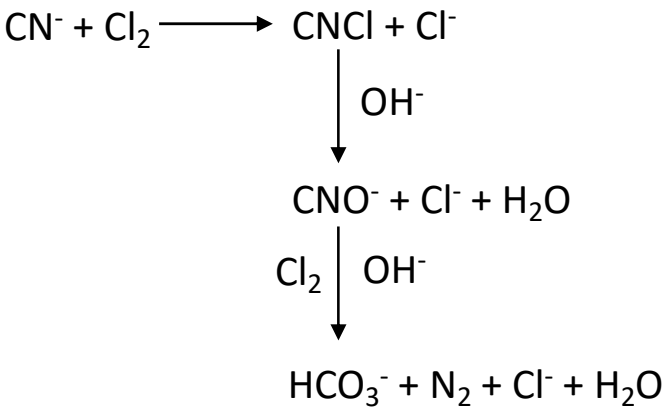

Figure 4. Degradation of free cyanide by alkaline chlorination. The process may be reduced to one stage resulting in the production of cyanate.

Significant disadvantages of this method are the toxicity of chemical compounds used or formed (chlorine, cyanogen chloride and chlorinated by-products) and the unfavorable price/ effectiveness ratio, i.e. high cost and low efficiency for some cyanocomplexes. The next generation of processes used SO_2/ air as an oxidizing agent. One example is the Inco process, which was created in 1984. This technology was followed, in 2003, by an improved process using a mixture of SO_2/ air/ H_2O_2 as oxidizing agents (CombinOx process by Inco-Degussa). This technology has proven to be effective and versatile, as it is also able to remove heavy metals (Kuyucak and Akcil 2013). Moreover, the application of the ozonation process to a model mixture of cyanide, phenol, and benzonitrile (50, 50, and 10 mg/l, respectively) was demonstrated on a 400-L scale (Acha et al., 2013). The oxidation process took place in a 5-meter column through which wastewater and ozone flowed.

2.2.2. Trends in chemical and physicochemical processes

Current trends in the field of cyanide coagulation are aimed at finding alternative coagulants and changing their quantity. It has been shown that the Fe^{2+}/ TCN ratio is decisive for the coagulation of $FeSO_4$ (Yu et al., 2016). A Fe^{2+}/ TCN ratio of more than 2.5 made it possible to almost completely remove TCN from coke plant wastewater.

Replacing the coagulant with a mixture of polyferric sulfate and a cationic polymer optimized this method. The effectiveness of the method has been shown on an industrial scale (wastewater flow 75 m^3/h, TCN concentration reduced by 20 times) (Shen et al., 2014).

Using electrocoagulation, fCN was completely degraded at a concentration of 100 mg/l. The purification process was as follows: enriched wastewater from the mining industry passed through a 2-liter electrochemical cell. The effectiveness of electrocoagulation turned out to be higher in comparison with classical chemical coagulation (Mamelkina et al., 2020). The use of electrocoagulation in combination with adsorption and biotreatment allowed the

removal of 96% fCN (initial concentration 6.4 mg/l) in jewelry wastewater on a scale of 1.5 m^3 (Pratiwi et al., 2021).

Alginate hydrogel (Pérez-Cid et al., 2020), organometallic resin (Chen et al., 2021) and activated carbon (Liu et al., 2020) have been tested in laboratory conditions as adsorbents. The effectiveness of the calcium alginate sorbent was 85% for a wastewater from electroplating industries with a fCN concentration of more than 50 g/l. In addition, the concentrations of metals present in the wastewater (approximately 5 g/l Ni and 2 g/l Cu) were reduced by 50 times (Pérez-Cid et al., 2020 The sorbent made of a metal-organic resin turned out to be effective for removing cyanide metal complexes with Fe^{3+}, Pd^{2+}, Pt^{2+}, Co^{3+} and, moreover, enabled to extract palladium and platinum. The concentration of metals in a model solution was 50 mg/l for each (Chen et al. 2021).

Innovative oxidation technologies or the use of new catalysts are aimed primarily at environmental safety and reducing the use of hazardous chemicals. An example is the use of compressed oxygen for liquid phase ("wet") oxidation, which does not require the use of hazardous chemicals (Oulego et al., 2013, 2014). Another example for safe oxidation is the use of H_2O_2 generated on site using argon as the discharge gas (Wang et al. 2017; Figure 5).

Using H_2O_2 as an oxidant requires 40 mg Cu^{2+}/l for an efficient oxidation (Wang et al. 2017). An example of an advanced catalyst was a mixed Cu–Mn oxide used under argon atmosphere at a temperature of 250 °C (Li et al., 2018). Another new approach represented the oxidation by H_2O_2 in combination with hydrodynamic cavitation, which resulted in the formation of free radicals ($OH^{\bullet}$) from water (Montalvo Andia et al., 2021).

Another oxidizer – sodium persulfate ($Na_2S_2O_8$) – was tested under laboratory conditions with coke plant wastewater, which was previously biologically purified and contained 4.8 mg TCN/l. It was combined with a flocculant – zero-valent iron (Fe^0). As a result, the TCN concentration was reduced to a level lower than 0.05 mg/l (Zhang et al., 2018).

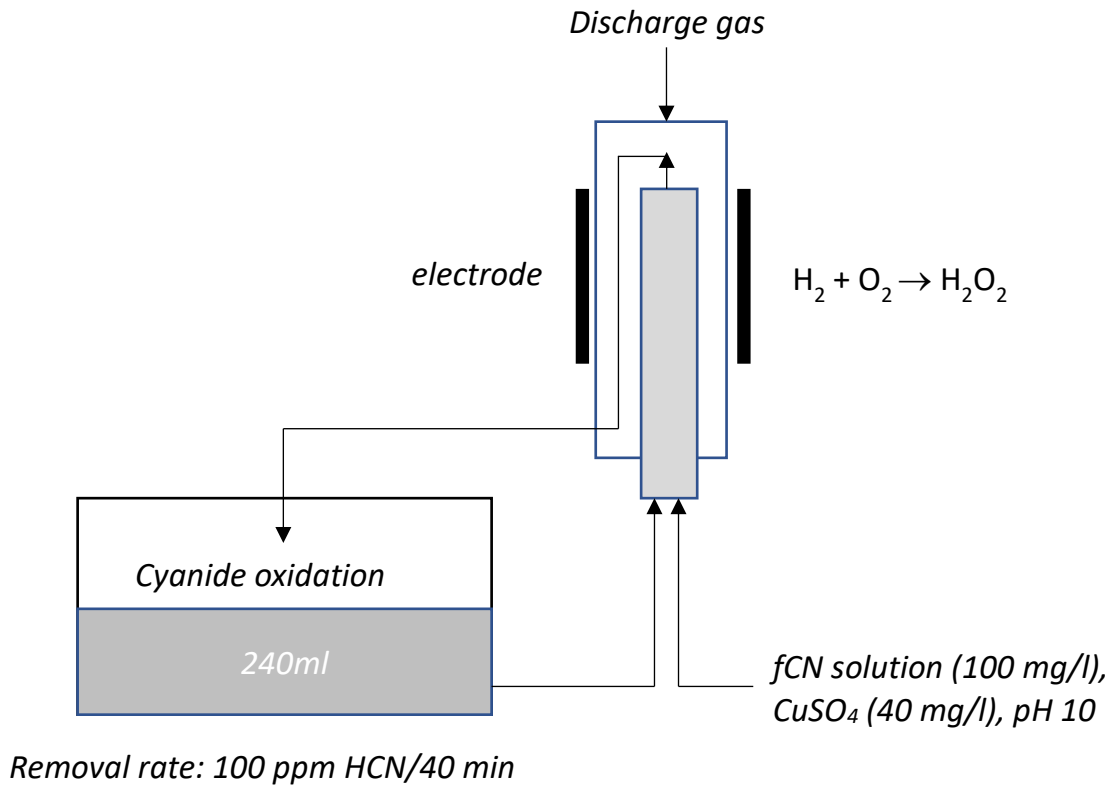

Figure 5. Removal of free cyanide (depicted as HCN) by oxidation with hydrogen peroxide generated in a plasma discharge reactor (Wang et al. 2017).

Other recent approaches have been based on new principles of cyanide removal. For example, the reaction of cyanide with an aldehyde yielded an insoluble cyanohydrin. Using 2-methoxybenzaldehyde under a carbon dioxide atmosphere (to optimize the cyanohydrin formation, 97% of 1M NaCN was removed (Figure 6) (Petersen et al., 2021).

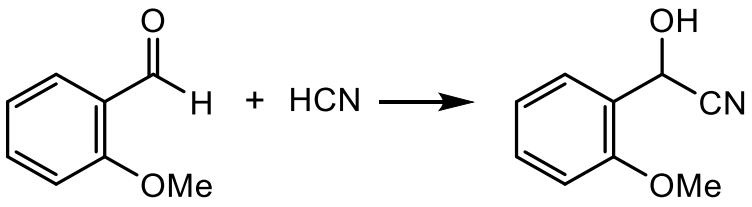

Figure 6. Scavenging of free cyanide by reacting HCN with an aldehyde (Petersen et al., 2021).

Another new process was electrochemical oxidation. In this approach, cyanides were oxidized with electric current, and the reaction product, cyanate, was converted into N_2 and CO_2 (Kuyucak and Akcil 2013) (Figure 7). An innovative feature in the possibility of removing several pollutants in one process (Jarrah and Mu´azu, 2016; Pillai and Gupta, 2015; Pillai and Gupta, 2016), reducing the cost of electrodes (Valiuniene et al., 2013; Pillai and Gupta, 2015; Pillai and Gupta, 2016). An example of such an approach is the use of an electrolytic facility with a graphite cathode and a biplanar boron-doped diamond (BDD) anode, which are commercially available. Elimination of more than 97% of fCN and the full elimination of phenol, ammonia and sulfide were demonstrated for a coke oven wastewater model (Jarrah and Mu´azu, 2016; Figure 8). In addition, the high efficiency of the BDD electrode in the degradation of cyanide, phenol and thiocyanate was demonstrated with real coking wastewater (Pillai and Gupta, 2016).

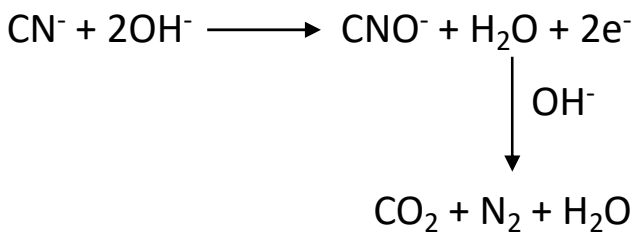

Figure 7. Electrochemical oxidation.

Another example of an electrode available at a reduced cost is the Ti electrode. It is coated with a nanolayer of Pt, which makes it much cheaper than a Pt-only electrode. The Ti electrode removed 2.6 g/l of cyanide almost completely in model mixtures of KCN and chlorides (Valiuniene et al., 2013). In electrochemical oxidation, chlorides have a positive effect on the oxidation efficiency due to the formation of Cl_2 and ClO^- that are very efficient in oxidizing cyanides (fCN, TCN) (Chen et al., 2020). In addition, a PbO_2 electrode was highly

effective in degrading fCN, thiocyanate and phenol in coke plant wastewater (Pillai and Gupta, 2016).

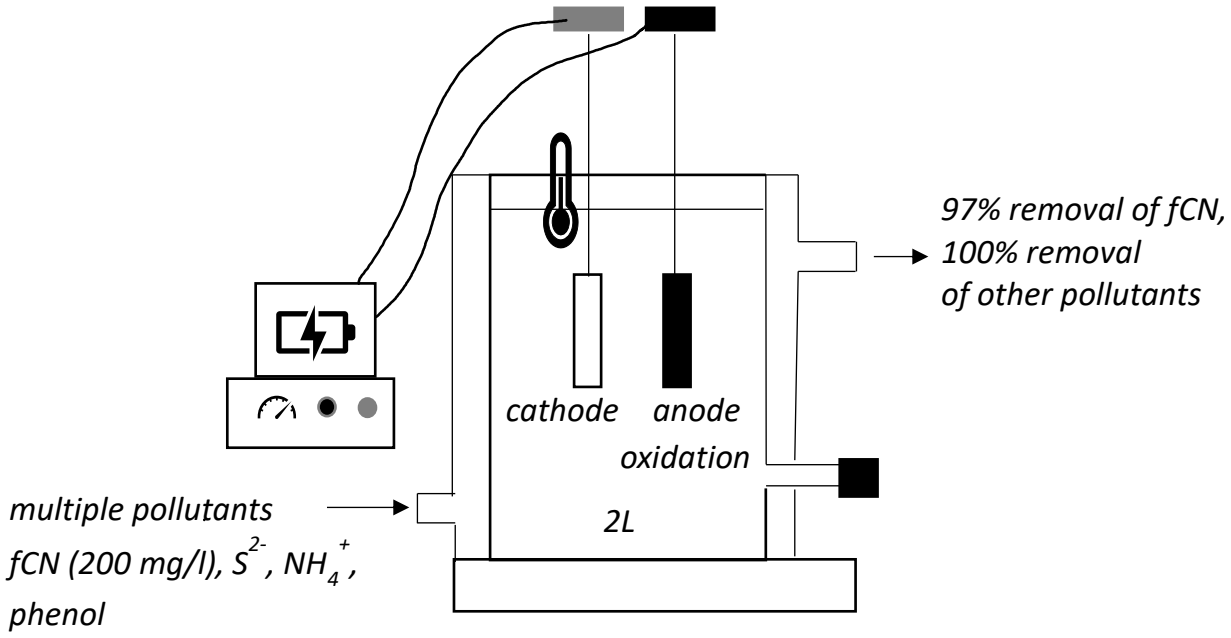

Figure 8. Electrolytic facility for removing free cyanide (fCN) and other pollutants (Jarrah and Mu´azu, 2016).

Electrodialysis is a method of separating and purifying solutions using an electric field and membrane filters. It is based on the principle of ion migration under the influence of electric field through selective ion-exchange membranes. Electrodialysis is used in industry and laboratories for various purification and separation tasks. Electrodialysis units made it possible to degrade almost 98% TCN in gold mine wastewater (initial concentration 231 mg/l) using a flow rate of 15 l/h (Zheng et al., 2015).

Photocatalysts are substances or materials that are capable of initiating and enhancing chemical reactions when exposed to light. The principle of operation of photocatalysts is based on the fact that they can absorb photons of light and transfer this energy into chemical reactions. Photocatalysts can be used to destroy cyanide in aqueous solutions. Titanium dioxide (TiO_2) can be used for this purpose. Well-known affordable TiO_2 powders are

produced by Aldrich (Anatase) and Evonik-Degussa (P25 catalyst). The latter is superior to Anatase Aldrich in removing cyanide from stream waste (Motegh et al., 2014). Thus, the P25 catalyst can remove almost 100% of TCN and 70% of thiocyanate in coking wastewater when exposed to artificial sunlight, as concluded from the computational model of the process (Viña Mediavilla et al., 2019).

In addition, it has been shown that the adsorption of TiO_2 on zeolite increases the efficiency of the catalytic agent. This catalyst was tested on a laboratory scale and was able to remove 94% of TCN (more than 7 g/l) in metallurgical waste, and was also effective in removing Cu and Zn (Pan et al., 2021). Immobilization of TiO_2 on polyurethane also increased the efficiency of the photocatalyst; when an iron porphyrin photosensitizer was added to the system, the fCN removal efficiency (100 mg/l) increased from 75% to 91% (Pattanayak et al., 2021).

Modern photocatalysts that are active in visible light have been studied. Examples are Nb/Ti, potassium lanthanum titanate ($K_2La_2Ti_3O_{10}$), cerium oxide (CeO_2), or gallium oxide (Ga_2O_3) photocatalysts (López and Castro, 2020; Pala et al., 2015; Baeissa and Mohamed, 2013).

2.2.3. Trends in biological degradation of cyanides

Bioremediation makes use of the metabolic potential of plants, fungi, insects, worms and other organisms for cleaning water, soil or atmosphere. A number of bacteria, fungi and plants are capable of cyanogenesis and produce cyanides but also have a significant potential to eliminate them through various routes (Bhalla et al., 2018).

There have been many studies showing the potential of innovative biological methods for the treatment of wastewaters that contain cyanide. These studies included the use of bacteria, both mixed and pure cultures, as well as the use of purified enzymes obtained from

homologously or heterologously producing strains. An industrial plant with a sequential change of phases without oxygen and with oxygen was used to treat waste products from the coking process. High rates of removal of cyanide, phenols, total nitrogen, and other contaminants were obtained. The researchers attributed this remediation efficiency to the abundance of *Thiobacillus*, *Thauera*, and an unidentified nitrifying bacterial strain and to the stability of the microbial community structure in this stepwise mode (Fan et al., 2021).

The ability of some anaerobic bacteria to remove not only fCN, but also its complexes with metals has been shown (Gupta et al., 2016). The aerobic and anaerobic cyanide-degrading consortia can be obtained and applied in different ways. Aerobic consortia have been derived from metallurgical effluents and enriched with media containing high concentrations of fCN (Mekuto et al., 2013). In another study, the source of aerobic consortia was mining wastewater residues (Guadalima and Monteros, 2018).

Mekuto et al. (2015, 2017) demonstrated the effectiveness of aerobic consortia to remove cyanide under laboratory conditions. The duration of cultivation of aerobic consortia ranged from 80 to 300 days, the concentration of fCN in the medium was 500 mg/l, and the decomposition of fCN was almost complete during the entire continuous process. The ammonia obtained as a reaction product was processed by nitrification and denitrification (Mekuto et al., 2015) (Figure 9).

The metabolic potential of the phylum Proteobacteria for the biological treatment of wastewater from a gold processing plant was also shown. Thus, a bioreactor with a combination of bacteria *Rhizobium daejeonense*, *Pseudomonas fluorescens* and *Pseudomonas stutzeri* showed decomposition of 93% of the present fCN (Shin et al., 2020). Another cell system (*Alcaligenes* sp. strain DN25) was immobilized with polyurethane foam and used for cyanide degradation. The effectiveness of the system based on simultaneous adsorption and biodegradation was shown to remove high concentrations of cyanide (up to 1,200 mg/l) in

model solutions. The continuous agitation bioreactor demonstrated an 85% cyanide removal efficiency in 52 days at fCN concentration of 100 - 200 mg/l (Li et al., 2019).

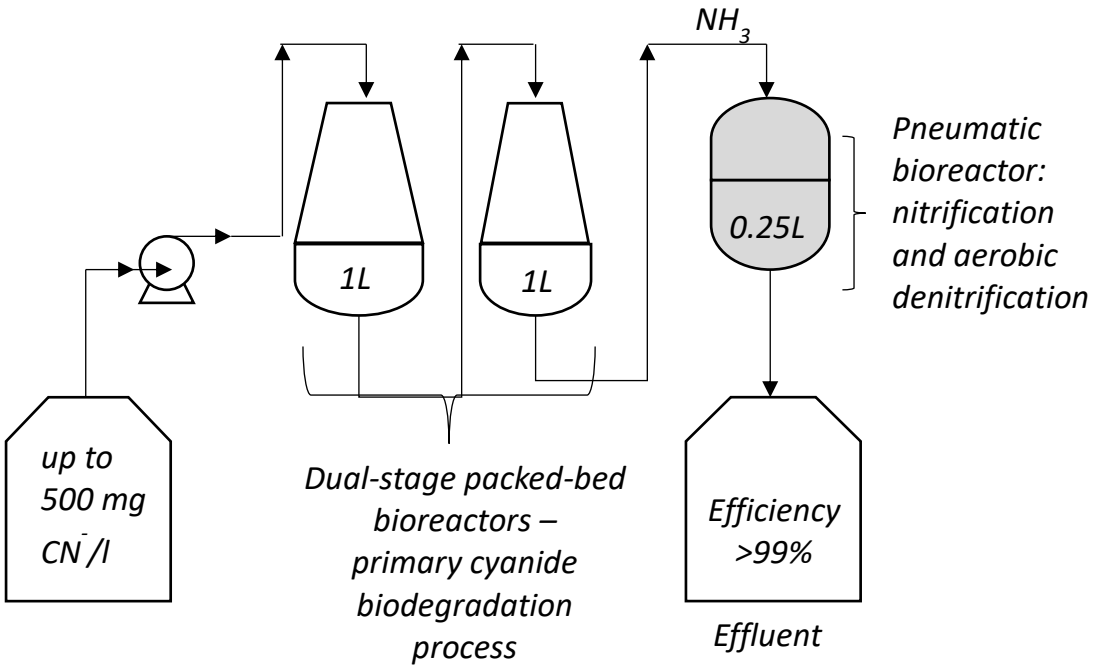

Figure 9. Long-term (80-day) continuous removal of fCN by aerobic microbial cultures (Mekuto et al., 2013).

A mixed consortium of bacterial strains has been used to biodegrade phenol and fCN in coke oven wastewater. The researchers used a two-step treatment consisting of *i*) oxidation and *ii*) biodegradation. The degradation of phenol (1000 mg/l) and fCN (100 mg/l) was 99% and 100%, respectively (Tyagi et al., 2020).

Another study demonstrated biodegradation of fCN (96%) in gold mining wastewater, and modeled the growth of a biofilm that used cyanide as a source of nitrogen and carbon. In this experiment, a biological reactor with separated compartments was used, in which disks with biofilm were partially immersed in the effluent and rotated (Burneo et al., 2020) (Figure 10).

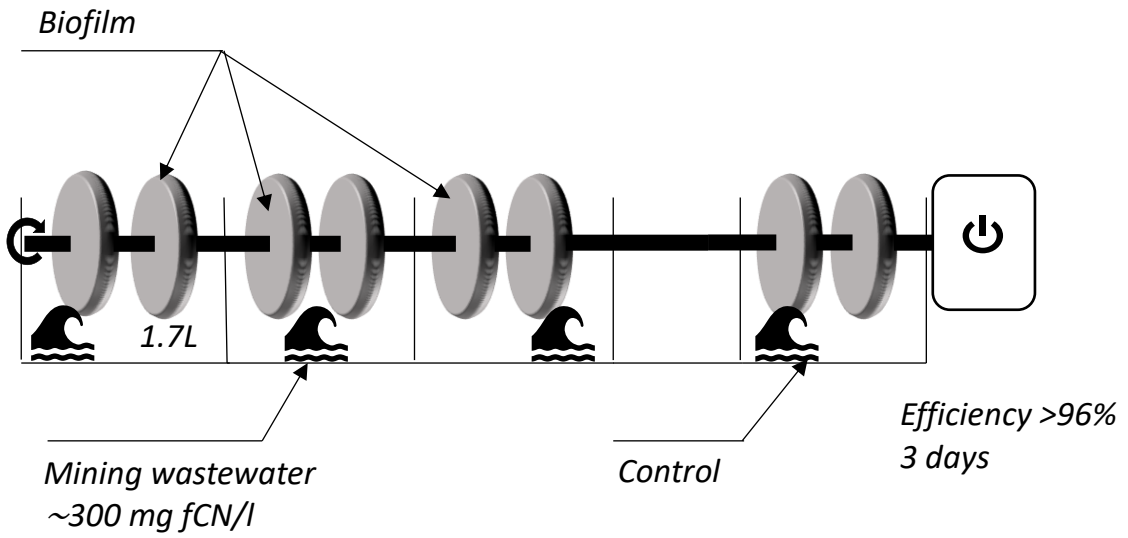

Figure 10. Facility for removal of fCN by microbial biofilm attached to rotating discs (Burneo et al., 2020).

Some bacteria were also effective in the degradation of organic cyanides – nitriles. For example, a bioreactor study (Chen et al., 2010) revealed the efficiency of propionitrile decomposition by immobilized cells of *Klebsiella oxytoca*. In another study, Li et al. (2018) used the recombinant bacterium *B. subtilis* N4/pHTnha-ami, which consisted of biofilms removing acetonitrile, acrylonitrile, and *cis*- and *trans*-crotononitrile. The study by An et al. (2018) revealed an effective treatment of nitrile-containing groundwater (removal of up to 99.8% CN^-) in a fluidized bed reactor based on mixed biofilms.

There are studies devoted to individual strains of cyanide-degrading bacteria, for example, *Pseudomonas pseudoalcaligenes* CECT5344 (Cabello et al., 2018) or *Pseudomonas fluorescens* NCIB 11764 (Fernandez and Kunz 2005). The products of cyanide conversion by the bacterium *P. fluorescens* NCIMB 11764 are CO_2 and ammonia (Figure 11A). The metabolic mechanism for cyanide conversion has been proposed to be mediated by enzymes such as oxidases, hydrolases and carbonic anhydrases, and genes encoding these enzymes have been found in the genome of the *P. fluorescens* strain (Vilo et al., 2012). The *P. pseudoalcaligenes* strain is an isolate obtained from river water. It is able to metabolize fCN

using cyanohydrin as an intermediate, and the cyanohydrin is then hydrolyzed by NLase (Cabello et al., 2018) (Figure 11B). Moreover, new insights into the metabolism of cyanide and cyanate by this strain were reported, such as the structure and function of the cyanate operon (Sáez et al., 2019), the role of small RNAs in the regulation of the strain metabolism (Olaya-Abril et al. 2019, Sáez et al. al., 2019) and the synthesis of metal chelators (Olaya-Abril et al. 2020). Studies on the cyanide degrading ability of this strain were conducted using dilute jewelry factory wastewater that contained approximately 300 mg TCN/l. The biodegradation process, which took place in a 10-liter bioreactor, removed about 95% of TCN (Ibáñez et al., 2017).

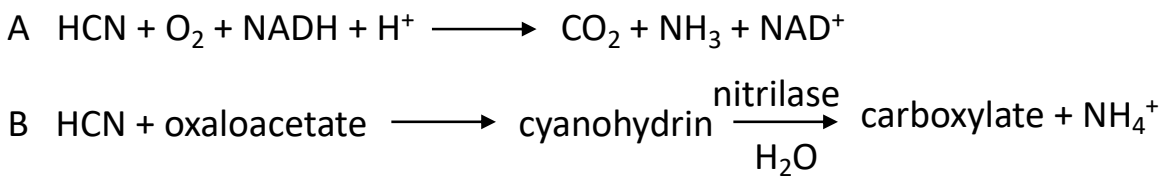

Figure 11. Metabolization of HCN in (A) *Pseudomonas fluorescens* (Fernandez and Kunz, 2005) and (B) *Pseudomonas pseudoalcaligenes* (Cabello et al., 2018).

The "Simultaneous Adsorption and Bioremediation" (SAB) process is a combination of methods for removing contaminants from aqueous solutions. It combines two main processes: adsorption on activated carbon and bacterial treatment. The SAB process can achieve a more effective water treatment than the physicochemical or biological methods alone. It can be particularly useful in cases where the water contains both organic and inorganic contaminants that can be easily removed by adsorption but also requires biological treatment for complete purification. The bacterium *Serratia odorifera* isolated from coking wastewater metabolized phenols in addition to cyanide. Activated carbon served as an adsorbent of fCN and phenols, and the bacteria restored the adsorbent by decomposing the compounds adsorbed. The optimal concentrations of fCN, phenol and activated carbon for the efficiency of this

process were 50 mg/l, 500 mg/l and 30 g/l, respectively. In this way, about 90% of fCN and almost all phenol were removed (Singh et al., 2016).

Phycoremediation is a process that uses microalgae to clean up contaminated aquatic environments. The ability of the autotrophic microalga *Tetraspora sp.* to decompose cyanide, ammonia and phenol has been studied. It has been shown that phycoremediation is effective only at a low cyanide concentration such as 2 mg/l. Microalgae are less resistant to cyanide than bacteria but this method can be applicable to a pre-treated wastewater (Rai et al., 2021).

2.2.4. Emerging enzyme processes

Isolated/purified enzymes, or whole cells that function solely as enzyme carriers (whole-cell catalysts) are probably the least developed tools investigated for cyanide remediation. However, their advantages are unequivocal: e.g., process simplicity, resistance to high concentrations of cyanides (compared with the resistance of growing microbial cultures), or operation at ambient temperatures. In addition, the cyanide-transforming enzymes that belong to the NLase group do not require cofactors. Nevertheless, sensitivity to highly polluted environments containing, e.g., heavy metals, need for sophisticated equipment, or costs of enzyme isolation or purification may be drawbacks.

The studies by Crum et al. (2015, 2016) showed the bioremediation potential of *Bacillus pumilus*. CynD is a good candidate for cyanide biodegradation, but the wild-type enzyme exhibits intolerance to alkaline pH. However, some CynD mutants of *Bacillus pumilus* C1 degraded fCN at pH up to 10 (Wang et al., 2012). Another work showed that agar- and polyacrylamide-immobilized *E. coli* cells overexpressing the *Bacillus pumilus* CynD were effective at pH 10, maintaining their activity at a high level, while cells immobilized on chitosan showed a low efficiency. The suitability of the immobilized cells for the degradation of fCN in wastewater from the gold processing industry was shown (Carmona-Orozco and

Panay, 2019). Therefore, the use of cyanide-degrading NLases is a promising tool for bioremediation of cyanide waste and for a potential use at sites of accidental release of cyanide into the environment (Banerjee et al., 2002; Gupta et al., 2010; Thuku et al., 2009). The origin, occurrence, production and biochemical/catalytic properties of the enzymes of interest are discussed below.

Cyanase (EC 4.2.1.104) is an enzyme that catalyzes the reaction of cyanate to carbon dioxide and ammonia (cyanate is the oxidation product of fCN) (Figure 12). Ranjan et al. (2019) demonstrated cyanate removal by cyanase from *Thermomyces lanuginosus*, which was obtained by expressing the gene in *Pichia pastoris*. The enzyme was immobilized on modified (magnetic) "multi-walled carbon nanotubes". The model mixtures contained heavy metals (Pb, Fe, Cu and Cr) in addition to cyanate (168 mg/l) (Ranjan et al., 2019). The aforementioned *P. pseudoalcaligenes* strain also contains cyanase and has been shown to be useful in removing cyanate produced by a prior chemical oxidation of cyanide (Sáez et al., 2019).

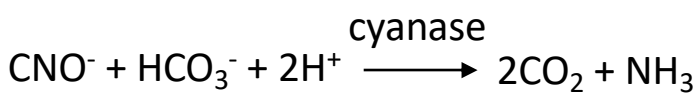

Figure 12. Reaction catalyzed by cyanase.

Rhodanese (thiosulfate sulfurtransferase, EC 2.8.1.1) catalyzes the reaction of HCN with thiosulfate to form thiocyanate (much less toxic than cyanide) and sulfite (Figure 13). It is the oldest of the cyanide-converting enzymes, known since 1933. It is common in all kingdoms of life. Its localization varies depending on the organism: rhodanese occurs in mitochondria (mammals, plants), chloroplasts (plants) or cytoplasm (plants, microbes). In mammals, its localization depends on the respective organism. In humans, activity is the highest in the kidneys, but it is also found in the liver and to a lesser extent in other organs. Disfunction of rhodanese is associated with various diseases (diabetes, colon diseases

including cancer, etc.). A number of papers also dealt with the biotechnological use of the enzymes (Buonvino et al., 2022). Bacteria and fungi are readily available sources of rhodanese for the remediation of cyanide waste. The enzyme could also serve as a therapeutic agent against cyanide intoxication.

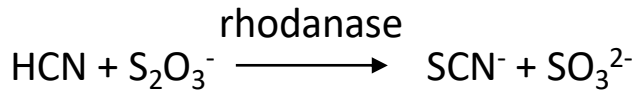

Figure 13. Reaction catalyzed by rhodanase.

2.3. Nitrilases in cyanide metabolism

Branch 1 of the NLase superfamily includes NLases that catalyze the hydrolysis of various nitriles but also HCN to the corresponding amides and acids. According to their activities, the enzymes acting on HCN belong to two different groups: CynD (EC 3.5.5.1, i.e., the same as NLase) belonging to the 3rd class – hydrolases, and CynH (EC 4.2.1.66), belonging to the 4th class - lyases. However, this classification is formal, and the enzymes are related, both having the Glu-Cys-Lys triad which is also common for all proteins of the NLase superfamily. The amino acid identities between CynH and CynD are only 25-30% (Benedik and Sewell, 2018). The CynD activity yields formic acid as the product of cyanide degradation, while the CynH activity yields formamide. Similarly, the hydrolysis of nitriles by NLases (EC 3.5.5.1) can proceed in two ways: hydrolysis of nitriles to ammonia and the corresponding carboxylic acid, or to the corresponding amides (Figure 14). Since NLases are capable of producing amide as a reaction product, it is important not to confuse them with nitrile hydratases (NHases; EC 4.2.1.84), metalloenzymes, that also yield amide as the reaction product from nitrile. NHase is not a member of the NLase superfamily.

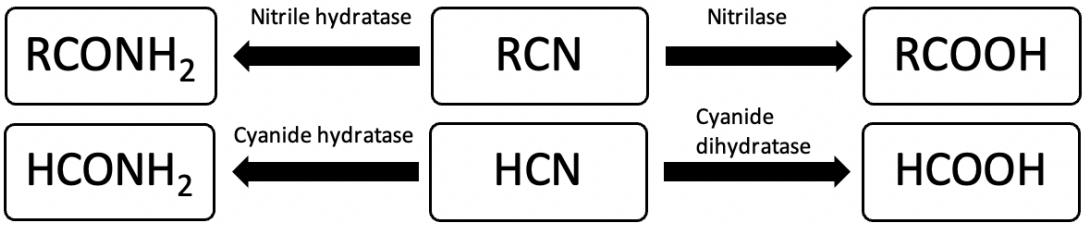

Figure 14. Pathways of the enzymatic conversion of cyanides and nitriles.

The mechanism of the conversion of cyanide catalyzed by the CynD and CynH enzymes can be represented by the scheme in Figure 15. The basic mechanism of NLase activity during cyanide transformation can be described as follows: the attack of the conserved NLase cysteine residue on the carbon atom of the cyanide in the presence of a water molecule results in the formation of a tetrahedral intermediate, and finally the acyl enzyme and NH_3. The following step is the hydrolysis of the acyl enzyme by another water molecule to yield a carboxylic acid and free enzyme. The formation of amide results from an alternative route. This includes a C-S bond cleavage in the tetrahedral intermediate (Jandhyala et al., 2005).

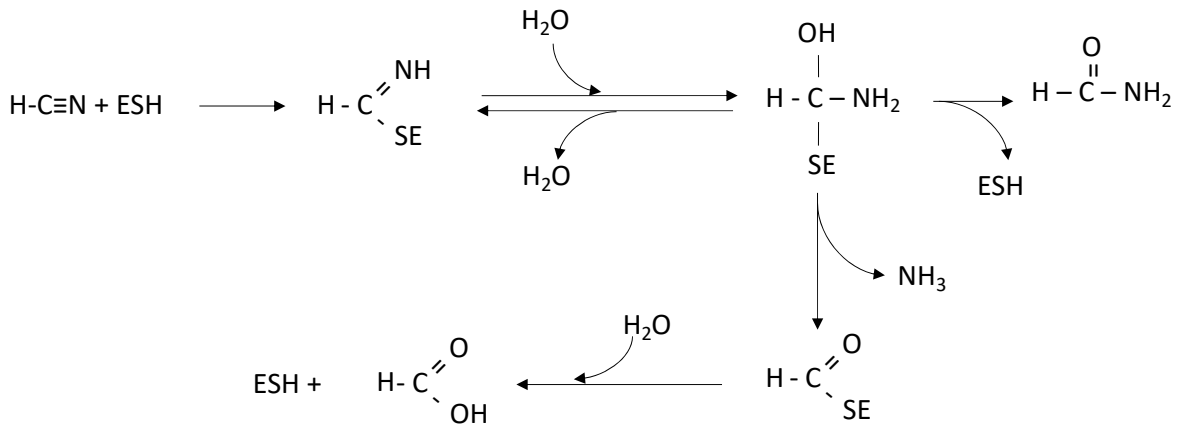

Figure 15. Nitrilase catalytic mechanism (E = enzyme).

2.3.1. Cyanide hydratase

CynH catalyzes the hydration of cyanide to formamide as the single reaction product (Basile et al., 2008) (Figure 14). The molecular weight of the subunit of all CynHs is about 40 kDa (Nolan et al., 2003). It is widely accepted that CynHs are fungal enzymes, although a report on a bacterial CynH from *Serratia marcescens* was published (Kushwaha et al., 2018). The paper described the structural analysis and computational modeling of this enzyme. The catalytic triad was Cys-Lys-Glu characteristic of the NLase superfamily. However, the evidence for the presence of CynH in this organism is indirect. This was based on finding formamide as a reaction product of the whole cells along with a NLase superfamily protein sequence in the genome of this organism.

Extensive data about the cyanide metabolism via CynH are available (Rinágelová et al., 2014). Enzymes of this type have been found in many fungi, particularly in the phylum Ascomycota.

The first CynH was discovered in *Stemphylium loti*, a fungus that parasitizes on the cyanogenic plant birdsfoot trefoil (*Lotus corniculatus L.*) (Fry and Millar, 1972). Later, CynHs were also characterized in other plant-parasitic fungi: *Gloeocercospora sorghi, Fusarium solani, Fusarium lateritium* and *Leptosphaeria maculans* (O'Reilly and Turner, 2003).

Several authors characterized CynHs obtained by genetic engineering technologies, since wild-type fungal strains with satisfactory CynH activities (*Fusarium oxysporum, G. sorghi*) are rare. *E. coli* is suitable as a heterologous host for the overproduction of these eukaryotic enzymes (Basile et al., 2008; Martínková et al., 2015). In this way, several CynHs were obtained by expressing the *cynH* genes from *Gibberella zeae, Aspergillus nidulans, Neurospora crassa, Gloeocercospora sorghi* (Basile et al., 2008), *Aspergillus niger* (Kaplan et al., 2013; Rinágelová et al., 2014), *Penicillium chrysogenum* (Kaplan et al., 2013), *Botryotinia fuckeliana*, and *Pyrenophora teres* (Veselá et al., 2016).

Even though the main natural function of the enzyme is probably to catalyze the conversion of cyanide to formamide (Benedik and Sewell, 2018), these enzymes have been also shown to transform nitriles. However, the relative activity for nitriles is very low compared to that for cyanide (Martínková et al., 2015). CynH from *F. lateritium* has a low NLase activity with benzonitrile, propionitrile and acetonitrile (Nolan et. al., 2003). Some nitriles, such as 2-cyanopyridine (2CP) and fumaronitrile (FN), have been shown to be degraded by CynH from *A. niger* (Kaplan et al., 2013; Rinágelová et al., 2014). The V_{max} for HCN is much higher than for FN or 2CP (Rinágelová et al., 2014). These two nitriles seem to be common substrates of CynHs, as they are also accepted by CynHs from *P. chrysogenum* (Kaplan et al., 2013), *B. fuckeliana*, or *P. teres* (Veselá et al., 2016).

Since the product of HCN conversion catalyzed by CynH is the corresponding amide, we can speak of a NHase reaction rather than a NLase reaction (O'Reilly and Turner, 2003). However, it is worth mentioning that cyanide metabolism is different *in vivo* due to cellular amidases, which can convert formamide to formate and ammonia. Thus, fungal cultures may produce a carboxylic acid product, while purified CynH does not (Benedik and Sewell, 2018).

2.3.2. Cyanide dihydratase

CynD catalyzes the conversion of cyanide into ammonia and formate and occurs probably in bacteria only (Benedik and Sewell, 2018). The first CynDs were discovered and characterized in the bacteria *Alcaligenes xylosoxidans* subsp. *denitrificans* (Ingvorsen et al., 1991), *Bacillus pumilus* C1 (Meyers et al., 1993) and *Pseudomonas stutzeri* AK61 (Watanabe et al., 1998).

The structure of the enzyme is a left-handed helical oligomer consisting of 10 or more subunits. The CynD enzyme from *P. stutzeri* AK 61 ($CynD_{stut}$) has a homooligomeric helical structure and consists of 14 subunits with twofold symmetry (Sewell et al., 2003). In contrast,

Bacillus pumilus C1 CynD consists of 18 subunits and has a peculiar structure that changes depending on pH (Jandhyala et al., 2003). Separate particles (oligomers) are transformed into long rods if pH drops from 8.0 to 5.4. When analyzing engineered mutants of the $CynD_{pum}$ enzyme from *Bacillus pumilus*, mutations were found that affected the oligomer size and enzyme activity. The R67C mutation resulted in a defect in oligomerization. Thus, the study indicates that the corresponding region is responsible for oligomerization and plays an important role in the structure of helical microbial NLases.The following regions were also found to be important for oligomerization of the CynDs: A-surface (conservative interface) between two monomers forming a dimer, and C-surface as the area of interaction of two dimers. Both surfaces are also very important for the activity of the enzyme and its temperature stability (Park et al., 2016).

The C-terminus is an extension that nteracts with both A surface and C surface (Sewell et al., 2003). The C-terminal domain of *Bacillus pumilus* CynD was shown to participate in changing such parameters as enzyme activity, thermal stability and pH tolerance. A hybrid protein $CynD_{pum-stut}$ which included the majority of sequence of $CynD_{pum}$ and the C-terminal part of $CynD_{stut}$ retained 100% activity at pH 9, while the parent $CynD_{pum}$ protein lost activity at pH above pH 8. The thermal stability of the hybrid was also better compared to the parent enzymes (Crum et al., 2015).

Another study compared recombinant forms of CynDs from *Bacillus pumilus* C1 and *Pseudomonas stutzeri*. After cloning their genes, expression in *Escherichia coli*, and purification, the enzymes were studied for their pH stability, thermal stability, and other characteristics. The pH range (pH 5.2 – 8.5), kinetic parameters (K_M 6–7 mM, V_{max} 0.1 mmol min^{-1} mg^{-1}) and tolerance to metals (Fe^{3+}, Cd^{2+}, Zn^{2+}, Hg^{2+}, Cr^{3+}, and Pb^{2+}) of both of the enzymes were similar (Jandhyala et al., 2005).

For the use of these enzymes in the biodegradation of cyanides, it is also possible to modify their catalytic properties by point mutations. Four point mutations in CynDs from *Bacillus pumilus* (K93R, D172N, A202T and E327K) exhibited effects on the properties of the enzyme (kinetics, thermal stability or pH stability). Thus, K93R and D172N mutations improved the stability of the enzyme. The D172N mutation increased the affinity of the enzyme for its substrate at pH 7.7. On the other hand, the A202T mutation had a destabilizing effect on the protein and led to the loss of its activity (Crum et al., 2016).

Recently, *Flavobacterium indicum* MTCC 6936 CynD and its ability to degrade cyanide has been described. At moderate temperatures, the enzyme exhibited a wide pH range (70% of enzyme activity was retained at pH 10). It exhibited thermal stability for 6.5 hours at 30 °C and for 5 hours at 35 °C. The kinetic parameters were K_M of 4.76 mM and V_{max} of 45 U mg^{-1} (Kumar et al., 2018).

2.3.3. Nitrilase NIT4

Type 4 NLase (NIT4) has a narrow substrate specificity for AlaCN, and analogues of this enzyme are widely distributed in the plant kingdom. Analysis of the purified NIT4 enzyme from *Arabidopsis* and *Nicotiana* showed that NIT4 is a distinct sub-branch of NLases that catalyze the hydrolytic reaction of AlaCN to a mixture of L-asparagine (Asn) and L-aspartic acid (Asp) (Piotrowski et al., 2001) (Figure 16). NIT4 has NLase and NHase activity. Both reactions share the same catalytic site.

Analysis of the sequence of "cyanoalanine hydratase" (classified EC 4.2.1.65) from blue lupine (*Lupinus angustifolius*) showed that this enzyme is a homologue of *Arabidopsis thaliana* and *Nicotiana tabacum* NIT4. Thus, plant cyanoalanine hydratase is a NIT4 enzyme. It has been proposed to replace the term cyanoalanine hydratase with the term cyanoalanine NLase or NIT4 (Piotrowski and Volmer, 2006).

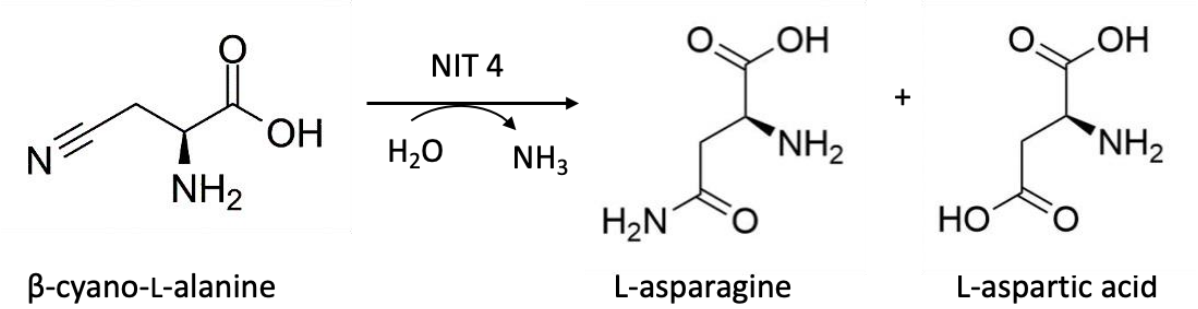

Figure 16. Transformation of β-cyano-L-alanine by nitrilase NIT4.

The NIT4 isoform of *A. thaliana* NLase is different from other forms of plant NLases NIT1, NIT2, and NIT3 which are similar to each other. NIT4 homologues were characterized in plants from different families, for example, *Nicotiana tabacum* and *Oryza sativa*. The ability of purified NIT4 protein from *N. tabacum*, *A. thaliana*, and *L. angustifolius* to transform AlaCN into Asp and Asn under *in vitro* conditions was shown (Piotrowski et al., 2001). The two activities of the NIT4 homologues, NHase activity (amide formation) and NLase activity (carboxylic acid plus ammonia formation) can produce different amide/ acid ratios from AlaCN in different plants (Piotrowski, 2008).

Cyanide is a by-product of the last stage of ethylene synthesis in plants (Figure 17). Cyanide is eliminated by a reaction with cysteine; this reaction is catalyzed by β-cyanoalanine synthase (CAS), resulting in the formation of AlaCN and sulfide (Sharma et al., 2019). The function of plant NLases NIT4 is to transform AlaCN to Asn, Asp and ammonia (Piotrowski and Volmer, 2006). Thus, NIT4 takes part in the process of cyanide detoxification in plants. The ability of plants to assimilate cyanide from the external environment is known (Ebbs, 2004). In wheat, under experimental conditions the rate of cyanide uptake was shown to correlate with nitrogen concentration, with nitrogen restriction leading to an increase in the rate (Ebbs et al., 2010). With an increase in exogenous cyanide, there is an increase in CAS activity in wheat (Machingura and Ebbs, 2010), tobacco (Liang, 2003) and rice (Yu et al., 2012). *Arabidopsis* studies have demonstrated that knocking out the gene encoding

mitochondrial CAS reduces CAS activity and increases the concentration of endogenous cyanide in plant roots. In addition, an increase in exogenous cyanide leads to an increase in endogenous cyanide when the gene is turned off (García et al., 2010).

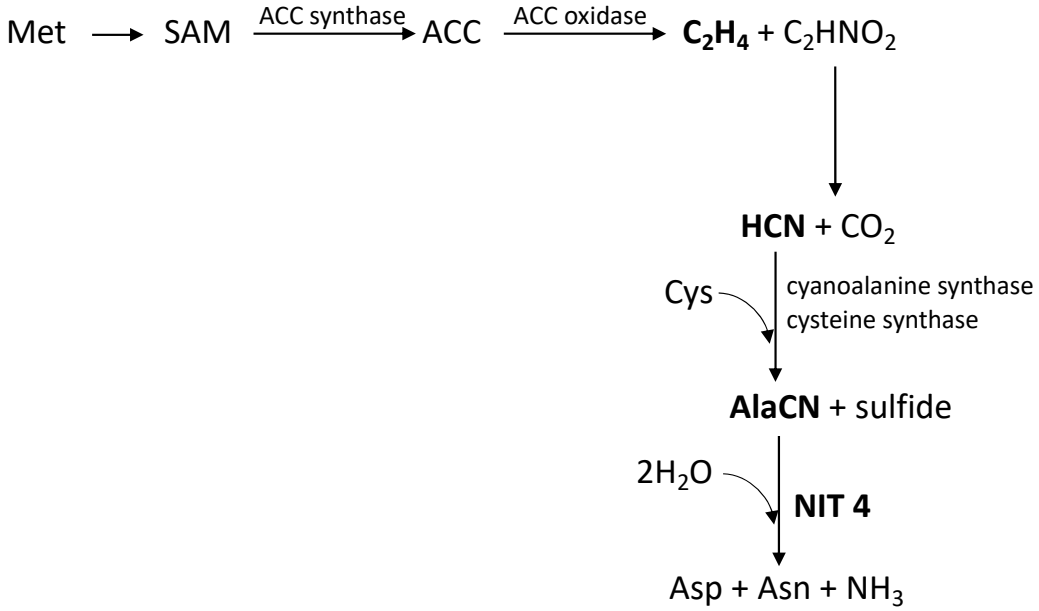

Figure 17. Metabolism of cyanide and synthesis of β-cyano-L-alanine in plants. Met, methionine; SAM, *S*-adenosyl-L-methionine; ACC, L-aminocyclopropane-L-carboxylic acid; Cys, cysteine; AlaCN, β-cyano-L-alanine; Asp, L-aspartic acid; Asn, L-asparagine.

The origin of endogenous cyanide in plants, in addition to its formation as a byproduct in the biosynthesis of the hormone ethylene, can be cyanogenic glycosides, which are present in many plant species and protect the plants from herbivores. Hydrolysis of cyanogenic glycosides, induced by injury to plant tissue, leads to the release of cyanide (Gleadow and Møller, 2014). NLases can participate in both primary and secondary metabolism of plants. NLases derived from the NIT4 ancestor are engaged in the endogenous catabolism of secondary metabolic products. The NLase heterocomplex NIT4A/B2 from *Sorghum bicolor* transforms the cyanogenic glycoside dhurrin (Figure 18) without cyanide release. Dhurrin can be metabolized in plants in two ways: through the intermediate decomposition product -

p-hydroxymandelonitrile, which then turns into *p*-hydroxybenzaldehyde and fCN, or through an intermediate product - *p*-hydroxyphenylacetonitrile - to hydroxyphenylacetic acid and ammonia. The second way proceeds without cyanide release (Figure 19) (Jenrich et al., 2007).

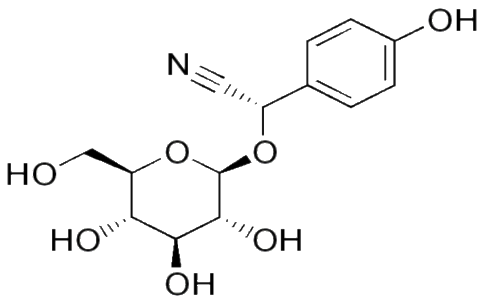

Figure 18. Cyanogenic glycoside dhurrin.

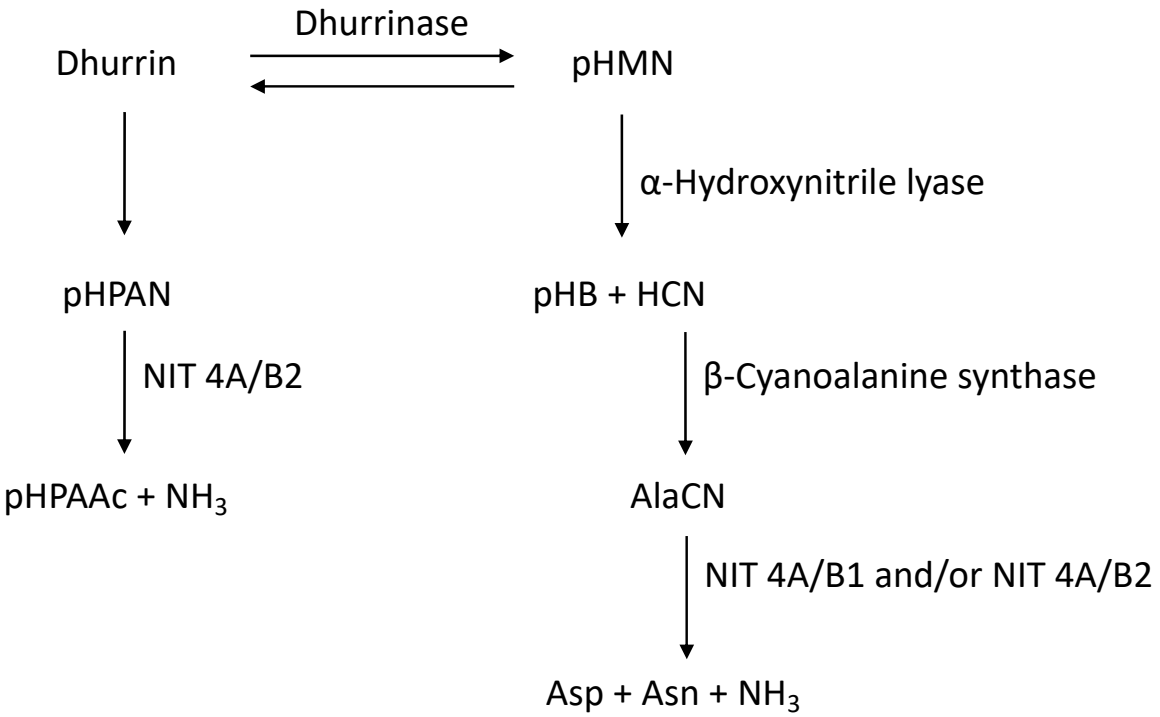

Figure 19. Scheme of dhurrin turnover pathways. pHPAN - *p*-hydroxyphenylacetonitrile; pHPAAc - *p*-hydroxyphenylacetic acid; pHMN - *p*-hydroxymandelonitrile; pHB - *p*-hydroxybenzaldehyde; AlaCN - β-cyano-L-alanine; Asp - L-aspartic acid; Asn - L-asparagine.

The specificity of plant NLase NIT4 from *Arabidopsis thaliana* depends on the helical turn of the enzyme. If this turn is changed by site-directed mutagenesis, the specificity of the mutant changes (Mulelu et al., 2019).

Plant NLases perform versatile functions and take part in the following processes: cyanide detoxification, which is probably their main function in plants, but also nitrogen restoration and recycling, catabolism of cyanogenic glycosides, and auxin biosynthesis. The importance of NLases for plants is supported by the fact that NIT4 homologues are ancient in higher plants, and the corresponding gene has been conserved during evolution (Piotrowski, 2008).

According to database searches, fungi and bacteria also contain a lot of NLases that are homologues of plant NLase NIT4 and can participate in cyanide degradation via AlaCN (Rucká et al., 2020). Hundreds of NIT4-like sequences have been published in bacteria. However, only few bacterial NIT4 enzymes were characterized. They were, e.g., the NIT4 of *Pseudomonas fluorescens* (Howden et al., 2009) and *Sinorhizobium fredii* (Veselá et al., 2016). In Basidiomycota fungi, subdivision Agaricomycotina, close homologues of NIT4 are encoded in *Dichomitus squalens*, *Trametes sp*., *Armillaria sp*., *Agaricus bisporus*, and many others (Rucká et al., 2019).

3. Methods

3.1. Genes and strains of microorganisms

The genes encoding putative NLases XP_006462086.1 (protein NitAb) and XP_008032838.1 (protein NitTv1), and putative CynHs XP_007307917.1 (protein NitSh) and KZV92691.1 (protein NitEg) were retrieved from the GenBank, based on homology searches. They were synthetically produced, per order, by GeneArt (part of ThermoFisher Scientific), Regensburg, Germany, according to nucleotide sequences optimized using the company´s original algorithm, i.e., the codons preferred by *Escherichia coli* were selected to allow for an efficient gene expression in this host (Figure 20). The software for gene design is available at https://www.thermofisher.com/cz/en/home/life-science/cloning/gene-synthesis/geneoptimizer.html.

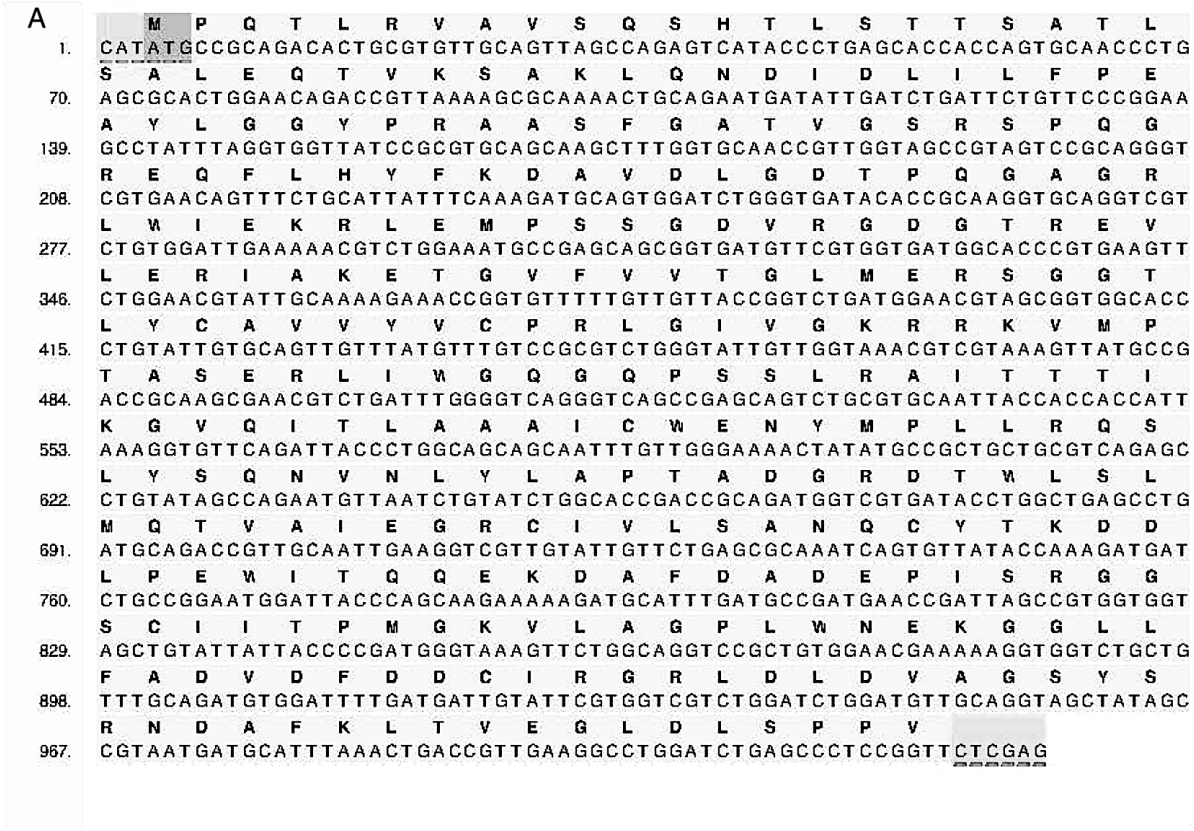

B

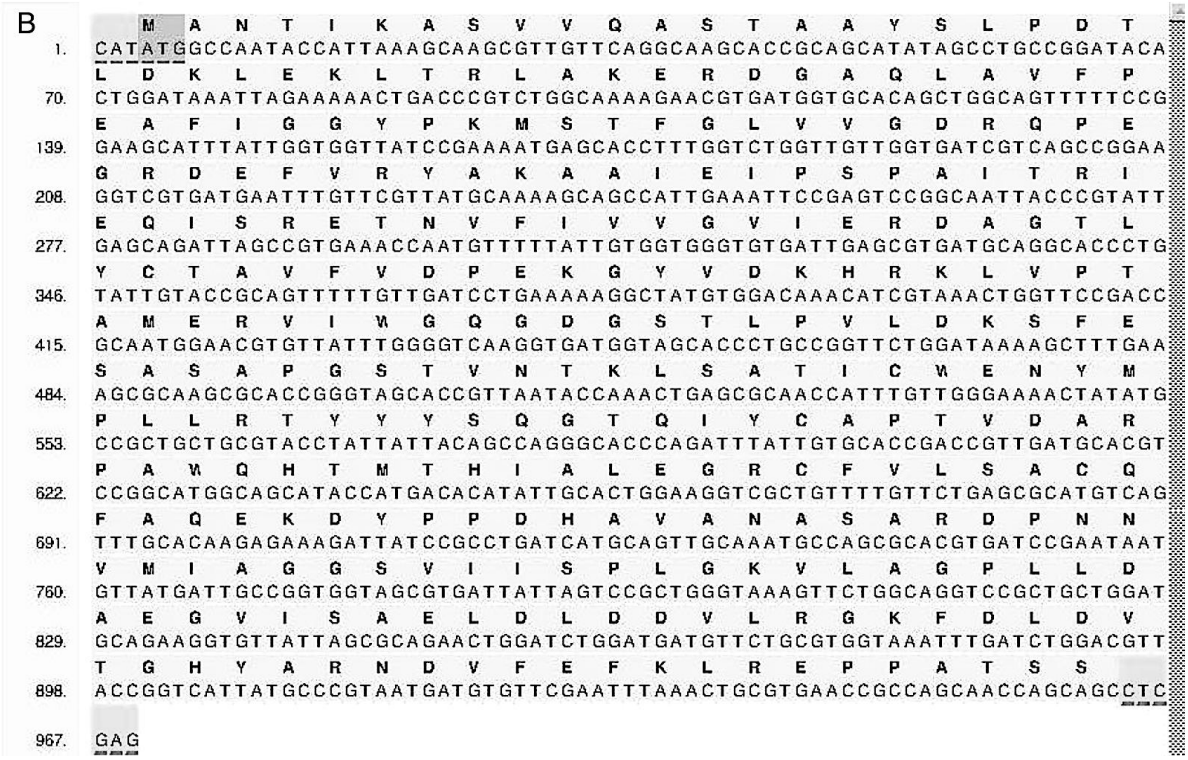
M A N T I K A S V V Q A S T A A Y S L P D T
1. CATATGGCCAATACCATTAAAGCAAGCGTTGTTCAGGCAAGCACCGCAGCATATAGCCTGCCGGATACA
L D K L E K L T R L A K E R D G A Q L A V F P
70. CTGGATAAATTAGAAAAACTGACCCGTCTGGCAAAAGAACGTGATGGTGCACAGCTGGCAGTTTTTCCG
E A F I G G Y P K M S T F G L V V G D R Q P E
139. GAAGCATTTATTGGTGGTTATCCGAAAATGAGCACCTTTGGTCTGGTTGTTGGTGATCGTCAGCCGGAA
G R D E F V R Y A K A A I E I P S P A I T R I
208. GGTCGTGATGAATTTGTTCGTTATGCAAAAGCAGCCATTGAAATTCCGAGTCCGGCAATTACCCGTATT
E Q I S R E T N V F I V V G V I E R D A G T L
277. GAGCAGATTAGCCGTGAAACCAATGTTTTTATTGTGGTGGGTGTGATTGAGCGTGATGCAGGCACCCTG
Y C T A V F V D P E K G Y V D K H R K L V P T
346. TATTGTACCGCAGTTTTTGTTGATCCTGAAAAAGGCTATGTGGACAAACATCGTAAACTGGTTCCGACC
A M E R V I W G Q G D G S T L P V L D K S F E
415. GCAATGGAACGTGTTATTTGGGGTCAAGGTGATGGTAGCACCCTGCCGGTTCTGGATAAAAGCTTTGAA
S A S A P G S T V N T K L S A T I C W E N Y M
484. AGCGCAAGCGCACCGGGTAGCACCGTTAATACCAAACTGAGCGCAACCATTTGTTGGGAAAACTATATG
P L L R T Y Y Y S Q G T Q I Y C A P T V D A R
553. CCGCTGCTGCGTACCTATTATTACAGCCAGGGCACCCAGATTTATTGTGCACCGACCGTTGATGCACGT
P A W Q H T M T H I A L E G R C F V L S A C Q
622. CCGGCATGGCAGCATACCATGACACATATTGCACTGGAAGGTCGCTGTTTTGTTCTGAGCGCATGTCAG
F A Q E K D Y P P D H A V A N A S A R D P N N
691. TTTGCACAAGAGAAAGATTATCCGCCTGATCATGCAGTTGCAAATGCCAGCGCACGTGATCCGAATAAT
V M I A G G S V I I S P L G K V L A G P L L D
760. GTTATGATTGCCGGTGGTAGCGTGATTATTAGTCCGCTGGGTAAAGTTCTGGCAGGTCCGCTGCTGGAT
A E G V I S A E L D L D D V L R G K F D L D V
829. GCAGAAGGTGTTATTAGCGCAGAACTGGATCTGGATGATGTTCTGCGTGGTAAATTTGATCTGGACGTT
T G H Y A R N D V F E F K L R E P P A T S S
898. ACCGGTCATTATGCCCGTAATGATGTGTTCGAATTTAAACTGCGTGAACCGCCAGCAACCAGCAGCCTC
967. GAG

C

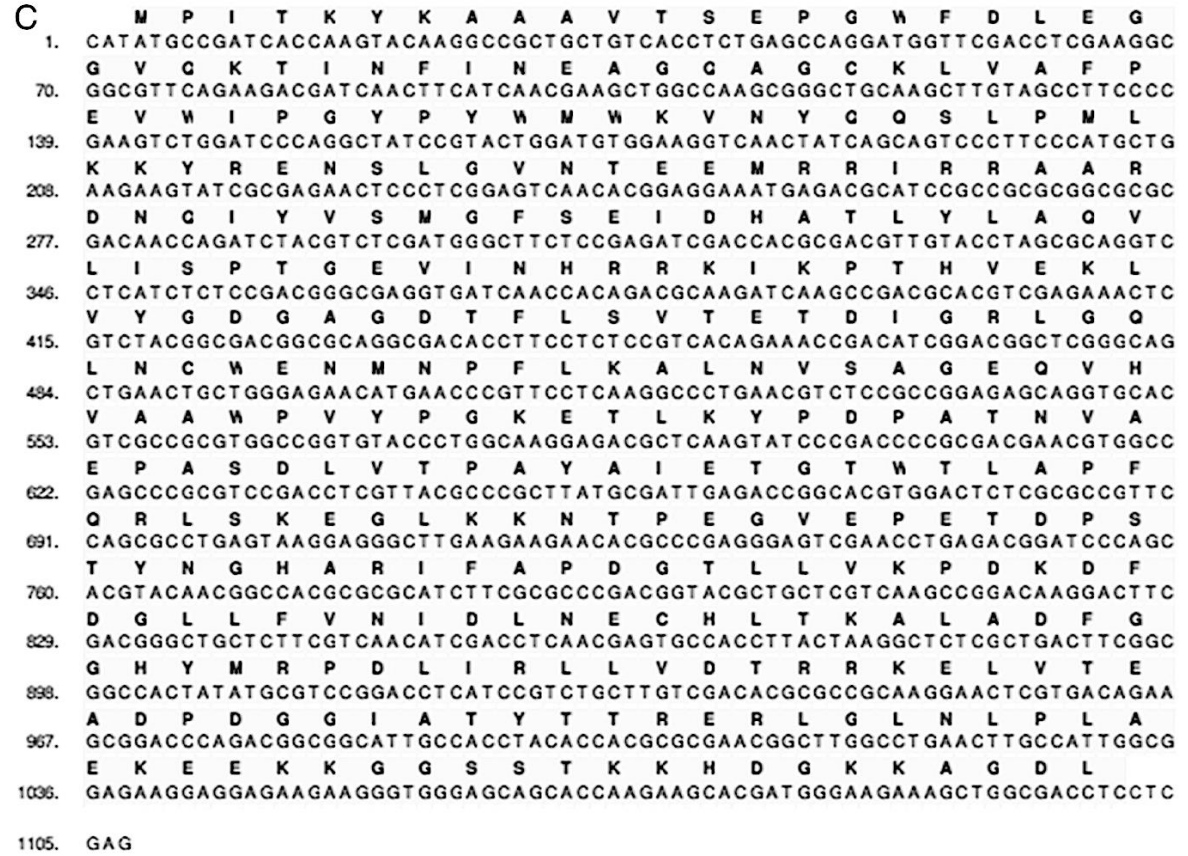
M P I T K Y K A A A V T S E P G W F D L E G
1. CATATGCCGATCACCAAGTACAAGGCCGCTGCTGTCACCTCTGAGCCAGGATGGTTCGACCTCGAAGGC
G V C K T I N F I N E A G C A G C K L V A F P
70. GGCGTTCAGAAGACGATCAACTTCATCAACGAAGCTGGCCAAGCGGGCTGCAAGCTTGTAGCCTTCCCC
E V W I P G Y P Y W M W K V N Y G Q S L P M L
139. GAAGTCTGGATCCCAGGCTATCCGTACTGGATGTGGAAGGTCAACTATCAGCAGTCCCTTCCCATGCTG
K K Y R E N S L G V N T E E M R R I R R A A R
208. AAGAAGTATCGCGAGAACTCCCTCGGAGTCAACACGGAGGAAATGAGACGCATCCGCCGCGCGGCGCGC
D N C I Y V S M G F S E I D H A T L Y L A Q V
277. GACAACCAGATCTACGTCTCGATGGGCTTCTCCGAGATCGACCACGCGACGTTGTACCTAGCGCAGGTC
L I S P T G E V I N H R R K I K P T H V E K L
346. CTCATCTCTCCGACGGGCGAGGTGATCAACCACAGACGCAAGATCAAGCCGACGCACGTCGAGAAACTC
V Y G D G A G D T F L S V T E T D I G R L G Q
415. GTCTACGGCGACGGCGCAGGCGACACCTTCCTCTCCGTCACAGAAACCGACATCGGACGGCTCGGGCAG
L N C W E N M N P F L K A L N V S A G E Q V H
484. CTGAACTGCTGGGAGAACATGAACCCGTTCCTCAAGGCCCTGAACGTCTCCGCCGGAGAGCAGGTGCAC
V A A W P V Y P G K E T L K Y P D P A T N V A
553. GTCGCCGCGTGGCCGGTGTACCCTGGCAAGGAGACGCTCAAGTATCCCGACCCCGCGACGAACGTGGCC
E P A S D L V T P A Y A I E T G T W T L A P F
622. GAGCCCGCGTCCGACCTCGTTACGCCCGCTTATGCGATTGAGACCGGCACGTGGACTCTCGCGCCGTTC
Q R L S K E G L K K N T P E G V E P E T D P S
691. CAGCGCCTGAGTAAGGAGGGCTTGAAGAAGAACACGCCCGAGGGAGTCGAACCTGAGACGGATCCCAGC
T Y N G H A R I F A P D G T L L V K P D K D F
760. ACGTACAACGGCCACGCGCGCATCTTCGCGCCCGACGGTACGCTGCTCGTCAAGCCGGACAAGGACTTC
D G L L F V N I D L N E C H L T K A L A D F G
829. GACGGGCTGCTCTTCGTCAACATCGACCTCAACGAGTGCCACCTTACTAAGGCTCTCGCTGACTTCGGC
G H Y M R P D L I R L L V D T R R K E L V T E
898. GGCCACTATATGCGTCCGGACCTCATCCGTCTGCTTGTCGACACGCGCCGCAAGGAACTCGTGACAGAA
A D P D G G I A T Y T T R E R L G L N L P L A
967. GCGGACCCAGACGGCGGCATTGCCACCTACACCACGCGCGAACGGCTTGGCCTGAACTTGCCATTGGCG
E K E E K K G G S S T K K H D G K K A G D L
1036. GAGAAGGAGGAGAAGAAGGGTGGGAGCAGCACCAAGAAGCACGATGGGAAGAAAGCTGGCGACCTCCTC
1105. GAG

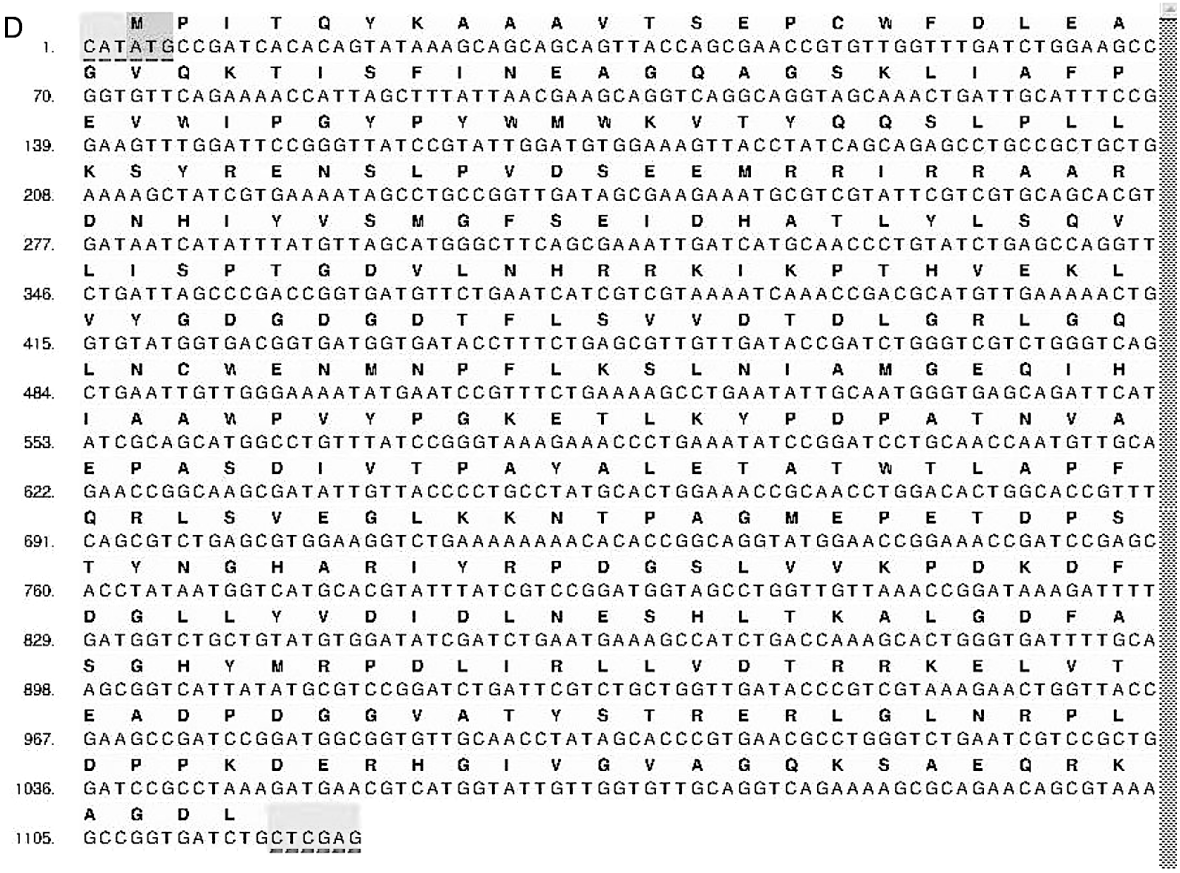

Figure 20. Optimized sequences of genes encoding nitrilases (A) NitAb and (B) NitTv1, and cyanide hydratases (C) NitEg and NitSh (D). Restriction sites *NdeI* and *XhoI* are underlined.

3.2. Overproduction and purification of enzymes

The genes were ligated between restriction sites *NdeI* and *XhoI* in the vector pET22b(+), which allowed to translate the genes into proteins with a C-terminal His_6-tag. The recombinant plasmids were used to transform competent *E. coli* Origami B (DE3) (Novagen) cells. The strains were prepared by Lenka Rucká, PhD. (Laboratory of Modulation of Gene Expression, Institute of Microbiology of the Czech academy of Sciences (IMIC), Prague). The 2xYT medium containing 16 g tryptone (ThermoFisher Scientific), 10 g yeast extract (ThermoFisher Scientific), 5 g NaCl, total volume 1 L, was used for cultivation of the transformed cells at 37 °C. Optical density at 600 nm (OD_{600}) was monitored using spectrophotometer UVmini-1240 (Shimadzu). To induce gene overexpression, 0.02 mM IPTG was added after OD_{600} achieved 1.0. The cultivation was continued for 20 h. The cell-free

extract (CFE) was prepared by sonication using sonicator Bandelin Sonopuls HD2200. Protein purification from the CFE was performed by immobilized metal affinity chromatography (IMAC) on TALON® Metal Affinity Resin (Clontech Laboratories, Inc.) with Co^{2+} as the metal ion. The methodology is summarized in Figure 21.

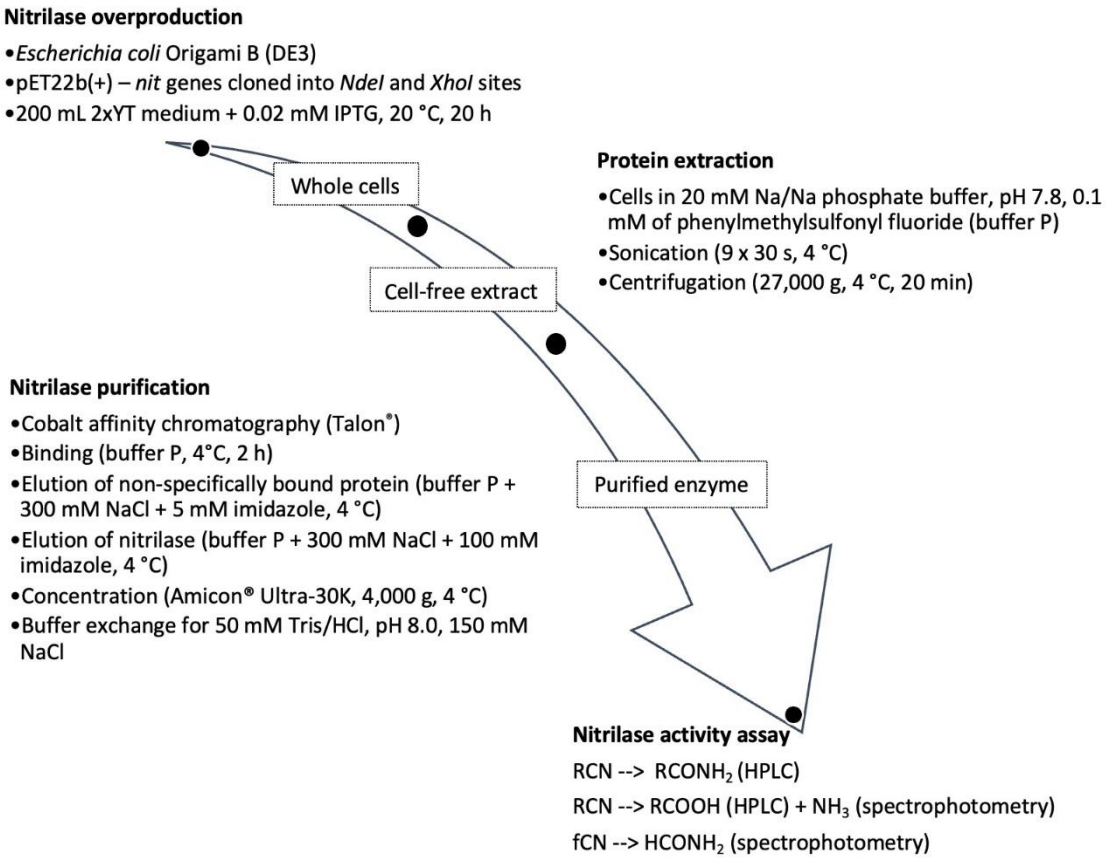

Figure 21. Scheme of the enzyme preparation protocol.

3.3. Enzyme Assays

3.3.1. Nitrilase NIT 4 assays

NIT4 activity assays were carried out in 1.5 ml Eppendorf tubes at 30 ºC under shaking (850 rpm) using Eppendorf ThermoMixer Comfort (Eppendorf). The total volume of the reaction mixture was 0.5 ml. Stock solutions of substrates (500 mM) were prepared in 200 mM buffer, pH 8.0, for 2CP, 3-cyanopyridine (3CP) and 4-cyanopyridine (4CP), and in

methanol for other nitriles (Table 3). The reaction mixture contained 0.025 ml of the stock solution of substrate (final concentration of 25 mM) in 50 mM Tris/HCl, pH 8.0, supplemented with 150 mM NaCl. After preincubation (5 min, 30 ºC), the reaction was initiated by adding an appropriate amount of the enzyme. After an appropriate interval, the reaction was stopped by adding 0.05 ml of 2 M HCl and the mixture was centrifuged (12 000 rpm, 2 min).

The reaction products formed from nitriles were analyzed by High-Performance Liquid Chromatography (HPLC); the nitrile, carboxylic acid, and amide were indentified by comparing retention times and UV spectra of products with those of authentic standards. The reaction product originated from AlaCN, ammonia, was determined spectrophotometrically (Brunner et al., 2018). Optionally, the reaction mixture was supplemented with asparaginase from *E. coli* (Sigma-Aldrich; 4 U) to convert Asn to Asp and ammonia.

The kinetic properties of the enzymes were determined analogously using 2.5 - 25 mM AlaCN. V_{max} and K_M were calculated using MyCurveFit program (https://mycurvefit.com).

To determine the temperature and pH stability of the enzymes, as well as to determine their pH and temperature optima, cinnamonitrile (CiN) was used as a substrate. Accordingly, the enzyme activity was calculated from the concentrations of cinnamic acid and cinnamamide. The following changes were made to the standard analysis: reactions were performed at temperatures from 20 to 50 °C to determine the temperature optima. The pH optima were determined using Britton–Robinson (B-R) buffers in the pH range of 4.0–11.2. B-R buffers consisted of solutions A (phosphoric acid, acetic acid, and boric acid, 40 mM each) and B (0.2 M NaOH) in different proportions.

Temperature stability was determined by pre-incubating the enzymes at different temperatures for 2 hours under shaking (850 rpm), followed by the determination of the residual activity. For activity determination, the reaction mixtures were brought to standard temperature (incubation for 10 min, 30 °C). Analogously, pH stability was determined by

incubating the enzymes for 2 hours at different pH values and standard temperature. The reactions were carried out under standard conditions; a 3-fold volume of 250 mM Tris/HCl buffer, pH 8.0, was added to adjust pH. Details of the reaction conditions are given in Table 3.

Table 3. NIT4 nitrilase assays – method details

<table>
<tr><th></th><th>Substrate (mM)</th><th>Reaction conditions</th><th>Compound determined</th><th>Analysis</th></tr>
<tr><td>Standard assay</td><td>AlaCN (25)</td><td rowspan="3">pH 8.0 [b], 30 °C, 5-10 min</td><td rowspan="2">Ammonia</td><td rowspan="2">Photometry (3.4.3)</td></tr>
<tr><td>Kinetics</td><td>AlaCN (2.5–25)</td></tr>
<tr><td>Relative activity</td><td>Aryl(aliphatic) nitriles (25) [a]</td><td>Acid, amide</td><td>HPLC (3.4.1)</td></tr>
<tr><td>Temperature optimum</td><td rowspan="4">CiN (25)</td><td>pH 8.0 [b], 20–50 °C, 5-10 min</td><td rowspan="4">Acid, amide</td><td rowspan="4">HPLC (3.4.1)</td></tr>
<tr><td>Temperature stability</td><td>Pre-incubation: pH 8.0 [b], 20-50°C, 2 h; Reaction pH 8.0 [b], 30 °C, 10 min</td></tr>
<tr><td>pH optimum</td><td>pH 4.0-11.2 [c], 30 °C, 10 min</td></tr>
<tr><td>pH stability</td><td>Pre-incubation: pH 4.0-11.2 [c]; 2 h, 30 °C; Reaction: pH 8.0 [c], 30 °C, 10 min</td></tr>
</table>

Abbreviations: AlaCN – β-cyano-L-alanine, CiN – cinnamonitrile.
[a] Allylcyanide, fumaronitril, indole-3-acetonitrile, phenylacetonitrile, 4-phenylbutyronitrile, 3-phenylpropionitrile, and phenylthioacetonitrile.
[b] 50 mM Tris/HCl buffer, pH 8.0, 150 mM NaCl.
[c] Britton–Robinson buffers.

3.3.2. Cyanide hydratase assays

CynH activity assays were carried out in 1.5 ml Eppendorf tubes at 30 °C under shaking (850 rpm) using an Eppendorf ThermoMixer Comfort (Eppendorf). The total volume of the reaction mixture was 0.5 ml. Stock solutions of KCN (500 mM) were prepared in 200 mM Tris/HCl buffer, pH 9.0. The reaction mixture contained 0.025 ml of the stock solution

of substrate in 50 mM glycine/NaOH buffer, pH 9.0. The reaction was stopped after 1-2 min by adding a two-fold volume of methanol.

Determination of fCN (substrate) or formamide (product) was carried out spectrophotometrically by the picric acid method (Fisher, 1952) and by the hydroxylamine method (Cluness, et al. 1993), respectively. The methods described in these papers were slightly modified (see section 3.4.2. for method details). Spectrophotometric measurements were performed against controls, which were prepared in the same way as the samples, but without KCN.

The amount of enzyme that degrades 1 μmol of fCN per minute or produces 1 μmol of formamide per minute was taken as a unit of CynH activity (conditions ofstandard assay: 30 ºC, pH 9.0). The kinetic properties of the enzyme, its thermostability and pH stability, as well as temperature and pH optima were also investigated. The parameters and conditions of the experiments are given in Table 4. The study of the shelf life of the purified enzyme at 4 ºC was carried out by periodically measuring its specific activity for 98 days.

Experiments using 2CP as a substrate were performed with the following differences from the standard assay: 50 mM Tris/HCl buffer, pH 8.0, with 150 mM NaCl was used, reaction time was 10 min, and 2 M HCl (0.05 ml per 0.5 ml sample) was used to stop the reaction; after centrifugation of the reaction mixture, the supernatants were analyzed by HPLC.

The temperature optimum was determined in the range of 20-50 °C. The optimum pH was determined in the pH range 4.0–10.8 using B-R buffers at 30 °C. To determine the pH stability, the enzyme was incubated in the same buffers for 2 h at 30 °C and then the residual activity was determined at pH 8.0 and 30 °C. The reaction products of the enzyme with 2CP are 2-pyridinecarboxylic acid and 2-pyridinecarboxamide. Their concentrations were determined by reverse phase HPLC (see section 3.4.1).

In the studies of the influence of copper and silver ions on the degradation of cyanide using the enzyme NitEg, the rate of consumption of fCN was monitored by the standard assay but in the presence of metal ions in different concentrations from 0 to 10 mM. Details of the reaction conditions are given in Table 4.

Table 4. Cyanide hydratase assays - method details

	Substrate (mM)	**Reaction conditions**	**Compound determined**	**Analysis**
Standard assay	KCN (25)	pH 9.0 [a], 30 °C, 1-2 min	Residual cyanide, formamide	Photometry (3.4.2)
Kinetics	KCN (2.5–25)			
Thermostability (long-term)	KCN (25)	Pre-incubation: 1-24 h at 27, 37, 43, 50 °C; Reaction: standard assay		
Cyanide conversion	KCN (0.6, 4.6, 25, 100)	pH 9.0-10.5, 30 °C, 5–180 min		
Temperature optimum	2-Cyanopyridine (25)	pH 8.0 [b], 20-50 °C, 10 min	Picolinic acid, picolinamide	HPLC (3.4.1)
Thermostability (short-term)		Pre-incubation: 20-50 °C, 2 h Reaction: pH 8.0 [b], 30 °C, 10 min		
pH optimum		pH 4.0–10.8. 30 °C, 10 min		
pH stability		Pre-incubation: pH 4.0–10.8, 2h, 30 °C, Reaction: pH 8.0 [b], 30 °C, 10 min		

[a] 100 mM glycine/NaOH, pH 9.0-10.5.
[b] 50 mM Tris/HCl buffer, pH 8.0, 150 mM NaCl.

The degree of fCN conversion was studied according to the following protocol: Eppendorf tubes of 2 ml contained reaction mixtures of 1 ml total volume. The mixtures were incubated at 30 °C and shaking (Eppendorf ThermoMixer Comfort, 850 rpm). Buffers were 100 mM glycine/NaOH, pH 9.0, 9.5, 10.0, or 10.5. The simulated wastewater was prepared according to the literature (Jarrah and Mu'azu, 2016; Papadimitriou et al., 2009). The following concentrations of fCN were used: 0.6, 4.6, 25 or 100 mM (added as KCN). Optionally, model compounds were added to the reaction mixtures - Na_2S, KSCN, NH_4Cl, phenol, $CuSO_4$, or $AgNO_3$ (see Table 5 for details). Reactions were also performed in the same buffer with 0.6 mM fCN or 4.6 mM fCN without other additives. Enzyme concentration was 2.5 μg/ml, and 5.0 μg/ml for the reaction with model coke plant effluent and model petrochemical effluent, respectively. Control reactions did not contain the enzyme. The reaction was stopped at various time intervals by taking 0.1 ml of the sample and adding 0.2 ml of methanol to it. Using the picric acid method (see above) or the Spectroquant® kit (Supelco), the residual fCN was determined.

Table 5. Composition of simulated wastewaters

Wastewaters	Pollutant, mM						
	free CN	S^{2-}	SCN^-	NH_4^+	Phenol	$AgNO_3$	$CuSO_4$
Coke oven	0.6	0	8.62	10.7	12.8		
Petrochemical	4.6	23.4	4.61	2,5	0.64		
Electroplating	100					1	1

3.4. Analytical methods

3.4.1. High-Performance Liquid Chromatography (HPLC)

Determination of concentrations of nitriles and their reaction products was performed using HPLC. For 2CP, 3CP, 4CP, and FN, the column used was an ACE C8 (5 μm, 250 mm × 4 mm; Advanced Chromatography Technologies Ltd.). The mobile phase was 10%

acetonitrile/ 5 mM sodium phosphate buffer, pH 7.2, used at a flow rate of 0.9 ml/min. For other nitriles (phenylacetonitrile (PAN), 3-phenylpropionitrile (PPN), allylcyanide, CiN, indole-3-acetonitrile (IAN), phenylthioacetonitrile (PTAN), 2CP) the column used was a Chromolith SpeedRod RP-18 (50 mm × 4.6 mm; Merck KgaA, Darmstadt, Germany). The mobile phase was 20% acetonitrile / 0.1% phosphoric acid used at a flow rate of 2 ml/min.

Calibration for nitriles used as substrates and the corresponding amides and carboxylic acids (if standards were available) was done by measuring peak area for different concentrations of each compound. Areas were read out at local spectrum maximum for each compound. The calibration curves are shown in Appendix A.

3.4.2. Liquid Chromatography – Mass Spectrometry (LC-MS)

The analysis of reaction mixtures was performed using liquid chromatography with tandem mass spectrometry on a Shimadzu Prominence system (Shimadzu Europa GmbH, Duisburg, Germany). The column used was an ACE C8 (5 µm, 250 mm × 4 mm; Advanced Chromatography Technologies Ltd., Aberdeen, UK) or Chromolith RP 18e (100 mm × 3 mm; Merck KgaA, Darmstadt, Germany) and a mobile phase of 10% acetonitrile, and the flow rate was 0.4 ml/min at a column temperature of 34 °C. MS analysis was performed using SCAN mode 50 – 250 *m*/*z* and LabSolutions software version 5.75 SP2. Other parameters of the negative-mode MS measuremets were as follows: ESI interface voltage - 4.5 kV, detector voltage - 1.15 kV, nebulizing gas flow - 1.5 ml/min, drying gas flow - 15 ml/min, heat block temperature - 200 °C, temperature DL - 250 °C. LC-MS measurements were performed and the data were interpreted by Ing. Lucie Petrásková, Ph.D. (Laboratory of Biotransformation, IMIC).

3.4.3. Spectrophotometric methods

The picric acid method was performed as follows: a mixture of the sample (0.01 ml), Tris/HCl buffer, pH 8.0 (0.09 ml), and 0.5% picric acid in 0.25 M Na_2CO_3 (0.2 ml) was incubated for 5 min at 100 °C in the water bath. The reaction mixture was then placed on ice to stop the reaction. Before measuring the optical density, 0.7 ml of distilled water was added, and absorbance was measured at 520 nm. The calibration curve is shown in Appendix B (Figure B.1).

Formamide comcentration was determined as follows: a mixture of the sample (0.2 ml) and 2.3 M hydroxylamine/3.5 M NaOH (1/1) (0.4 ml) was incubated for 10 min at 60 °C. Then 0.2 ml of 4 M HCl and 0.2 ml of 1.23 M $FeCl_3$ were added, and the absorbance was measured at 540 nm. The calibration curve is shown in Appendix B (Figure B.2).

Protein concentration was determined by the Bradford method. The method is based on binding of the protein with Coomassie brilliant blue R-250 dye, which thus changes the absorption maximum from 465 to 595 nm (Bradford, 1976). The enzyme was diluted 20 times in 50 mM Tris/HCl buffer, pH 8.0, with 150 mM NaCl. The resulting enzyme solution (20 µl) was added to a cuvette containing 1 ml of Bradford solution and mixed. After 5 min the spectrophotometric measurement was carried out at a wavelength of 595 nm against a blank sample (1 ml Bradford solution with 20 µl buffer without enzyme).

Ammonia concentration was determined using the *o*-phthaldehyde reagent as described in the literature (Brunner et al., 2018). The total volume of the reaction mixture was 0.9 ml, and the absorbance was measured using spectrophotometer UVmini-1240 (Shimadzu). Semi-microcuvettes contained dimethyl sulfoxide (186 µl) and 132 µl of *o*-phthalaldehyde (OPA) reagent (80 mg OPA dissolved in 400 µl of methanol was added to 40 ml of 15 mM Na-tetraborate, pH 9.25). Aliquots (66 µL) taken from the reaction mixtures were added, followed by 66 µL of 10% (*v*/*v*) trichloroacetic acid. Next, dimethyl sulfoxide (450 µl) was

added, the solutions were vigorously mixed, and the cuvettes were incubated for 10 min at a room temperature. Finally, the absorbance at 675 nm was measured spectrophotometrically. Calibration curves were generated using defined concentrations of NH_4Cl (1–15 mM). The calibration curve is shown in Appendix B (Figure B3).

3.4.4. SDS-PAGE

Electrophoresis was carried out according to Laemmli (1970); a 10% polyacrylamide gel with sodium dodecyl sulfate was used. Samples were incubated at 95 °C for 5 min in sample buffer (Tris/HCl (pH 6.8) 100 mM, dithiothreitol 200 mM, SDS (for electrophoresis) 4% wt., bromophenol blue 0.2% wt., glycerol 20% wt.) and added to the gel in an amount of 5 - 10 µl (protein concentration approximately 0.3 mg/ml). Standards with molecular weights ranging from 14.4–97 kDa (GE Healthcare) were used. The gel was stained with Coomassie brilliant blue R-250.

4. Results

4.1. Nitrilases NIT4

Based on database searches, Basidiomycota genomes were recently shown to contain a large number of genes encoding for potential proteins of the "nitrilase superfamily" (Rucká et al., 2019). Since these enzymes are considered as promising biodegradation tools, the enzymes NitTv1 (sequence XP_008032838.1) and NitAb (sequence XP_006462086.1) from *Trametes versicolor* and *Agaricus bisporus*, respectively, were selected in this thesis as representatives of fungal NIT4 NLase homologues to study their functions and their capability to degrade toxic cyanide.

4.1.1. Analysis of published NIT4 sequences

The sequences of NLases from the division of Basidiomycota previously found by GenBank database analysis (Rucká et al., 2019) were divided into two main clades: 1 - similar to plant NIT4 NLases (up to >50% identities); 2 - similar to putative NLases in *Ascomycota* (up to ca. 50%). The producers of both selected NLases belong to the division *Basidiomycota* (subdivision *Agaricomycotina*). The enzymes studied in this thesis were chosen so that one of them is a representative of clade 1 (more than 50% sequence identity with plant NLases), and the other enzyme is outside clade 1 on the phylogenetic tree (Figure 22).

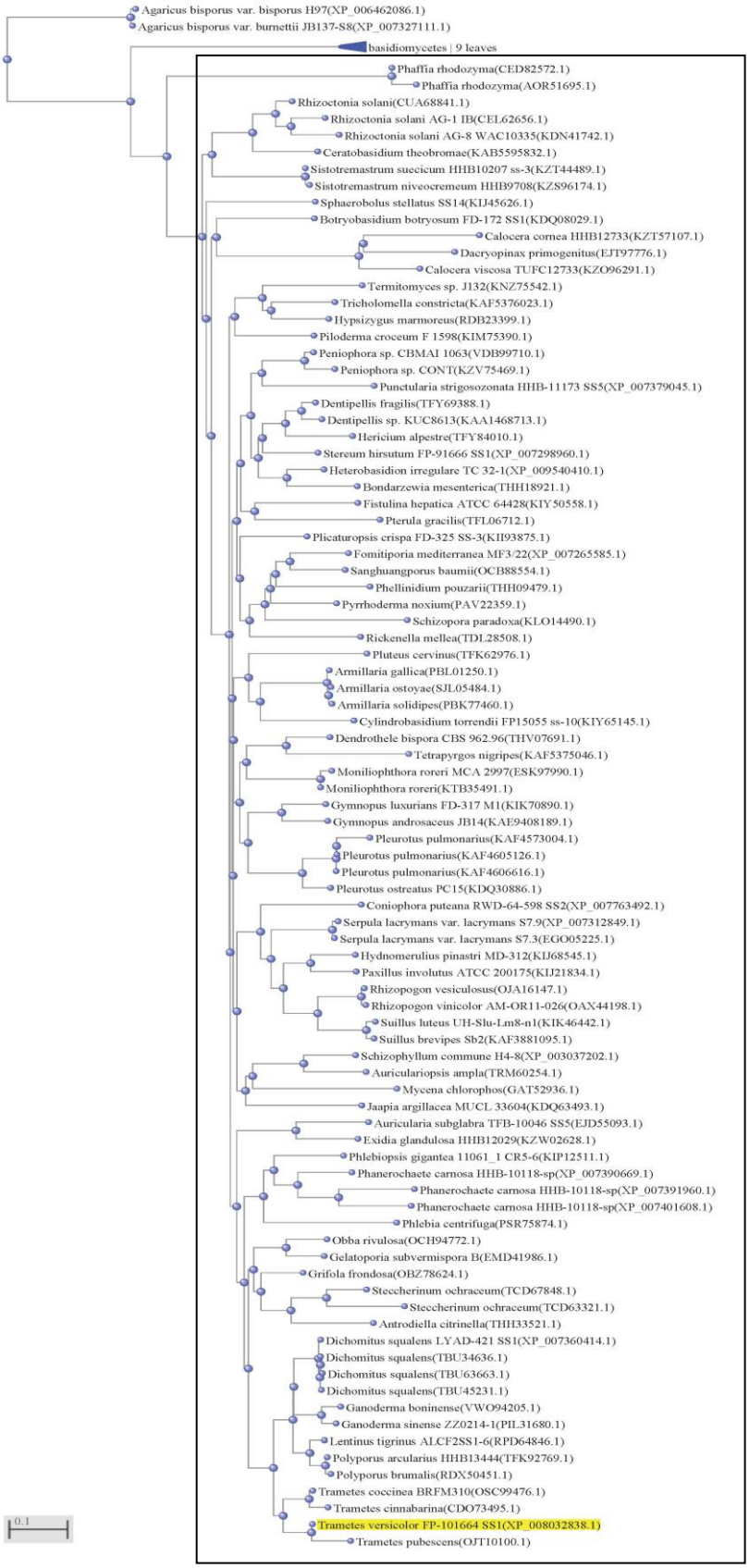

Figure 22. Phylogenetic tree of homologues of plant nitrilases in Basidiomycota (Rucká et al., 2019). Clade 1 in the box; NitTv1 nitrilase (template) highlighted in yellow.

4.1.2. Characterization of fungal nitrilases NitAb and NitTv1

E. coli Origami B (DE3) served as a heterologous host for the overproduction of NLases. The conditions for gene expression were the same as in the previous study (Rucká et al., 2019). After sonicating the cells, the enzymes were purified by IMAC using TALON® resin (Figure 21 in section 3 Methods), affording approximately 9.6 mg and 6.6 mg of protein per 100 ml of culture medium for NitAb and NitTv1, respectively (Figure 23). Each of the NIT4 nitrilases was detected as two protein bands of very similar molecular weights. Mass spectrometry did not show any difference between the two bands in either enzyme. These phenomena are apparently caused by the conditions under which the SDS-PAGE analysis proceeds (e.g., the composition of the sample buffer) and may reflect two different oxidation states of the enzymes.

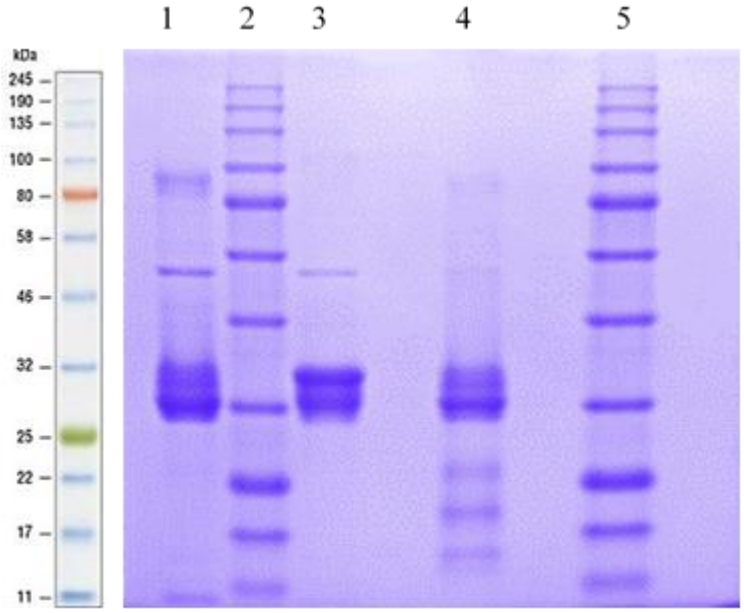

Figure 23. SDS-PAGE of nitrilases NitTv1 and NitAb. Lane 1 – partially purified NitTv1 (lot 1), 1.59 mg/ml, 4 µl; lane 2 – marker; lane 3 – partially purified NitAb, 20.9 mg/ml, 5 times diluted, 2 µl; lane 4 – partially purified NitTv1 (lot 2), 7.23 mg/ml, 1 µl; lane 5 – marker.

Both enzymes were investigated for their catalytic properties (Table 6). The specific activities for 25 mM substrates (AlaCN, PPN) and kinetic parameters for AlaCN were calculated based on ammonia production, which was determined spectrophotometrically. The ratio of activities for AlaCN and PPN were also determined, which is characteristic of each NIT4 enzyme.

Table 6. Catalytic properties of fungal nitrilases NitTv1 and NitAb

Enzyme	**Substrate AlaCN**					**AlaCN:PPN**
	specific activity [U mg^{-1} protein]		V_{max} [U mg^{-1} protein] K_M (mM)		NHase:NLase Activity	**Activity**
	Asparaginase					
	+ (Total Activity)	− (NLase Activity)	NLase Activity	NHase Activity		
NitTv1	131.5 ± 0.5	94.2 ± 1.0	129.8 ± 11.4 7.72 ± 1.82	53.2 ± 9.2 6.74 ± 3.35	0.40 ± 0.02	91 ± 3
NitAb	40.1 ± 0.1	26.8 ± 0.4	34.8 ± 2.0 7.38 ± 1.40	19.6 ± 2.5 4.97 ± 2.12	0.50 ± 0.02	56 ± 4.0

AlaCN – β-cyano-L-alanine, PPN – 3-phenylpropionitrile, NHase – nitrile hydratase, NLase – nitrilase.
Note: Determined with 25 mM substrates at pH 8 and 30 °C.

All known NIT4 NLases can be characterized as enzymes with a dual – NLase and NHase – activity. The designation "NHase" is formal, as both activities belong to a single enzyme which is a NLase in terms of structure. The products of the action of NLase activity on a nitrile are the corresponding carboxylic acid and ammonia, while the product of the reaction of a nitrile with an enzyme with NHase activity is the corresponding amide. Thus, dual activity NLases produce a carboxylic acid acid and the corresponding amide as the reaction products. Accordingly, NIT4 converts AlaCN to Asp and ammonia (i), or to Asn (ii).

$AlaCN + H_2O \rightarrow Asp + NH_3$ "nitrilase" activity of NIT4 (i)

$AlaCN + H_2O \rightarrow Asn$ "nitrile hydratase" activity of NIT4 (ii)

After supplementing the reaction medium with asparaginase, which converts Asn to Asp (iii), the amount of ammonia increased by 40-50%.

$Asn + H_2O \rightarrow Asp + NH_3$ asparaginase activity (iii)

Other nitriles investigated as substrates of the studied enzymes were aliphatic and arylaliphatic nitriles (Table 7). As potential auxin precursors, PAN and IAN were tested. The formation of reaction products - carboxylic acids and amides - was determined using HPLC. The relative activities of enzymes with the above substrates were calculated using AlaCN as the reference substrate.

Table 7. Relative activities of nitrilases NitTv1 and NitAb

Enzyme	**Relative Activity [%]**
NitTv1	AlaCN (100), FN (8.6), 4CP (1.7), CiN (1.6), PPN (1.1), PAN (1.0), PTAN (<1), IAN (<1)
NitAb	AlaCN (100), CiN (3.3), PPN (1.8), PAN (1.1), FN (<1), PTAN (<1), 4CP (<1), IAN (<1)

FN – fumaronitrile, 4CP – 4-cyanopyridine, CiN – cinnamonitrile, PPN – 3-phenylpropionitrile, PAN – phenylacetonitrile, PTAN – phenylthioacetonitrile, IAN - indole-3-acetonitrile.
Note: Determined with 25 mM of substrate at pH 8 and 30 °C. Specific activities of 131.5 and 40.1 U mg^{-1} protein for AlaCN - β-cyano-L-alanine (Table 6) were taken as 100% in NitTv1 and NitAb, respectively. No significant activities were found with allylcyanide and 4-phenylbutyronitrile.

For NitTv1, the best substrate after AlaCN was FN. With arylaliphatic substrates such as CiN, PPN, PAN, or PTAN, the activity was present but significantly lower compared to FN. The activity of NitAb enzyme for these substrates was lower than that of NitTv1. In contrast to NitTv1, NitAb did not show a significant activity for FN.

Studies of the influence of temperature and pH on the activity and stability of the enzymes were carried out using CiN as a substrate. The reaction products were the corresponding acid and amide (cinnamic acid and cinnamamide) for both enzymes. The advantage of using CiN as a substrate was the possibility of analyzing the effect of temperature and pH on the ratio of NLase and NHase activity.

For the NitTv1 enzyme, the temperature optimum for NHase activity (30–35 °C) was slightly higher than for NLase activity (30 °C) (Figure 24).

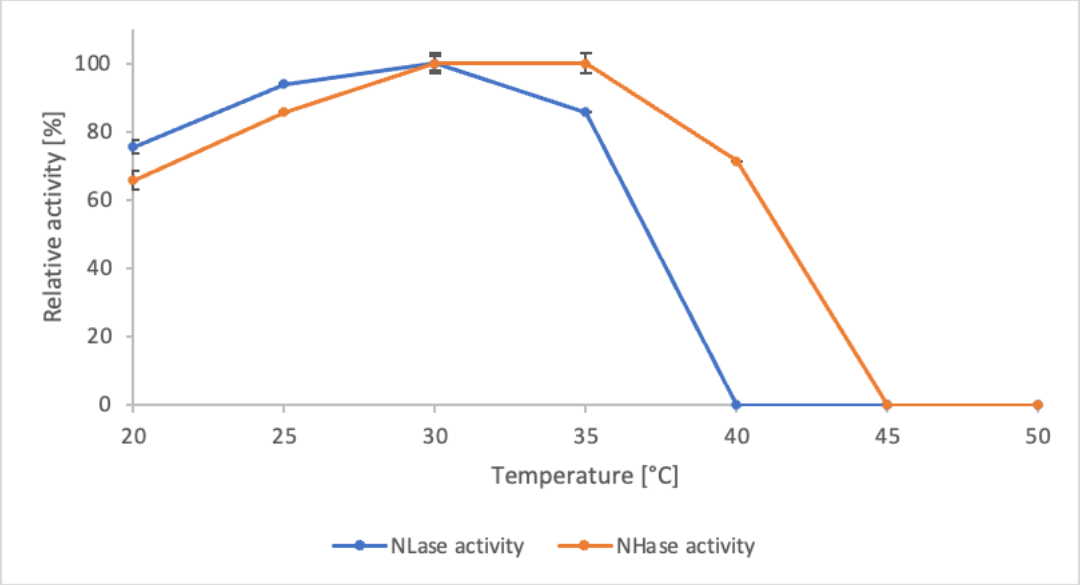

Figure 24. Relative activities of NitTv1 at different temperatures and pH 8.0. The acid-forming activity (nitrilase) is named NLase activity; the amide-forming activity is named nitrile hydratase (NHase) activity. 25 mM cinnamonitrile was used as a substrate (see Methods and Table 3 for method details).

The stability of the enzyme was determined from the activity left after preincubation for 2 hours at different temperatures (Figure 25). For the NitTv1 enzyme, NLase activity remained stable up to 35 °C, with the NHase activity being more stable than that of NLase.

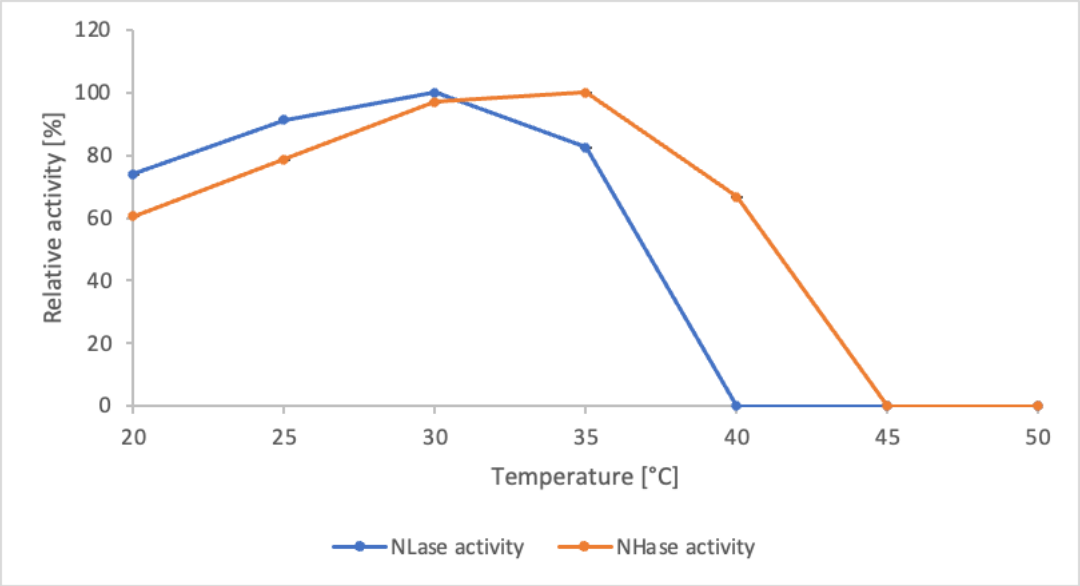

Figure 25. Relative stabilities of NitTv1 at different temperatures. See Fig. 24 for legend.

The effect of pH on the activity and on the ratio of NHase and NLase activities of the NitTv1 enzyme is shown in Figures 26. The pH optimum for both activities was approximately 7.5-8.5; however, NHase was more active than NLase at pH 4.5-6.5. The stability of the NitTv1 enzyme was good in the pH range of 5.2 to 9.3, with both activities remaining stable over this pH range (Figure 27). At strongly acidic and alkaline pH (approximately 4 and 11) the enzyme was unstable.

Thus, the NHase/ NLase ratio was affected by the reaction temperature, i.e., an increase in temperature led to an increase in this ratio. A pH shift to acidic also led to an increase in this ratio (Figures 24, 25).

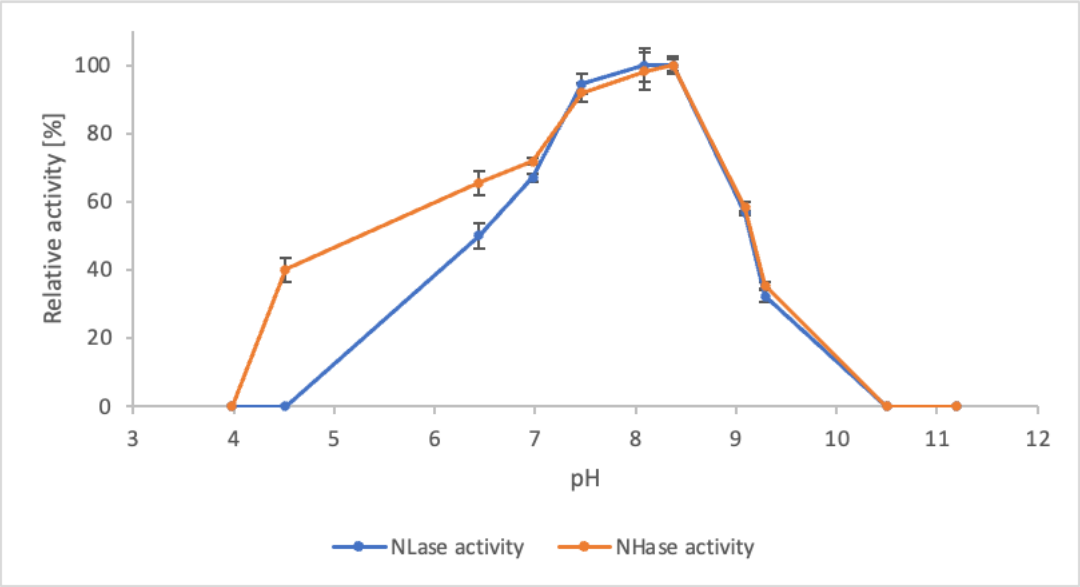

Figure 26. Relative activities of NitTv1 at different pH. See Fig. 24 for legend.

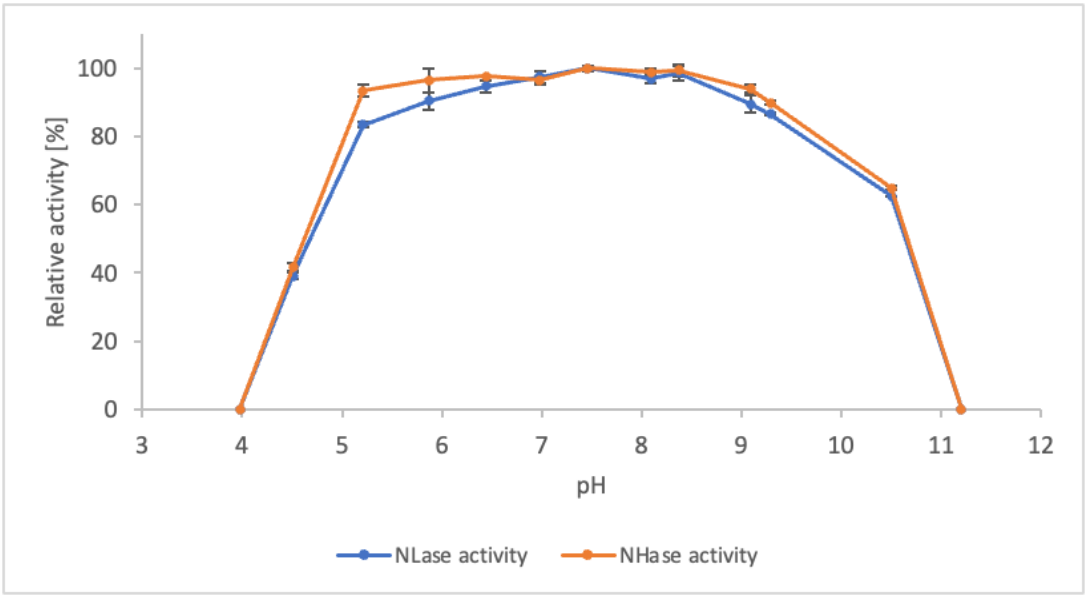

Figure 27. Relative stabilities of NitTv at different pH. See Fig. 24 for legend.

A study of the activity of NitAb at different temperatures showed that the temperature optimum of the enzyme is 25–30 °C, and at a temperature of 40 °C, almost no enzyme activity was detected (Figure 28). No effect of temperature on the ratio of NHase and NLase activities was found, in contrast to the NitTv1 enzyme. The stability of the enzyme was good at

temperatures of up to 35 °C. After preincubation of the enzyme at higher temperatures (40 – 45 °C), the activity was very low or absent (Figure 29).

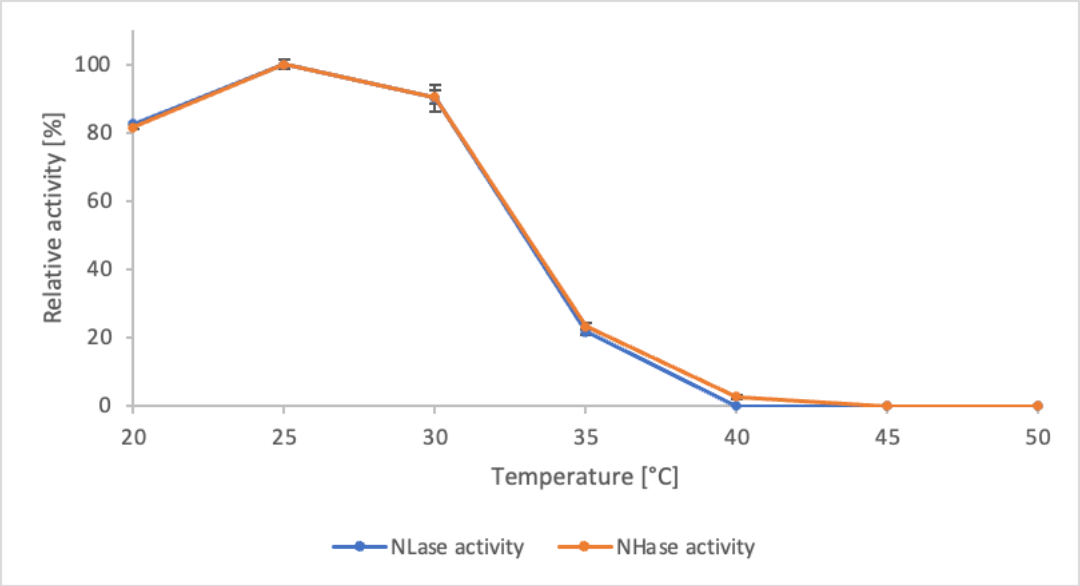

Figure 28. Relative activities of NitAb at different temperatures. See Fig. 24 for legend.

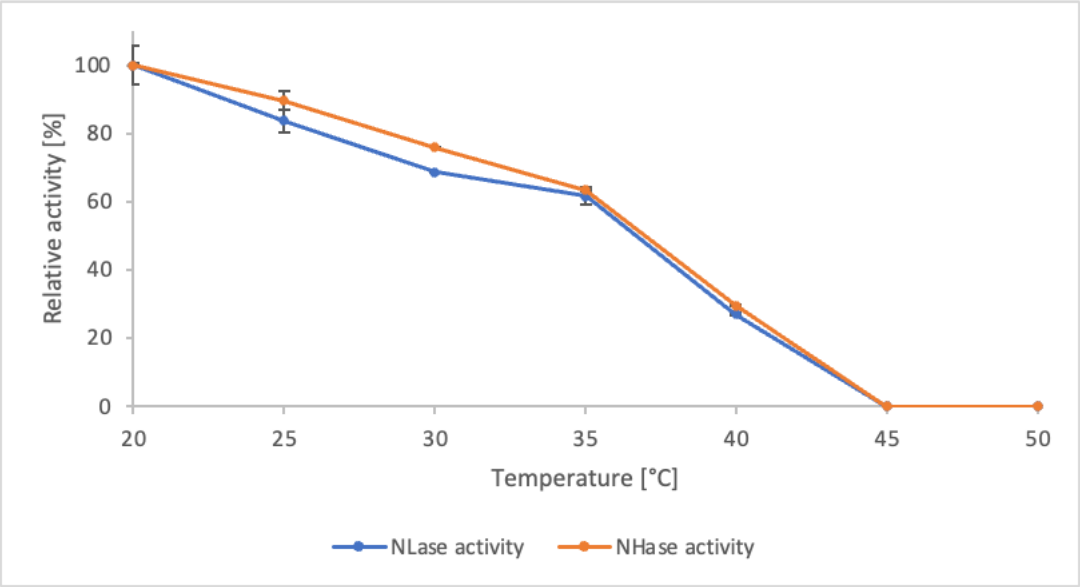

Figure 29. Relative stabilities of NitAb at different temperatures. See Fig. 24 for legend.

A study of the effects of pH on the activity of NitAb showed that the activity of the enzyme was the highest at pH between 6–8 (Figure 30). Unlike the NitTv1 enzyme, NitAb was unable to maintain its activity at acidic pH such as 4.5 or below.

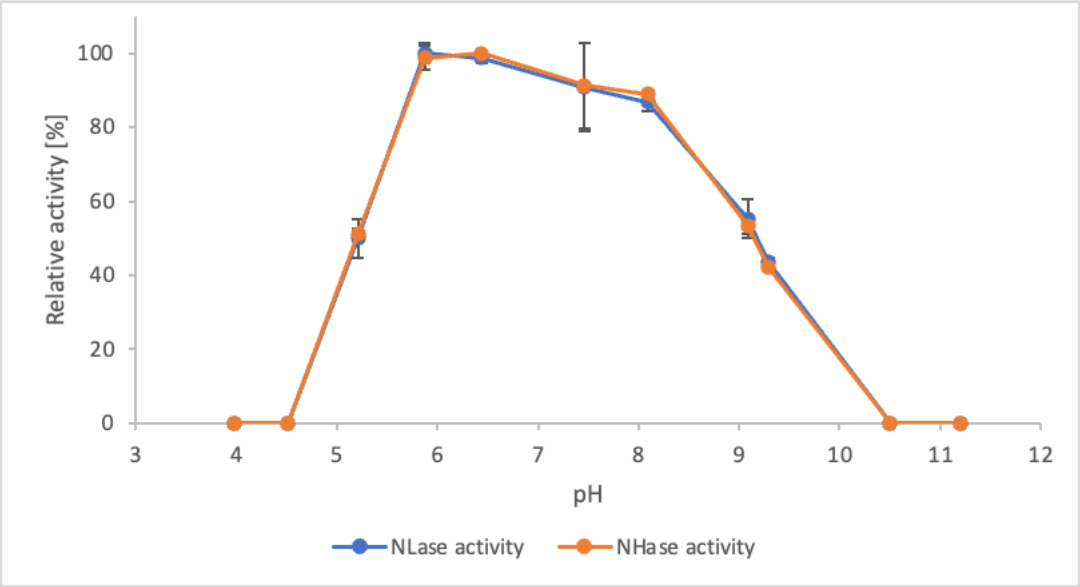

Figure 30. Relative activities of NitAb at different pH. See Fig. 24 for legend.

NitAb enzyme was stable at pH 5-7 but lost a part of its activity at more alkaline pH values (pH 8-9) (Figure 31). The effect of pH did not differ significantly between NLase and NHase activity, in contrast to more significant differences in the NitTv1 enzyme.

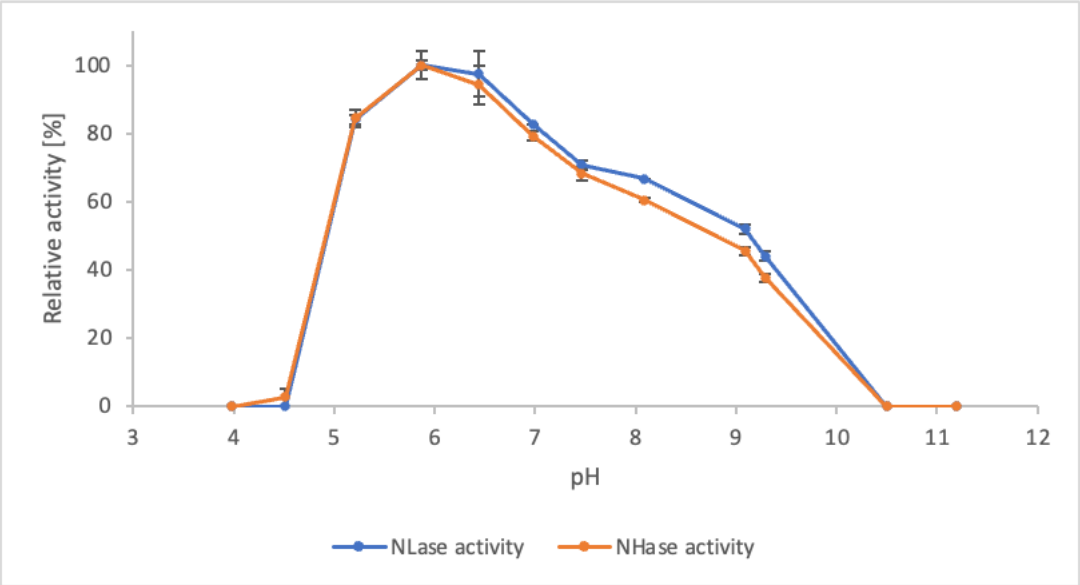

Figure 31. Relative stabilities of NitAb at different pH. See Fig. 24 for legend.

NitTv1 enzyme was more stable than NitAb during storage, retaining 95% activity after 15 days at 4 ºC, while the residual activity of NitAb was 42% after 18 days.

4.1.3. Computational studies of NitAb and NitTv1 enzymes

NitAb homology model construction and ligand docking were performed by Ing. Natalia Kulik, Ph.D. (Laboratory of Photosynthesis, Algatech Centre, IMIC) in a similar way as for the previously constructed NitTv homology model (Rucká et al., 2019). The active sites of NitTv1 and NitAb have been shown to be similar to those of other NLases (Rucká et al., 2019). In NitTv1, the catalytic triad consists of E46, K133, C178, E140, and the NitAb catalytic triad consists of E45, K157, C195 and E164 (Figure 32 - 34).

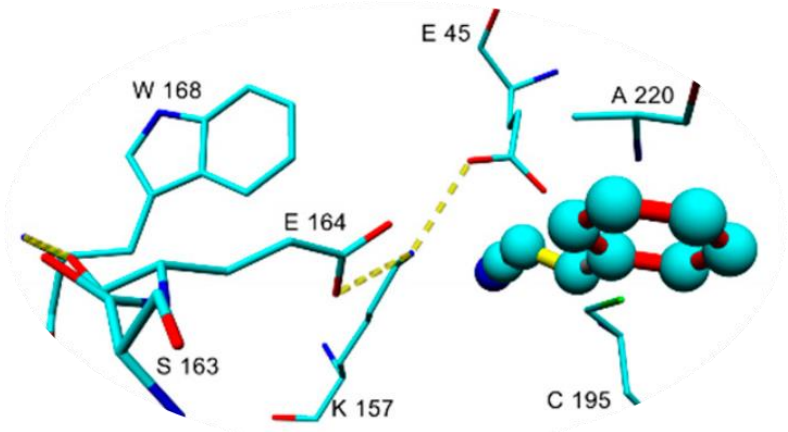

Figure 32. Active site residues of NitAb with docked cinnamonitrile.

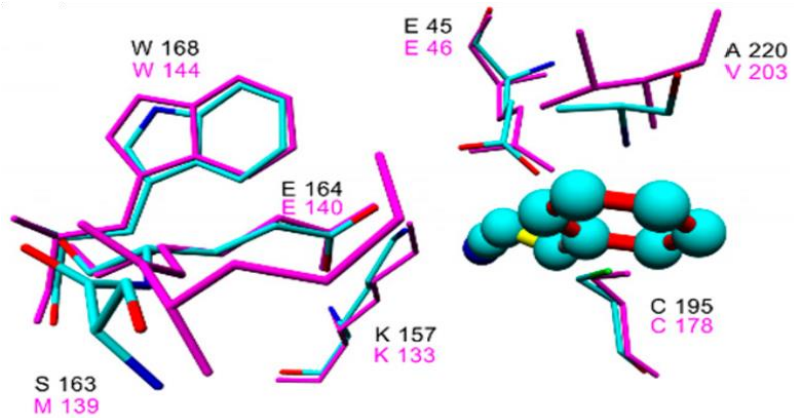

Figure 33. Overlay of the active site residues of NitAb (element color, black labels) and NitTv1 (magenta color, magenta labels).

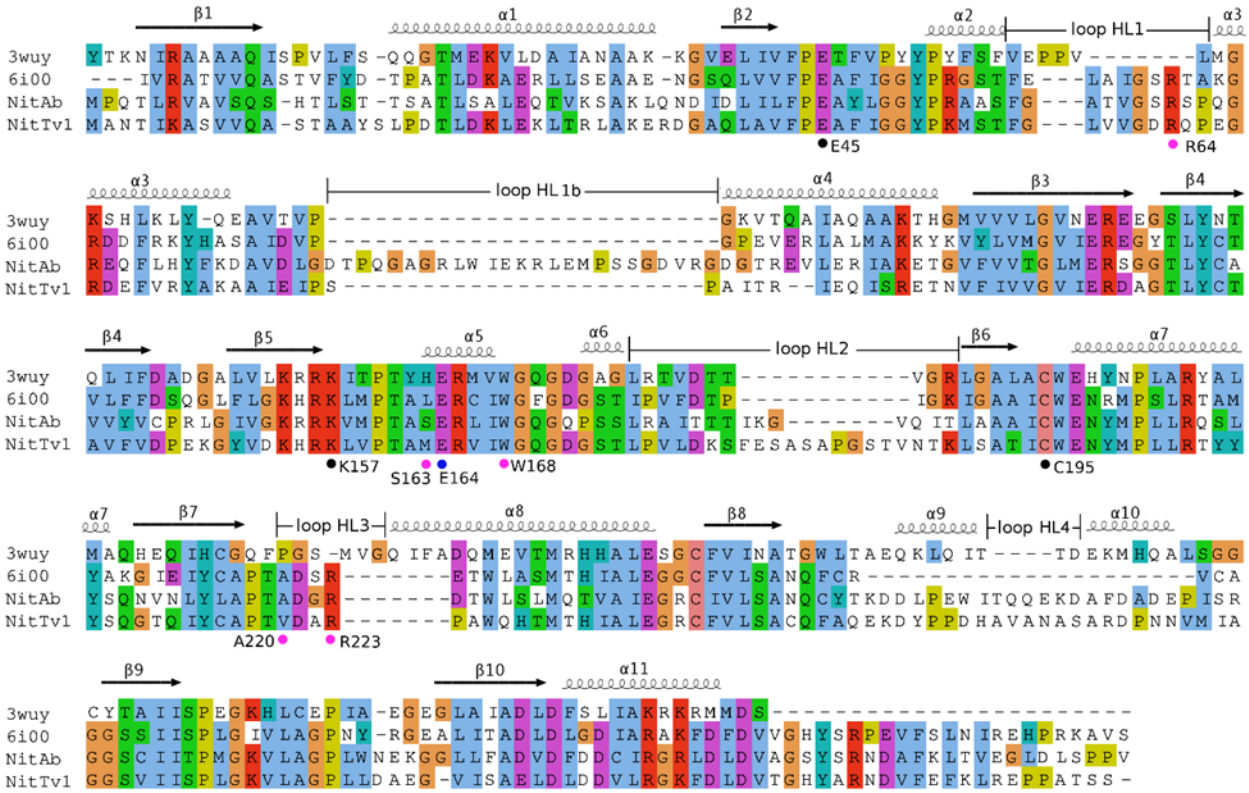

Figure 34. Multiple sequence alignment of crystallized nitrilases and NIT4 nitrilases NitAb and NitTv1. Distribution of secondary structure elements was assigned according to the crystal structure of nitrilase from *Synechocystis* sp. (pdb code 3wuy) (Cuff et al., 1998). The catalytic triad (E, K, C) is labeled with black dots, an additional important E residue is marked with a blue dot. Amino acid residues proposed to be important for substrate recognition are marked with cyan dots. The numbers of residues below the alignment correspond to NitAb. Loops are designated HL1-HL4 in accordance with the previous data (Rucká et al., 2019).

For both enzymes, it is characteristic that the HL1, HL2, and HL4 loops (Figures 32-33) are extended, and the NitAb enzyme also has an extension of the HL1b loop, which was not found in the first clade NLases (clade 1 includes NitTv1; Figure 22).

The affinities of ligands (substrates) to the active sites of NitTv1 and NitAb monomers and tetramers were expressed as “standard precision scores” (SP score) calculated by the Glide program Table 8. A lower (more negative) SP score indicates a higher affinity of the ligand to the active site. In the monomer or tetramer of each enzyme, binding of all ligands in the active

site is possible, with a certain advantage in binding of arylaliphatic nitriles. For NitAb and NitTv1, oligomerization promoted better binding.

Table 8. Binding SP scores calculated by program Glide

Ligand	Glide SP Score [kcal/mol]			
	NitTv1		NitAb	
	Monomer	Tetramer	Monomer	Tetramer
Cinnamonitrile	ni [1]	- 2.569	- 2.409	- 2.569
Fumaronitrile	- 0.150	- 0.085	- 1.118 [2]	- 0.870 [2]
Phenylpropionitrile	- 3.838	- 4.639	- 4.170	- 4.669
3-Phenylpropionitrile	- 3.490	- 3.571	- 3.146	- 4.099
4-Cyanopyridine	- 3.260	ni [1]	ni [1]	- 3.057
Phenylthioacetonitrile	- 3.591	- 3.602	- 3.453	- 4.343
Methylthioacetonitrile	ni [1]	- 3.897	- 3.694	- 3.250
β-Cyano-L-alanine	- 2.713	- 2.758	- 2.416	- 2.557
Indole-3-acetonitrile	- 4.310	- 5.798	- 4.112	- 5.718
4-Phenylbutyronitrile	- 4.201	- 3.873	- 3.072	- 2.932
Allylcyanide	ni [1]	- 1.004	- 1.487	- 1.355

[1] ni = not identified (no position with a negative binding score was found for the ligand). [2] Docking of ligand was only possible with increased distance (0.35 nm) between the catalytic C residues (sulfur atom) and the ligand (cyano group). SP = standard precision.

4.2. Cyanide hydratases

4.2.1. Analysis of published cyanide (di)hydratase sequences

Using the GenBank database (https://blast.ncbi.nlm.nih.gov; accessed on December 5, 2022) and based on selected validated CynHs, 60–99% identical sequences were found with greater than 90% coverage. A total of 389 homologous sequences were obtained, and all

belonged to fungi, with 98.5% identified in Ascomycota fungi and only six belonging to Basidiomycota (Table 9).

Table 9. Cyanide hydratases (CynHs) identified in GenBank

Phylum	Class	Genus [1]	Sequences Found [2]	Species with confirmed cynHs (Reference)
Ascomycota	Dothideomycetes	*Aureobasidium*	39	
		Alternaria	17	
		Hortaea	12	
		Pyrenophora	4	*P. teres* (Veselá et al., 2016)
		Leptosphaeria	2	*L. maculans* (Sexton et al., 2000)
		Stemphylium	1	*S. loti* (Fry and Millar, 1972)
		Other	46	
	Lecanoromycetes	*Mycoblastus*	2	
		Letharia	2	
		Other	6	
	Leotiomycetes	*Botrytis*	8	
		Monilinia	4	
		Botryotinia	1	*B. fuckeliana* (Veselá et al., 2016)
		Other	20	
	Sordariomycetes	*Fusarium*	43	*F. solani* (Barclay et al., 2002), *F. lateritium* (Nolan et al., 2003), *F. graminearum* (Basile et al., 2008) [3]
		Colletotrichum	21	
		Monosporascus	8	
		Diaporthe	6	
		Verticillium	6	
		Neurospora	2	*N. crassa* (Basile et al., 2008)
		Microdochium	2	*M. sorghi* (Basile et al., 2008) [4]
		Other	39	
	Eurotiomycetes	*Aspergillus*	52	*A. nidulans* (Basile et al., 2008), *A. niger* (Rinágelová et al., 2014)
		Penicillium	29	*P. chrysogenum* (Kaplan et al., 2013)
		Other	9	
	Xylobotryomycetes	*Cirrosporium*	1	
	Sareomycetes	*Sarea*	1	
Basidiomycota	Agaricomycetes	*Auricularia*	3	
		Stereum	2	*S. hirsutum* (Rucká et al., 2019
		Exidia	1	*E. glandulosa* (Sedova et al., 2021)

[1] The following templates were used to search the GenBank: CynH from *Fusarium solani* (CAC69666.1) (Barclay et al., 2002) and *Gloeocercospora sorghi* (designated *Microdochium sorghi* in NCBI; AAA33353.1) (Basile et al., 2008). Redundant sequences were excluded using the tool https://web.expasy.org/decrease_redundancy. Sequences with identities of 60–99% and coverage of 90% were selected. [2]Genera that contain the highest numbers of CynHs or whose CynHs were experimentally confirmed are shown. [3]Previously *Gibberella zeae*. [4]Previously *Gloeocercospora sorghi*.

A similar search yielded 230 CynD sequences (Table 10). Their identity and coverage were ≥ 70% and ≥ 90%, respectively, using $CynD_{pum}$, $CynD_{stut}$ (*P. stutzeri* has been reclassified as *Stutzerimonas stutzeri*) or $CynD_{ind}$ templates. The number of corresponding sequences with 70–99% identity to $CynD_{pum}$ or $CynD_{stut}$ was 79 (81 including templates). It was assumed that these proteins have CynD activity, but it is difficult to predict the activities of those that have a lower level of identity (at a threshold level of 50%, the number of sequences is approximately 70 more). The hypothetical CynDs found were almost all from bacteria; only one putative CynD was from yeast (*Sheffersomyces stipites*).

Table 10. Cyanide dihydratases (CynDs) identified in GenBank

Phylum	Class	Genus	Sequences Found [1]	Species with Confirmed CynD Activity (Reference)
Firmicutes	Bacilli	*Bacillus*	52 [2]	*B. pumilus* (Park et al., 2016; Park et al., 2015: Sewell et al., 2017)
		Paenibacillus	12 [3]	
		Other	4	
	Clostridia	*Clostridium*	6	
		Lacrimispora	1	
Proteobacteria	Gammaproteobacteria	*Acinetobacter*	1	
		Stutzerimonas	1	*S. stutzeri* (Crum et al., 2015)
	Betaproteobacteria	*Burkholderia*	2	
Actinobacteria	Actinomycetia	*Brevibacterium*	1	
Bacteroidota	Flavobacteria	*Flavobacterium*	147	*F. indicum* (Kumar et al., 2018)
		Other	5	
Ascomycota	Saccharomycetes	*Scheffersomyces*	1	

[1] The following templates were used to search the GenBank: $CynD_{pum}$ from *Bacillus pumilus* (AAN77004.1), $CynD_{stut}$ from *Stutzerimonas stutzeri* (BAA11653.1) and $CynD_{ind}$ from *Flavobacterium indicum* (CCG52320.1). Sequences with identities of 70–99% and coverage of 90% were selected.
[2] The number of sequences found in the species *Bacillus safensis*, *Bacillus pumilus*, *Bacillus thuringiensis* and *Bacillus cereus* was 17, 15, 5, and 4, respectively.
[3] The number of sequences found in the species *Paenibacillus alvei* was 8.

The results of these searches show that CynDs and CynHs constitute a small portion of NLases which comprise several thousand sequences. Not surprisingly, the well-known Glu-Lys-Cys triad is also found in the CynDs and CynHs (e.g., C164, E48 and K130 in the CynD from *Bacillus pumilus*). Enzymes of the NLase family also possess a second conserved Glu

residue. Both Glu residues and the Lys residue determine the positioning of the substrate in relation to the catalytic residue (Cys) and are important for activity (Makumire et al., 2022; Weber et al., 2013). CynDs and CynHs, as representatives of NLases, also have two conserved Glu residues at the corresponding positions (Figure 35).

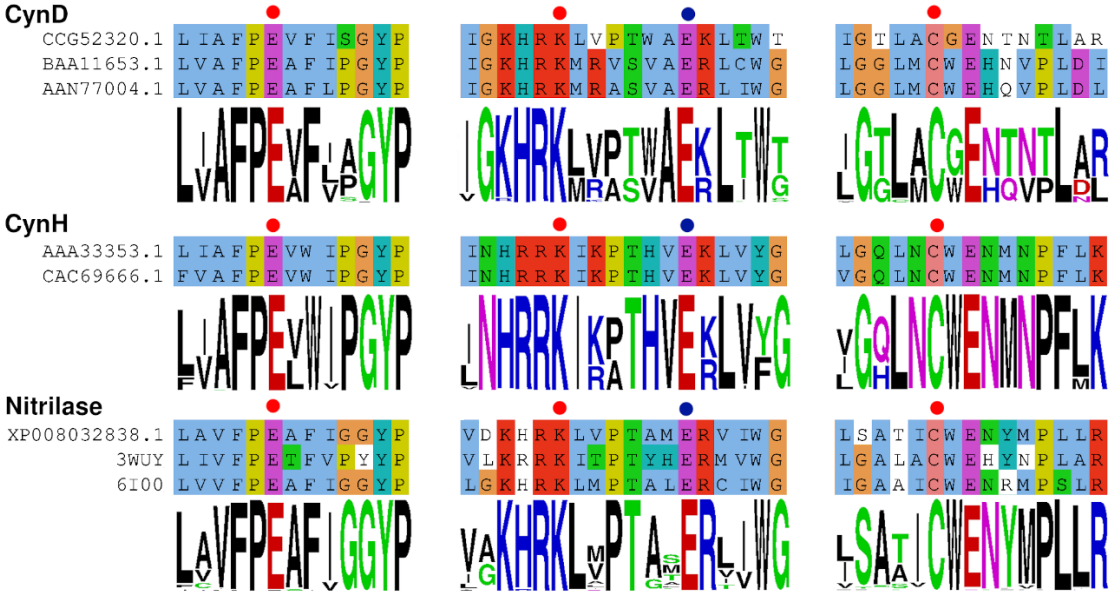

Figure 35. Conservation of key regions surrounding the active site residues in the following nitrilases: cyanide dihydratases (CynDs) from *Flavobacterium indicum* (CCG52320.1), *Stutzerimonas stutzeri* (BAA11653.1), and *Bacillus pumilus* (AAN77004.1), cyanide hydratases (CynHs) from *Microdochium sorghi* (AAA33353.1) and *Fusarium solani* (CAC69666.1), and other nitrilases – NIT4 from *Trametes versicolor* (XP_008032838.1), aliphatic nitrilase from *Synechocystis* sp. (pdb 3wuy), and NIT4 nitrilase from *Arabidopsis thaliana* (pdb 6i00). The active site residues are indicated by red dots. The second Glu is indicated by blue dots. Sequences were aligned with the CLUSTAL Omega tool, and the diagrams were generated using the WebLogo tool (http://weblogo.berkeley.edu/logo.cgi). The active site amino acids were identified based on a previous study (Thuku et al., 2009).

4.2.2. Obtaining enzymes

Only six putative CynHs have been found in the sequenced genomes of Basidiomycota. Two of them were chosen for overproduction and characterization. These were CynHs from

the fungi *Stereum hirsutum* (NitSh; GenBank: XP_007307917) and *Exidia glandulosa* (NitEg; GenBank: KZV92691). The enzymes were overproduced and purified by Ing. Lenka Rucká, Ph.D. (Laboratory of Modulation of Gene Expression IMIC). The enzymes were obtained in a similar way as the above NIT4 NLases: briefly, the optimized genes were ligated into the pET22b(+) vector, which was then used to transform the cells of *E. coli* Origami B (DE3). The synthesis, optimization and ligation procedures were performed by GeneArt. Here, both enzymes were characterized in terms of their reaction optima and other catalytic properties (see below).

Using SDS-PAGE, the molecular mass of NitEg in CFE (lane 1 in Fig. 36A) and the (partially) purified enzyme (lanes 4-8 in Figure 36A, purity ca 90%) was estimated to be approximately 43.8 kDa (Figure 36B) and this value is not too far from the theoretical molecular mass of NitEg fused with a His_6 tag (41,800 Da).

4.2.3. Cyanide-degrading activities of cyanide hydratases

To measure the specific activity of the CynHs, 25 mM KCN was used as substrate. The specific activity of CFE from *E. coli* cells producing the NitEg enzyme was 280 ± 14 U/mg as determined by the picric acid method. Pooled and concentrated fractions of the (partially) purified enzyme (lanes 4-8 in Fig. 36A) exhibited a specific activity of 697 ± 95 U/mg protein as determined by the same method. This was in accordance with the specific activity calculated from the amount of formamide produced: 784 ± 32 U/mg protein. The specific activity was 206 ± 32 U/mg protein for the purified NitSh enzyme.

Formamide is the main product of the CynH-catalyzed reaction of HCN (one form of fCN formed by dissolution of simple cyanide) (Figure 37). In accordance with this, the final concentration of formamide (22 mM) produced by NitEg was close to the initial concentration of fCN (25 mM) (Figure 38). This formamide concentration corresponds even better to the

fCN concentration in the control sample, in which the enzyme is absent (Figure 37). This indicated that a small part of fCN load was removed abiotically under the conditions used (pH 9.0).

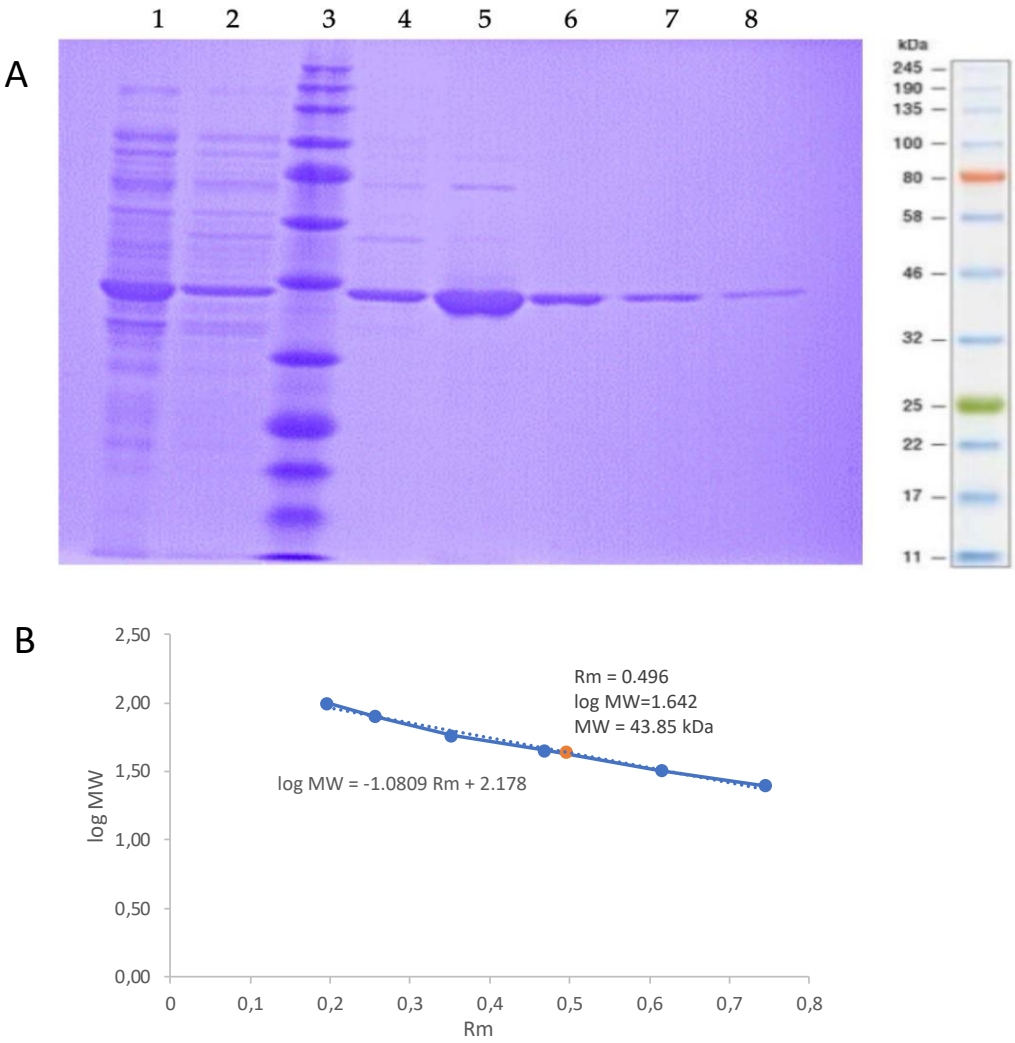

Figure 36. (A) SDS-PAGE of cyanide hydratase from the fungus *Exidia glandulosa* (NitEg) in 10% polyacrylamide gels. 1 - Cell-free extract, 2 - column wash (unbound protein), 3 - marker, 4-8 - fractions from cobalt-affinity chromatography; right - prestained marker. (B) Determination of molecular weight (MW) of NitEg using relative mobility (Rm) calculated as the ratio of distance travelled by the NitEg band and the distance traveled by the dye on the SDS-PAGE gel. Calibration (blue curve) was made for protein standards of 25, 32, 45, 58, 80 and 100 kDa. The position of NitEg is shown in orange.

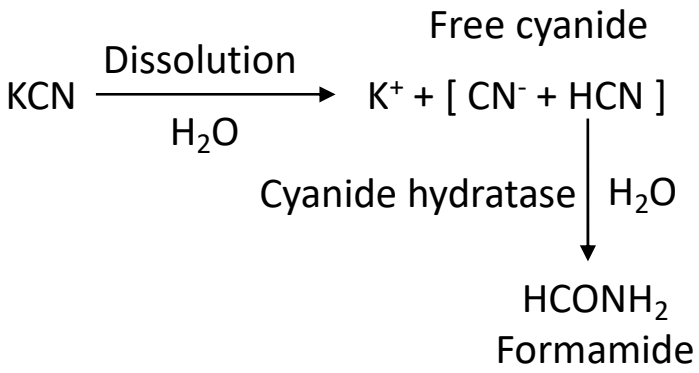

Figure 37. Detoxification of free cyanide catalyzed by cyanide hydratases.

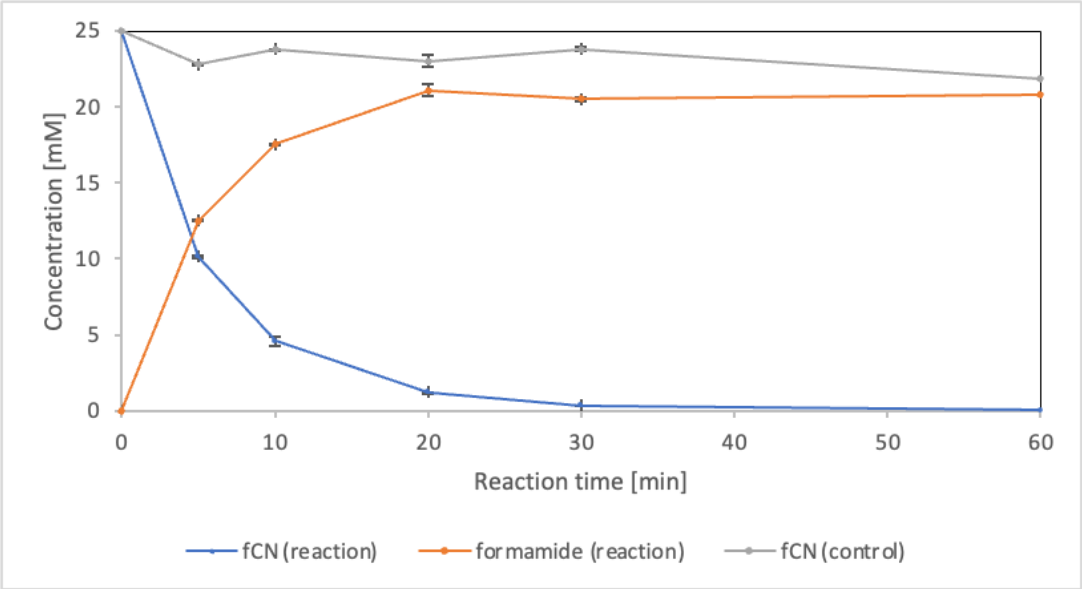

Figure 38. Conversion of fCN (fCN; 25 mM) by cyanide hydratase NitEg (4.0 µg protein/ml of reaction mixture) at pH 9.0 (100 mM glycine/NaOH buffer). Concentrations of fCN were determined using picric acid reagent. The control did not contain the enzyme.

4.2.4. Dependence of activity of NitEg and NitSh cyanide hydratases on temperature and pH

The influence of temperature and pH on the activity of the enzymes was studied using 2CP as substrate, since this substrate is less sensitive to changes in temperature and pH, in contrast to fCN. The specific activity of the CynHs with 2CP was about 2.4 U/mg protein for NitSh and 6.6 U/mg protein for NitEg and these values were estimated by the amounts of

products determined by HPLC. In the reaction of NitSh and NitEg with 2CP, pyridine-2-carboxylic acid (picolinic acid) and pyridine-2-carboxamide (picolinamide) were obtained as products, indicating the presence of both acid-forming and amide-forming activities, which were designated as NLase and NHase activities, respectively (Figure 39). Reactions with 2CP made it possible to evaluate the effect of temperature and pH on the ratio of the two activities, similar to the reaction of substrate CiN in NIT4 NLases (section 4.1.2.).

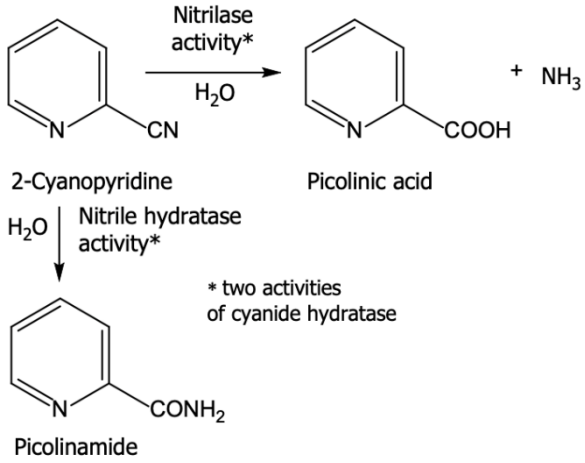

Figure 39. Dual activity of cyanide hydratase for 2-cyanopyridine.

NitSh was most active at 35 °C, but significantly less at 40 ºC (Figure 40). As the temperature increased (above 35 ºC), the NHase/NLase ratio increased. The enzyme was fairly stable at up to 30 ºC (Figure 41), and NHase activity was more stable than NLase activity. This finding is similar as that made for NIT4 NLases (section 4.1.2.).

The activity of NitEg was the highest at 40-45 ºC (Figure 42). The effect of the temperature on the NHase/ NLase ratio was only significant at 25-30 °C. At 50 ºC, the activity of the enzyme dropped significantly. The NLase activity was fairly stable at up to about 30 °C, while NHase activity remained stable at up to 40 °C after 2 hours. (Figure 43).

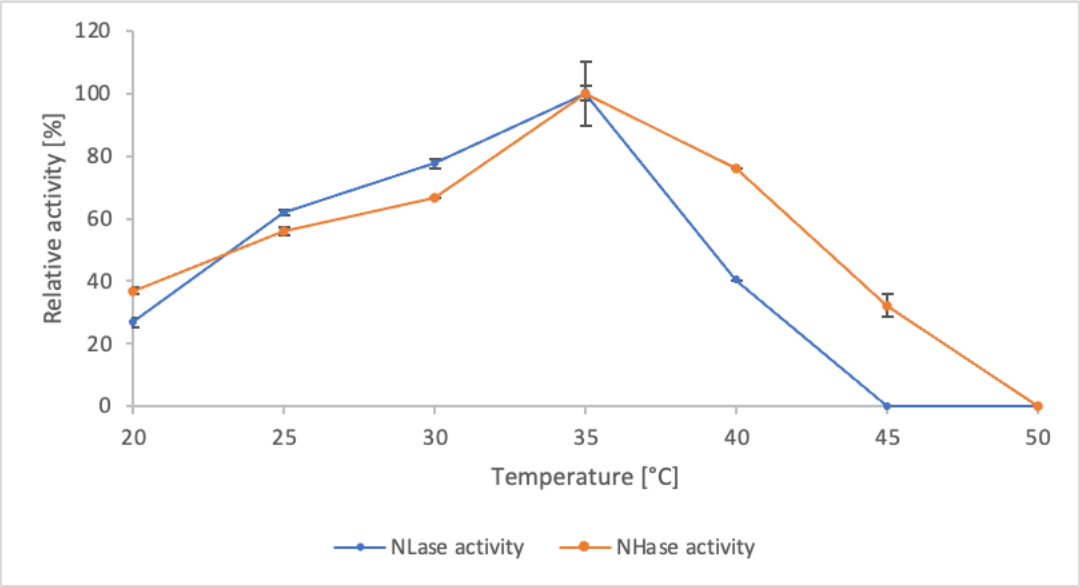

Figure 40. Relative activities of NitSh at different temperatures and pH 8.0. The acid-forming activity is named nitrilase (NLase); the amide-forming activity is named nitrile hydratase (NHase) activity. 2-Cyanopyridine (25 mM) was used as substrate (see Methods and Table 3 for method details).

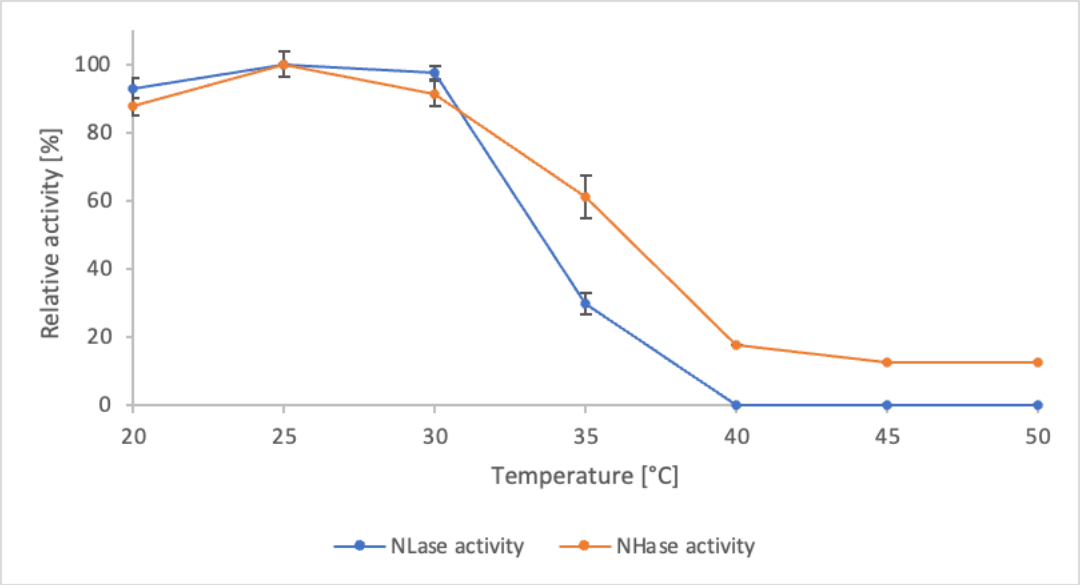

Figure 41. Relative stabilities of NitSh at different temperatures. See Fig. 40 for legend.

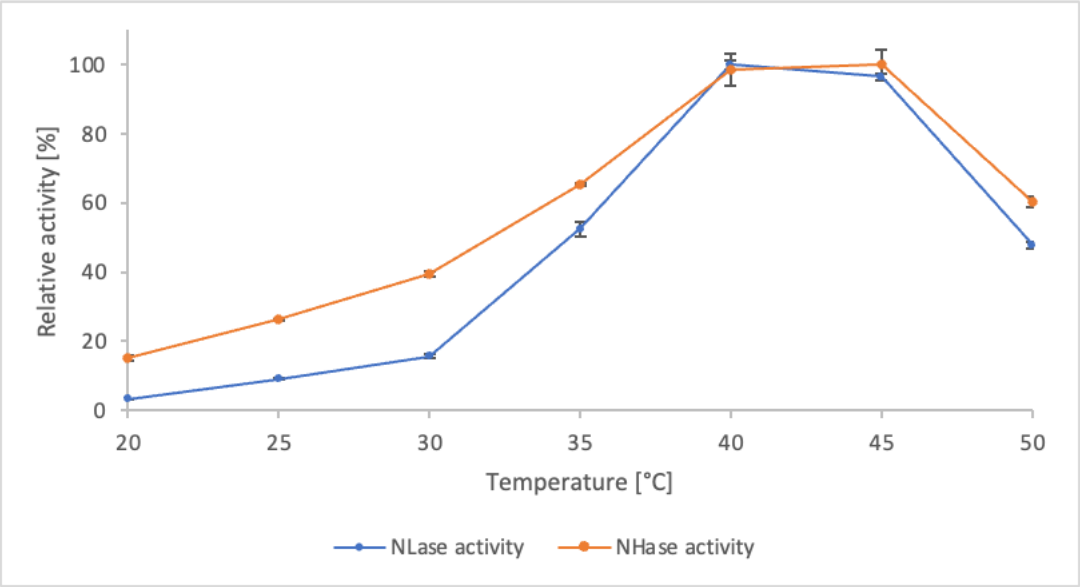

Figure 42. Relative activities of NitEg at different temperatures. See Fig. 40 for legend.

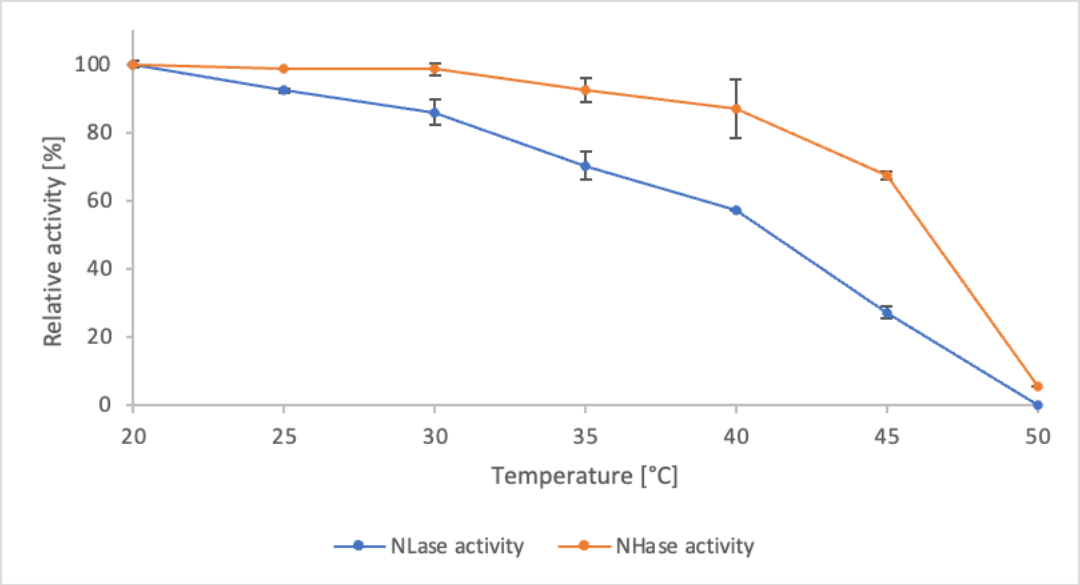

Figure 43. Relative stabilities of NitEg at different temperatures. See Fig. 40 for legend.

The maximum activity of the enzyme was found at pH 7-8, while the range of enzyme activity was from 6 to 10 (Figure 44). The range of pH was wider for NHase activity than for the NLase activity. The enzyme remained active after 2-hour preincubation at pH 6-8 (Figure

45). The NHase activity of the enzyme was stable over a wider pH range than the NLase activity.

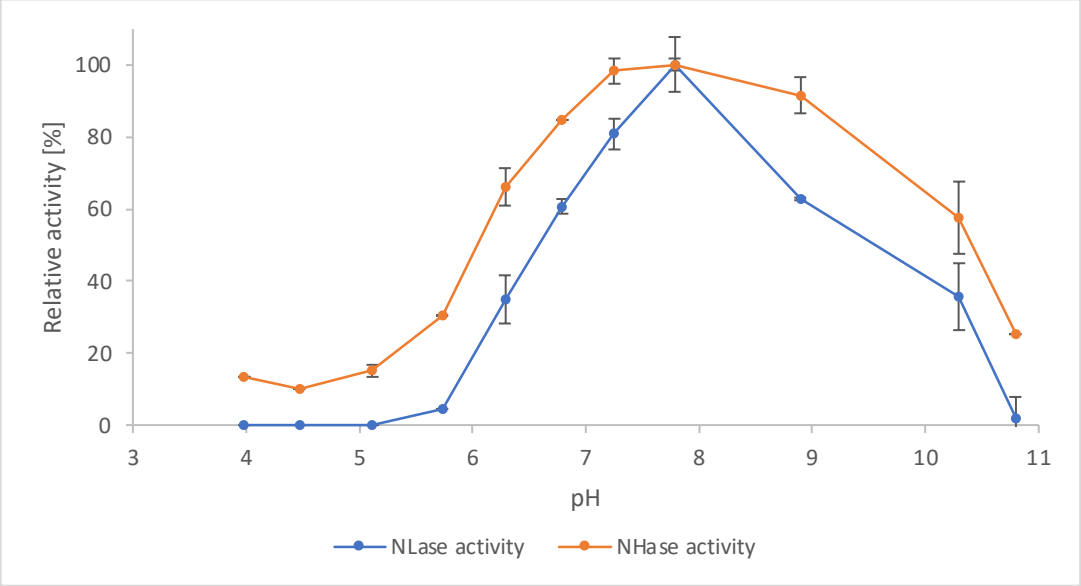

Figure 44. Relative activities of NitSh at different pH. See Fig. 40 for legend.

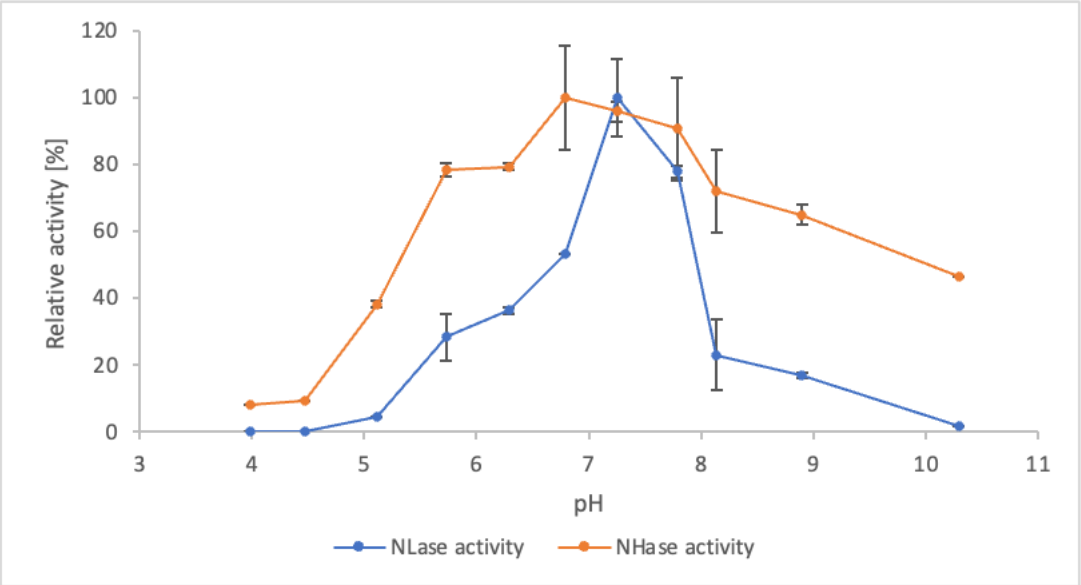

Figure 45. Relative stabilities of NitSh at different pH. See Fig. 40 for legend.

The pH optimum of NitEg was approximately 6-10 for both NLase and NHase activities. Thus, the pH range of NitEg activity was wider compared to NitSh. The residual activity of the enzyme at pH range of 5 to 10 was high, but the enzymes did not retain significant activity outside this range. Similar as for NitSh, NHase activity was stable over a wider pH range than NLase for NitEg.

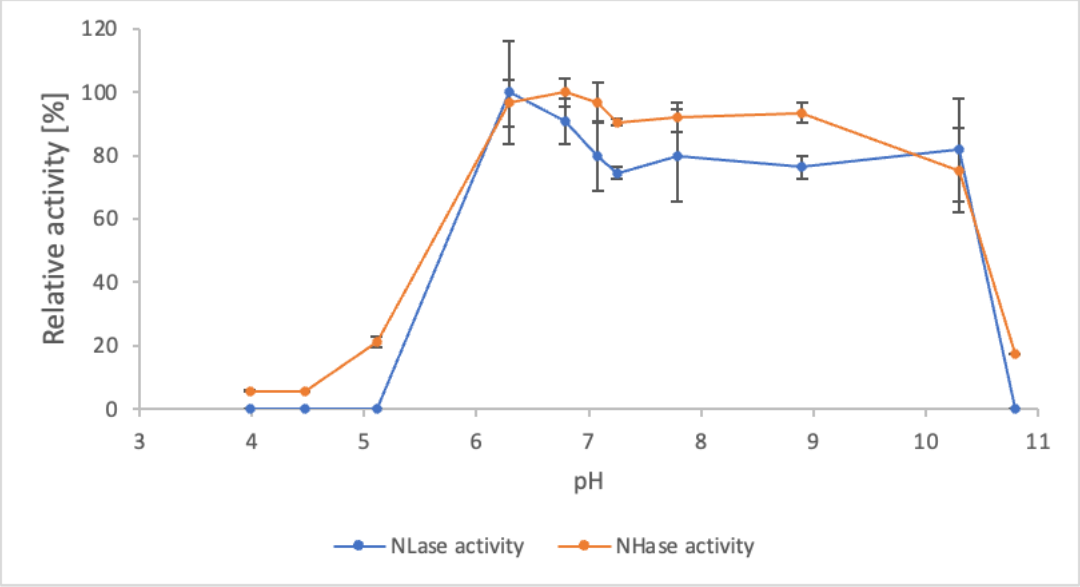

Figure 46. Relative activities of NitEg at different pH. See Fig. 40 for legend.

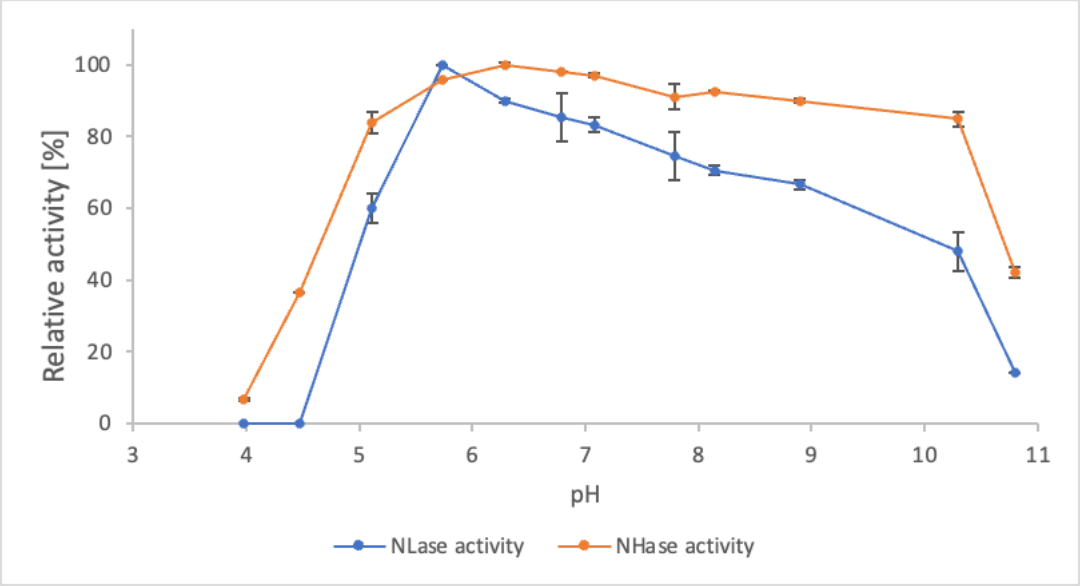

Figure 47. Relative stabilities of NitEg at different pH. See Fig. 40 for legend.

The above studies have shown that NitEg is more promising in terms of its reaction optima and stability. Comparing the effect of temperature and pH on the activity of the two enzymes, NitEg had a wider range of activity and pH stability. Moreover, the specific activity of NitEg enzyme was higher than that of NitSh enzyme.

4.2.5. Biodegradation abilities and potential applications of NitEg enzyme

From the above results it follows that NitEg is a more promising candidate for the use in the biodegradation of cyanide in wastewater. Therefore, for the NitEg enzyme, we investigated the influence of other parameters (presence of other pollutants, long-term storage etc.) on its activity. These factors can affect the real working conditions of the enzyme, when it is used for the biodegradation of cyanide in industrial wastewater, or for analytical purposes.

Effect of silver and copper on the activity of NitEg enzyme

The activity of purified NitEg was determined in the presence of silver and copper ions. This parameter is important, since the content of these metals, for example, in silver and copper galvanic baths, is obligatory (Basile et al., 2008). NitEg activity was assessed by the rate of the decrease in fCN at 30 °C and pH 9 (Table 11).

Table 11. Influence of copper and silver ions on the activity of NitEg

Metal Concentration [mM]	Relative Activity [%]	
	Ag^{+}	Cu^{2+}
-	100	100
0.1	66 ± 5	93 ± 7
1	61 ± 5	68 ± 8
5	31 ± 10	14 ± 3
10	n.d.	0

n.d. - not determined (fCN formed a complex with silver).

At a concentration of silver from 0.1 to 1 mM, the activity of NitEg decreased by approximately 30%; at 5 mM, the activity decreased by 70%, and at 10 mM, no activity was detected. It should be added that in the control samples that did not contain the enzyme, a decrease in the concentration of fCN was also observed: at 5 mM silver, from 25 mM to approximately 15.7 mM fCN, at 10 mM silver to 5 mM fCN. This is probably due to the ability of cyanide to form complexes with metals.

The presence of copper ions in the reaction mixture in the concentration of 0.1 mM did not significantly reduce the enzyme activity, but the activity of the enzyme was significantly inhibited at above 5 mM copper.

Temperature stability and shelf life

Additionally, prolonged monitoring of the NitEg activity was carried out, aimed at studying the long-term effect of temperature on the activity, as well as the shelf life of the enzyme.

The specific activity of the purified enzyme remained consistently high for 98 days when the enzyme was stored at 4 °C. A statistically significant but slight decrease was observed after day 69, while after 98 days the enzyme activity was still approximately 83% of the original value (Figure 48).

To study the stability of the enzyme at different temperatures, the temperature range from 27 to 50 °C was chosen according to the literature data published for other CynHs (Basile et al., 2008). Residual enzyme activity was measured at various time points of incubation up to 24 hours using fCN as substrate. After 24 hours, the enzyme retained 60% of its initial activity at 27 °C and 40% at 37 °C. A temperature of 43 °C significantly reduced the activity of NitEg already after 3 hours (retention of 40% of the initial activity), and after 24 hours the

enzyme retained only 10% of its activity. At a temperature of 50 ºC, already after 1 hour the enzyme activity was less than 10% (Figure 49).

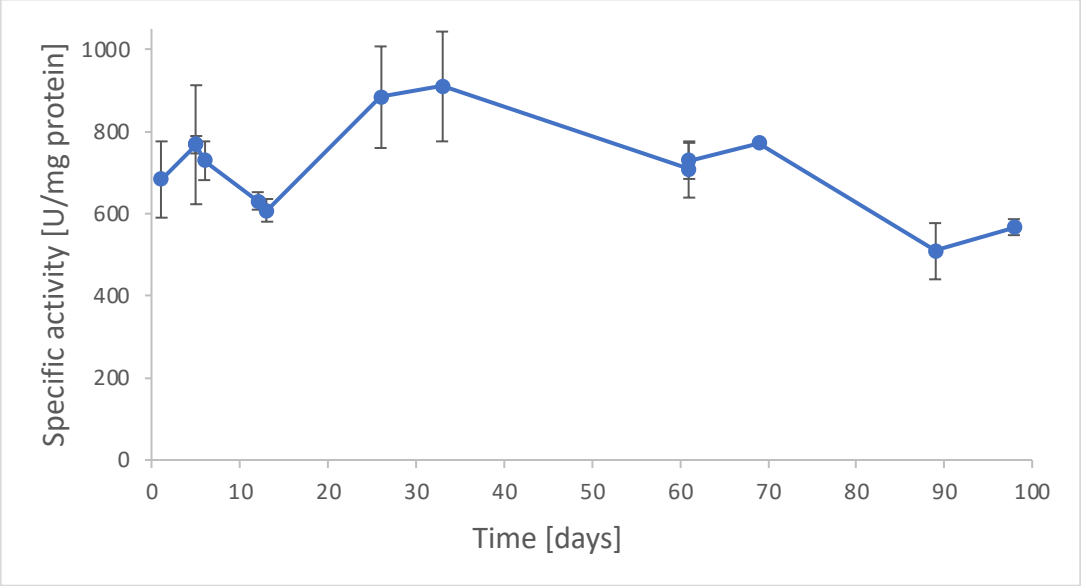

Figure 48. Stability of NitEg during storage at 4 °C. Specific activity was determined by picric acid method.

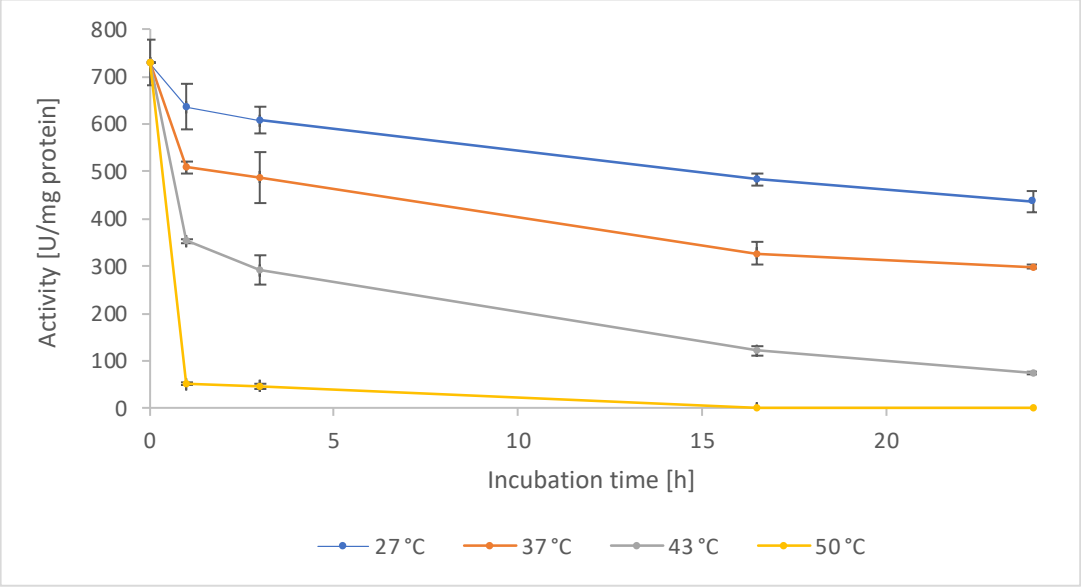

Figure 49. Effect of temperature on the residual activity of purified enzyme NitEg at different temperatures. Conditions: 10.3 mg protein/ml of reaction mixture, 50 mM Tris/HCl buffer, pH 8.0, supplemented with 150 mM NaCl. Specific activities were calculated based on the production of formamide.

Study of the efficiency of NitEg under conditions simulating wastewater

The ability of the enzyme to work under the conditions close to real industrial wastewater was studied using simulated wastewater. Taking into account the literature data on the analysis of wastewater, in particular the amount of fCN, pH, and the presence of other components, solutions were modeled (see below). However, it must be noted that thezy are still simple mixtures compared to multicomponent real wastewaters.

The efficiency of the enzyme in an alkaline environment is of fundamental importance since cyanide-containing wastes are stored at an alkaline pH to avoid volatilization of cyanide as HCN. Accordingly, investigations of enzyme activity were carried out at pH from 9.0 to 10.5 using 4 and 20 µg enzyme per ml (Figures 50 - 51).

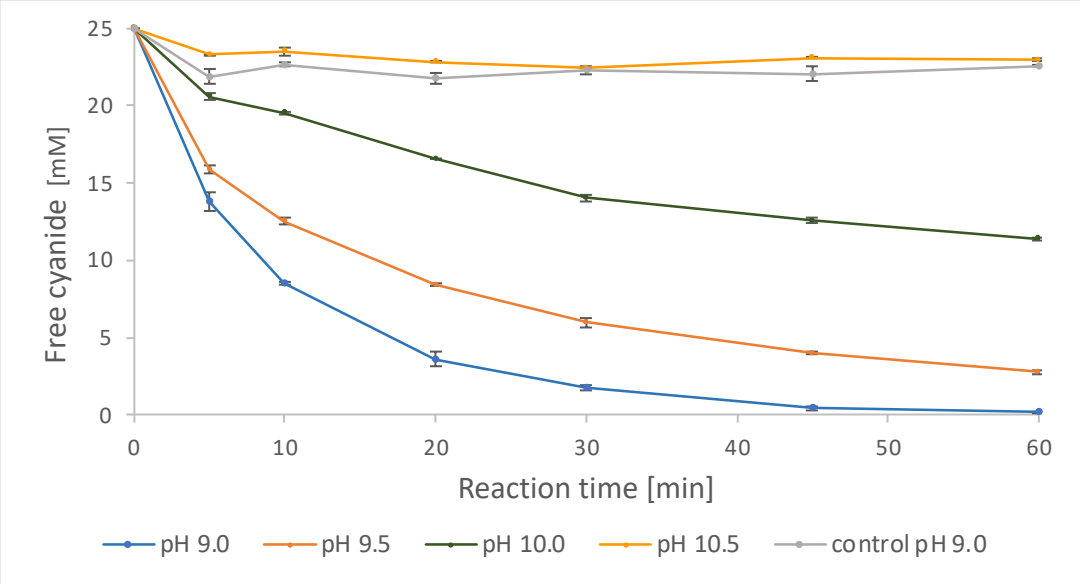

Figure 50. Effect of pH on the enzyme transformation of 25 mM free cyanide. Concentration of enzyme NitEg was 4.0 µg enzyme/ml, buffer - 100 mM glycine/NaOH. Controls were without enzyme, pH 9.0. Concentration of residual fCN was determined by picric acid method.

The efficiency of NitEg in a concentration of 4 µg of enzyme per ml at pH 9.0 to eliminate 25 mM fCN was high - after 1 hour all cyanide was completely removed. With an increase in pH, the efficiency of the enzyme decreased: at pH 9.5, 89% of cyanide were

degraded in one hour, but only 54% at pH 10.0. At pH 10.5, the enzyme had a very low efficiency. The degradation of cyanide associated with abiotic factors was only 10% after 1 hour (Figure 50).

Next, the performance of an increased concentration of NitEg (20 µg per ml) was investigated at the same pH values (9.0-10.5) (Figure 51). At pH 9.0 and 9.5, more than 80% of fCN were removed after only 30 min. In 1 hour, the same amount of cyanide was removed at pH 10. Even at pH 10.5, a certain decrease in the amount of cyanide was observed (Figure 51). The obtained data show that the rate of the enzymatic reaction is important to achieve high cyanide removal efficiency. It can be assumed that this is due to the fact that the enzyme has some limitations in stability, judging by its pH stability profile (Figure 47).

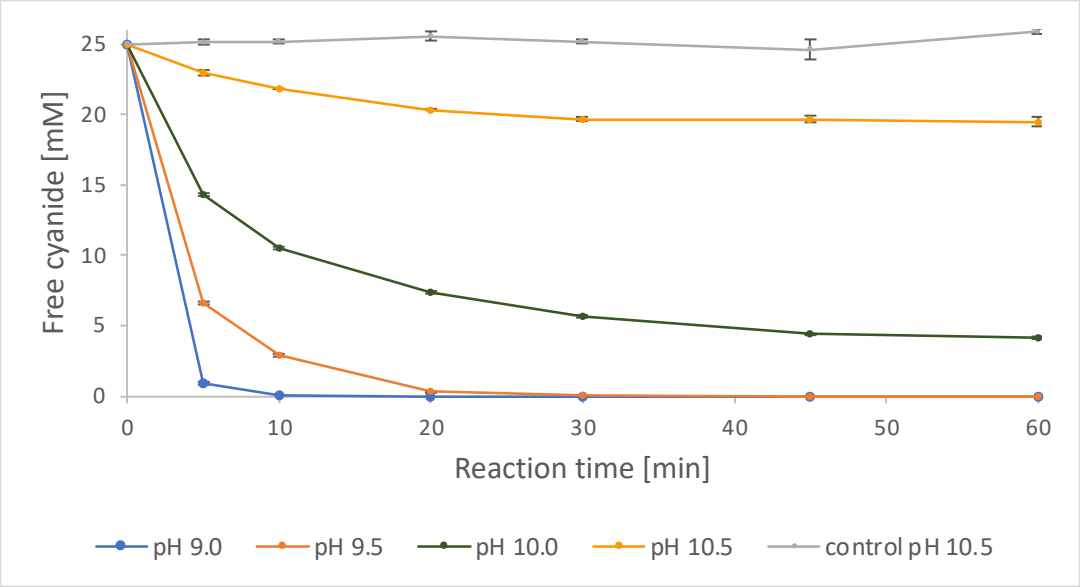

Figure 51. Effect of pH on the enzymatic degradation of 25 mM free cyanide. Concentration of enzyme NitEg was 20 µg enzyme/ml. See legend of Fig. 50 for further details.

The effect of the presence of inorganic salts and phenol in the reaction mixture on the activity of NitEg

The composition of wastewater from coking industries can contain up to 10 mM fCN (Pillai and Gupta, 2016), although more often the fCN concentration is around 0.6 mM fCN. This wastewater also contains phenol, ammonia and thiocyanate. According to the literature data (Papadimitriou et al., 2009), a mixture simulating wastewater from coke production was prepared with certain concentrations of phenol, CN^-, SCN^-, NH_4^+ (Table 5, Methods). The maximum reported concentrations of impurities (12.8 mM phenol, 8.6 mM SCN^- and 10.7 mM NH_4^+) were used in the model mixture, the fCN concentration was 0.6 mM; pH was 9.1 in accord with the real wastewater. The enzyme in an amount of 2.5 μg/ml decomposed fCN almost completely in 90 min under the above conditions. Control runs (without additives or without enzyme) were used in the experiment. Thus, the sample labeled "buffer" in Figure 52 contained the same amount of fCN but it was free from the salt and phenol additives, while the enzyme concentration was also 2.5 μg/ml. The time of decomposition of fCN in this sample was slightly shorter than in the "wastewater" sample. The control run without enzyme showed that abiotic degradation of cyanide was rather insignificant (Figure 52).

Another model effluent was prepared according to the composition of wastewater from petrochemical industry (Jarrah et al., 2016). This mixture contained a significant concentration of S^{2-}, while the concentration of fCN was eight times higher than in the above coke-plant effluent model. Both model effluents contained phenol and ammonia, but the petrochemical effluent model contained them in lower concentrations, and it did not contain SCN^- (Figure 53). Under conditions simulating petrochemical wastewater, 96% fCN was removed after 45 min by the enzyme at 5 μg/ml (Figure 53). A zero response of fCN could not be achieved, probably due to the measurement error caused by the background signal from the mixture components.

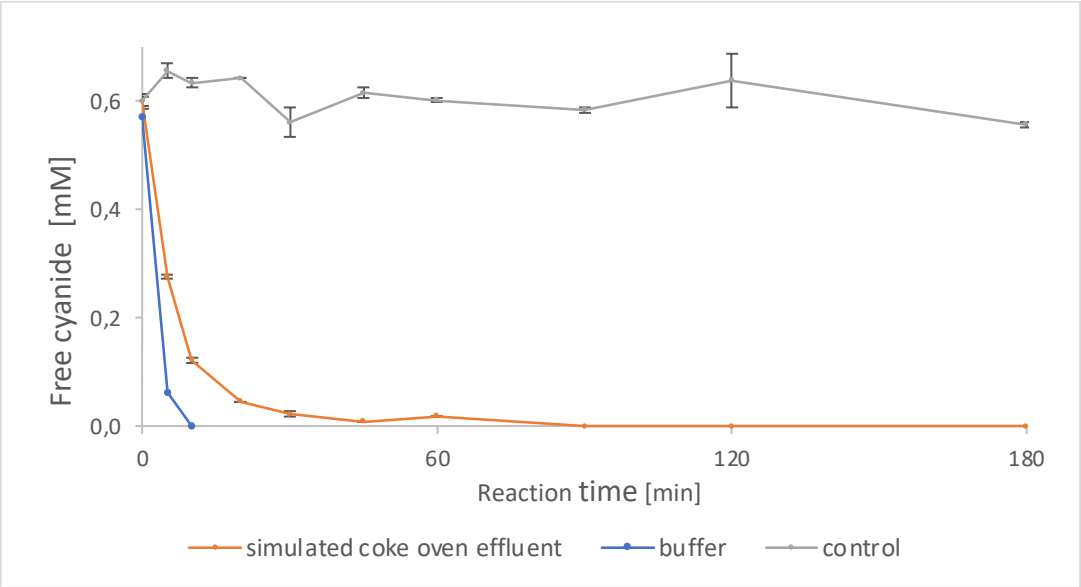

Figure 52. Biodegradation of free cyanide (fCN) by NitEg enzyme (2.5 µg/ml) in simulated coke plant wastewater (0.6 mM fCN, 8.6 mM SCN^-, 10.7 mM NH_4^+ and 12.8 mM phenol in 100 mM glycine/NaOH, pH 9.1) (Papadimitriou et al., 2009). The reaction in the same buffer with 0.6 mM fCN but without other additives is labeled "buffer". Control did not contain the enzyme. The concentration of fCN was determined using the picric acid method.

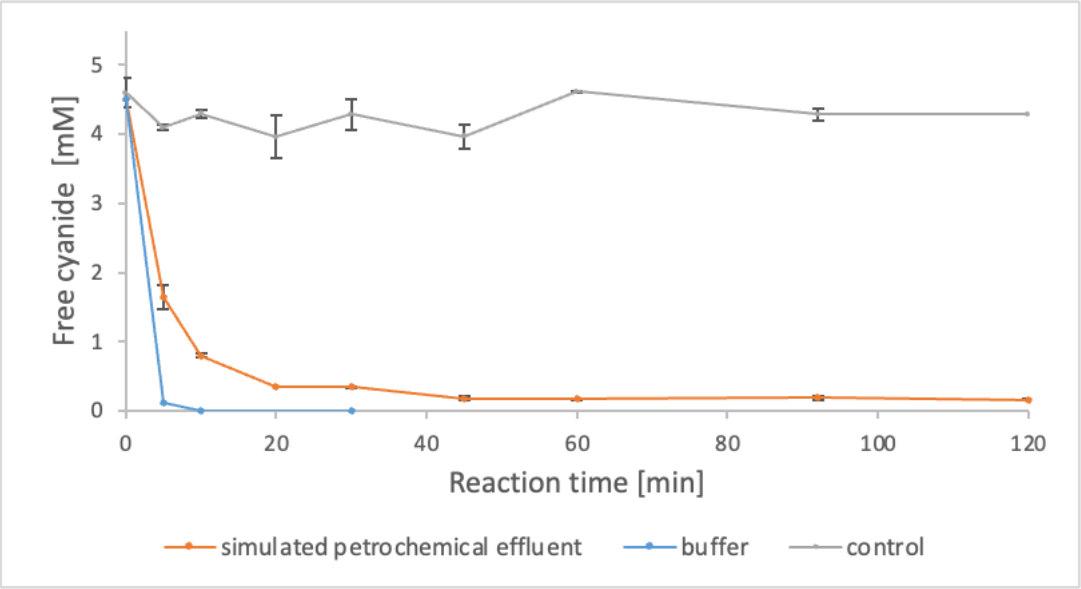

Figure 53. Biodegradation of free cyanide (fCN) by enzyme NitEg (5.0 µg/ml) in a model petrochemical effluent (4.6 mM fCN, 23.4 mM S^{2-}, 2.5 mM NH_4^+ and 0.64 mM phenol in100 mM glycine/NaOH, pH 9.1) (Jarrah et al., 2016). The reaction in the same buffer with 4.6 mM fCN but without other additives is labeled "buffer". Control did not contain enzyme. The concentration of fCN was determined by Spectroquant® kit.

Because S^{2-} is capable of causing interference, we could not use the picric acid method to measure fCN (Fisher, 1952) in this case. At H_2S concentrations of 0.029 mM and 0.29 mM, the interference reduced the signal by 2.5% and 27.5%, respectively. Higher concentrations led to the opposite effec; as a result, at the amount of H_2S 2.9 mM and 29 mM, the interference increased the signal two and twenty times, respectively (Fisher, 1952). Thus, the Spectroquant® kit containing 1,3-dimethylbarbituric acid as a reagent was used to measure fCN in petrochemical effluent models.

Since wastewater from gold mining, electroplating and processing of precious metals contain heavy metals (copper, zinc and nickel), we studied the effect of heavy metals on the degree of conversion of fCN by the enzyme. The wastewaters from the above industries can contain very high concentrations of cyanide of up to approximately 0.5 – 2 M (Carmona-Orozco et al., 2019, Basile et al., 2008, Pérez-Cid et al., 2020) and they were usually diluted prior to the enzymatic treatment experiments (Carmona-Orozco et al., 2019, Basile et al., 2008).

To study the function of the enzyme under the conditions of high fCN concentration, we studied the biocatalytic degradation of a 100 mM fCN solution (simulating a diluted effluent) using NitEg at various concentrations (14, 20, and 30 μg/ml). The pH of the reaction mixture was 9.0, since at this value fCN is more stable than, for example, at pH 8.0 used in the previous study (Basile et al., 2008). The results obtained demonstrate that even 14 μg/ml of the enzyme is sufficient to degrade more than 97% of cyanide within 60 min (Figure 54). However, approximately 2% of fCN was not removed during the entire experiment time of 3 hours, even at an enzyme concentration of 30 μg/ml. According to the data obtained in the control sample, the loss of cyanide associated with abiotic factors was about 17%.

Enzyme activity in simulated galvanic effluents was studied at a concentration of fCN of 100 mM and a concentration of copper and silver of 1 mM. It was shown that an enzyme

concentration of 14 µg/ml is sufficient to remove 97% of fCN at a concentration of 100 mM in one hour in a solution without metal ions (Figure 55).

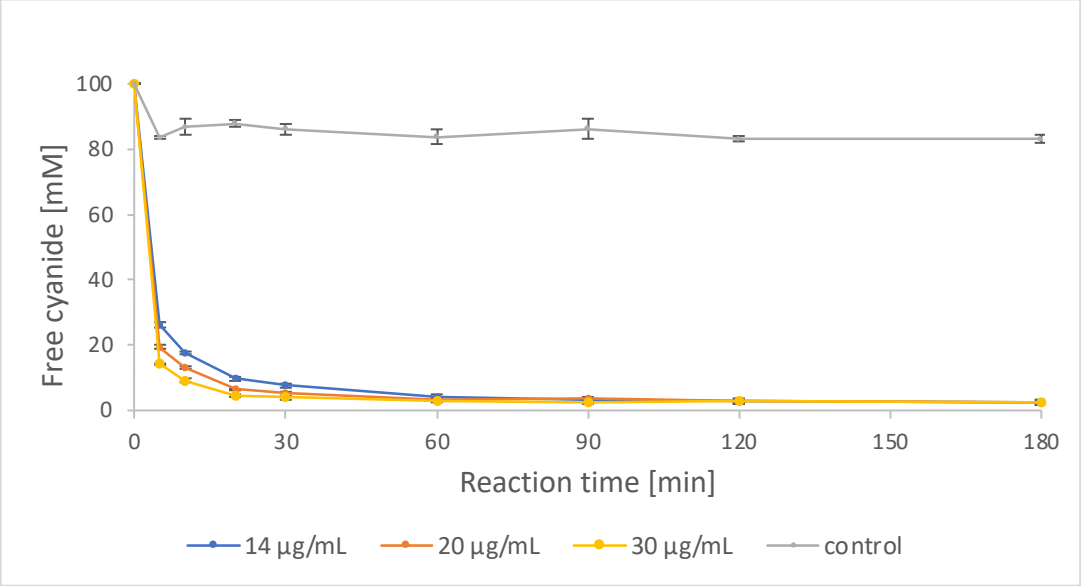

Figure 54. Biodegradation of 100 mM free cyanide (fCN) in 100 mM glycine/NaOH, pH 9.0, by various NitEg enzyme concentrations (14, 20, 30 µg/ml). Controls did not contain enzyme. The concentration of fCN was determined using the picric acid method.

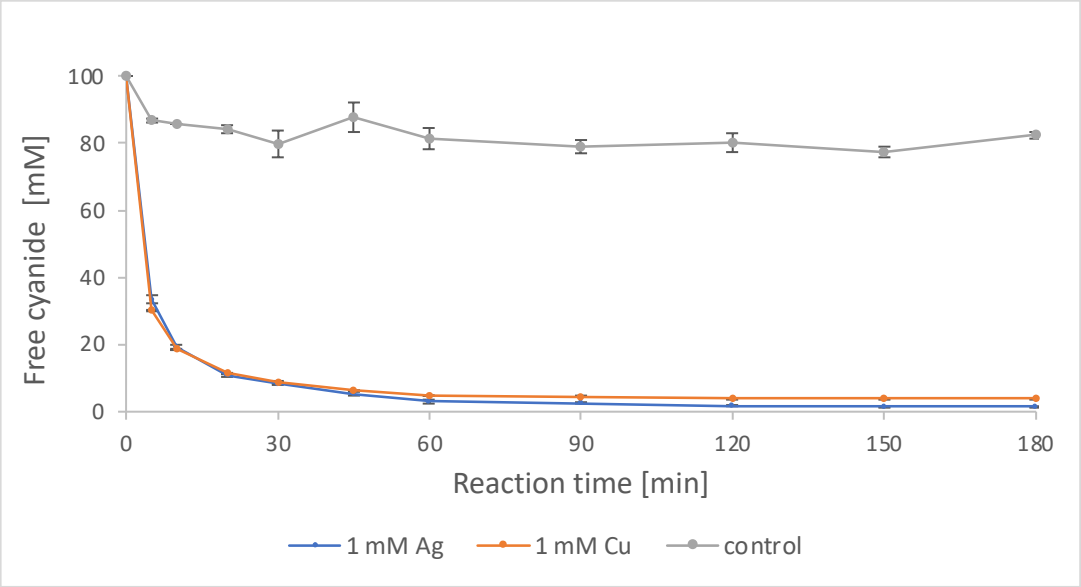

Figure 55. Biodegradation of 100 mM free cyanide in 100 mM glycine/NaOH, pH 9, by 14 µg/ml enzyme in the presence of 1 mM $AgNO_3$ or 1 mM $CuSO_4$. Controls did not contain enzyme. The concentration of fCN was determined using the picric acid method.

The percentage of removal of fCN in the presence of metal ions was 96-98% (Figure 55), and thus similar to that in the reaction without metals (Figure 54). In the presence of metals, the initial reaction rate was slightly lower (Figure 55).

5. Discussion

Enzymatic degradation of cyanide is an emerging and promising alternative to the current processes of removal of free and complex cyanides, toxic compounds that can be released into the environment as a result of certain industrial processes or by accidents. Since they represent a threat to the environment and population, green and sustainable ways of their removal are extremely attractive. New biodemediation strategies using robust enzymes with a high specific activity are among these prospective methods. This work is focused on two types of NLases involved in the biodegradation of cyanide – CynH and NIT4. The involvement of these enzymes in specific metabolic routes in microorganisms or plants was explained in the Literature review (section 2.). The wealth of sequences resulting from genome sequence projects allowed us to use an efficient approach to search for new enzymes important in cyanide degradation.

Previous searches of the GenBank database (Rucká et al., 2019; last update on December 5, 2022) focused on CynH and NIT4 representatives in the phylum Basidiomycota which was heavily underexplored as for these enzymes. This phylum was found to contain several dozens of NIT4 homologues and a few CynH homologues, apart from other NLase types. The majority of NLases have been found in the subdivision Agaricomycotina (about 60 species contain NIT4 homologues).

Basidiomycota are known destroyers of toxic pollutants, primarily phenolic compounds. This is since they produce a wide range of oxidases (laccases, peroxidases). In contrast, their ability to decompose cyanides was almost unknown, although these fungi grow on living or decaying plants containing cyanides (fCN, nitriles).

Selected enzymes were then obtained by heterologous expression in *E. coli* by optimizing the previously developed protocol for the production of NLases (Veselá et al., 2016). Enzyme purification was performed in one step using IMAC, which was enabled by

the presence of the His_6-tag in the heterologously produced enzymes. Further optimization of the expression and purification protocols would enable to increase the amount of the enzymes obtained if needed. For example, lowering the cultivation temperature would lead to improved protein solubility or using an autoinduction culture medium would enable to obtain high-density cultures.

Especially, one representative of the CynHs, and two of the NIT4 NLases were studied in detail. Among NLases, only NIT4 enzymes are widely distributed in plants. As a result of this thesis, the "plant" NLase homologues have been newly found in the genomes of Basidiomycota.

Cloning of the NLase genes NIT1-NIT3 and NIT4 from plants and their expression in *E. coli* cells were published previously (Piotrowski et al., 2008). However, the catalytic properties of fungal homologues of plant NLases have not been studied until recently, when the activity of the first fungal NIT4 homolog, NitTv1, was shown for AlaCN using whole cells (Rucká at al., 2019).

Studies of purified NitTv1 and NitAb enzymes showed that the enzymes have substrate specificity for AlaCN, similar to NIT4. Screening for activity to different substrates showed that NitTv1 and NitAb are also active, although with a lower transformation rate, with arylaliphatic nitriles, which are characteristic substrates for the NIT1-NIT3 enzymes (Vorwerk et al., 2001, Osswald et al., 2002). Although a plant NIT4 is also able to transform PPN and PAN, these activities are minor (Piotrowski et al., 2001). Thus, this is a significant difference between plant and fungal NIT4 NLases.

The study of the influence of temperature and pH on the activity of the enzymes was important to assess their effectiveness as catalysts. Comparing the catalytic and biochemical properties of fungal NLases NitTv1 and NitAb and plant NIT4 NLases from *Arabidopsis thaliana* (GenBank: AAM65906) and *Nicotiana tabacum* (NP_001312683.1), it was shown

that the temperature optima of fungal NLases are lower than those of plant NIT4 (Piotrowski et al., 2001). The pH optima of NitAb and NitTv1 were like those of NIT4 (pH 7-9) (Piotrowski et al., 2001) and lower than those of NIT1 (pH 9) (Osswald et al., 2002). Comparison of the temperature stabilities of fungal and plant NLases is difficult due to different pre-incubation and reaction conditions.

In NitTv1, the pH stability profile was wider than the activity profile, i.e., at slightly acidic or slightly alkaline pH, the relative stability of the enzyme is higher than its relative activity. This effect can be explained by the so-called enzyme-specific pH effects that are possible with some NLases. For example, when the pH shifts from slightly alkaline to slightly acidic, the transformation of short helices into long ones can occur in the molecule of CynD (Jandhyala et al., 2003).

The ability of plant NLases and their fungal counterparts to form an amide as a reaction product has been termed NHase activity, and the NIT4 enzyme can be designated "bifunctional NLase/ NHase NIT4" (Piotrowski et al., 2001). It is necessary to clarify that amide-forming NLases differ from "true" NHases, which are metalloenzymes and do not belong to the "NLase" superfamily. NLases are more stable than NHases and they are often enantioselective unlike NHases whose enantioselectivity is limited.

The ratio of acid/ amide reaction products depends on the substrate, pH, temperature and enzyme. A pronounced effect of temperature and pH on acid/amide ratio was found in NitTv1. Similar effects were previously shown for the NLase from *P. fluorescens* (Fernandes, 2006). In the reactions of AlaCN, the products were Asp (acid) and Asn (amide), and their ratio was higher in NitTv1 and NitAb compared to NIT4 (Piotrowski, 2001).

The role and importance of NLases in biological processes may be related to the detoxification of both exogenous and endogenous nitriles some of which can participate in plant hormone biosynthesis (Howden and Preston 2009). Probably, fungal NLases are

important in the interaction of plants and fungi, and studying the properties of fungal NLases will help to understand the mechanism and nature of these interactions.

The NitEg enzyme from the fungus *Exidia glandulosa* is the first CynH characterized in Basidiomycota. The amino acid sequence is 86.29% (coverage 95%) identical to CynH from *Neurospora crassa* (GenBank XP_960160.2; UniProtKB: Q7RVT0). NitEg consists of 366 amino acid residues, while *N. crassa* consists of 351 residues. The CynH from *N. crassa* is one of the few CynHs that were previously purified (Basile et al., 2008) and at least partially characterized. *N. crassa* belongs to the phylum Ascomycota which contains the majority of CynH sequences known. A well characterized CynH (GenBank ABX75546) from another species of Ascomycota, *Aspergillus niger* (Rinágelová et al., 2014), is more distant from NitEg in terms of their sequences (cca. 65% identity). Its biochemical properties also slightly differ from those of NitEg (see below).

The use of a purified enzyme for wastewater treatment has an advantage over the use of whole cells of a recombinant organism, since the use of the latter can be regulatorily difficult (moreover, it could cause a contamination of the environment with genetically modified cells). However, purification of the enzyme inevitably leads to an increase in the cost of catalyst production. An alternative solution would be to use CFE, as it had a high specific activity (280 U/mg for NitEg) and can be made void of whole cells. The disadvantage of this alternative is that CFE is inferior in terms of specific activity compared to the purified enzyme.

CynHs have more than 60% amino acid sequence identity and yet they have different specific activities or pH profiles. Experimental conditions undoubtedly influence the results, but it is difficult to judge the strength of these factors. Nevertheless, even under identical reaction conditions, differences in pH profiles were shown (Basile et al., 2008). The resistance of the enzyme to alkaline conditions is of fundamental importance if the enzyme is intended

to be used in industrial wastewater. This is because the cyanide-containing wastewaters must have an alkaline pH to minimize the formation of gaseous HCN (extremely hazardous).

The efficiency of NitEg at alkaline pH was studied in this thesis and seems to be promising. Thus, the enzyme completely removed 25 mM cyanide at pH 9-9.5, or over 80% of it at pH 10. These data are in good agreement with the pH profile of the enzyme activity, with a fairly wide pH range (cca. 6-9).

NitEg showed more attractive properties than CynDs whose ability to biodegrade cyanide under alkaline conditions was studied previously (Carmona-Orozco et al., 2019, Park et al., 2017, Wang et al., 2012, Crum et al., 2015). Its specific activity of over 600 U/mg at pH 9 leaves other alternative biocatalysts behind. The ability of NitEg to remain active at high pH for a long time makes the catalyst efficient and allows it to degrade cyanide in highly concentrated solutions almost completely. A stabilizing effect of CynD immobilization was shown for alkaline conditions (Carmona-Orozco et al., 2019), and a similar effect is possible for NitEg and other CynHs.

Studies of CynDs from bacteria (*Bacillus*, *Pseudomonas* – reclassified *Stutzerimonas*) and CynH from *N. crassa* have shown that the C-terminus is of great importance for the thermal stability of these enzymes (Park et al., 2017, Crum et al., 2015). CynH was superior to CynD in resistance to elevated temperatures; it retained 90% activity after 4 hours at 42 °C (Crum et al., 2015) and 50% after 24 hours at 43 °C (Basile et al., 2008). Other CynHs (from *G. sorghi* and *Aspergillus nidulans*) were less stable under the same conditions (Basile et al., 2008). CynH from *Aspergillus nidulans* is very similar to CynH from *A. niger* (Rinágelová et al., 2014) in terms of sequence. The thermostability of CynH from *A. niger* was studied by a different method with pre-incubation of the enzyme for 1 hour, and the enzyme did not show sufficient stability at temperatures above 35 °C. The NitEg enzyme showed a good thermal stability at 27 or 37 °C with retention of activity after 24 hours, but at 43 °C the enzyme

retained only 10% residual activity after the same time interval. At a temperature of 50 °C, NitEg quickly lost its activity like other CynHs (Basile et al., 2018).

Comparison of the kinetic parameters V_{max} and K_M of NitEg with those of previously studied CynHs from *A. niger* (Rinágelová et al., 2014) and *G. sorghi* (Jandhyala et al., 2005) showed that both parameters were the lowest in NitEg: V_{max} was 1335 U/mg, and K_M was 22 mM, while in the CynH from *A. niger* V_{max} was 6800 U/mg, K_M was 109 mM and in the CynH from *G. sorghi* V_{max} was 4400 U/mg, and K_M was 90 mM.

When comparing the ratio of V_{max} to K_M, it was found that NitEg and CynH from *A. niger* have similar values of catalytic efficiency, 60 and 62 U.l/mg/mmol, respectively, while this parameter is lower in CynH from *G. sorghi* (49 U.l/mg/mmol).

The effect of high K_M on the ability to degrade lower concentrations of cyanide was not as significant, since the removal of 0.6 mM fCN by NitEg was almost complete. Degradation of the 100 mM cyanide solution was not complete with 96–98% and this can be explained by inactivation of the enzyme.

The values of k_{cat} were calculated for CynHs with known V_{max} and identical molecular weights (40-42 kDa). NitEg and CynHs from *G. sorghi* and *A. niger* have k_{cat} (in s^{-1}) of 927, 3000, 4500, respectively, and the k_{cat}/K_M (1/s/mmol) ratios were 42, 33, and 41, respectively. According to the BRENDA database, similar NLases have k_{cat}/K_M values ranging from 0.001 to 205 1/s/mmol and the highest value belonged to NLase from *Pyrococcus sp.* for benzonitrile, but in other parameters this NLase was inferior to NitEg (Dennett et al., 2016).

A future scale-up of the CynH production is important for the envisioned industrial uses of the enzyme as a prospective tool for environmental and population protection. Previously, the enzyme has been prepared from fungal cultures. Fungal cultivation can be carried out on a large scale; for instance, the fungus *Fusarium oxysporum* has been cultivated in a volume of 45 liters (Yanase et al., 2000), and the fungus *Fusarium solani* in a volume of

10 liters (Barclay et al., 1998). However, production of the CynH in heterologous strain was only carried out on a small scale (Basile et al., 2008, Rinágelová et al., 2014). Nevertheless, heterologous production of another NLase enzyme was successful at large scale; the culture was grown in a fermenter with a capacity of 500 l and cultivation protocol was optimized (using lactose as an inducer). Under such conditions, 13 g dry biomass per liter were obtained (Xue et al., 2015). Accordingly, the production of the enzyme NitEg may be possible in large volumes. Taking into account the much higher specific activity of the CynH enzymes compared to other NLases, the production of the order of 10^6–10^7 U/l may be realistic.

CynHs and CynDs were shown to be effective in cyanide degradation in wastewaters from some industries. Table 12 combines data on the use of these enzymes in simulated and real wastewaters. In the study with the CynH from *N. crassa*, real wastewaters (electroplating bath residues) contained approximately 100 mM fCN and, optionally, silver or copper ions (Basile et al., 2008). For the degradation of cyanide in a solution with silver ions, the enzyme was used at a concentration of 7–13 μg/ml, while for the reaction mixture with copper ions, the concentration of the enzyme was 10 times higher. The presence of silver and copper ions reduced the cyanide removal efficiency by 10% and 30%, respectively. However, the comparison of these results with those obtained for NitEg is difficult due to insufficient data on the types of wastewater used in the previous study (concentration of metal ions unknown). Moreover, pH of the previous solutions was 8, while for NitEg pH was 9.

CynH from *N. crassa* was able to completely remove 100 mM cyanide in the absence of metal ions within 1 hour (Basile et al., 2008) similar to NitEg but, also here, pH of the solutions was different (pH 8 and pH 9 for CynH from *N. crassa* and NitEg, respectively). However, other CynHs took 12-48 hours to degrade a similar amount of cyanide (Basile et al., 2008). Studies of the kinetic parameters of the enzyme, degradation of fCN in various reaction mixtures, and the shelf life of the enzyme were carried out only for NitEg. The characteristics

of the enzyme obtained in this work showed a high promise of the enzyme for the degradation of cyanide; moreover, according to the data accumulated in this thesis, this enzyme may be one of the best known biocatalysts with this ability.

Table 12. Enzyme efficiency of CynH and CynD in real wastewater and simulated mixtures

Reaction mixture, free cyanide (mM), pH	Biocatalyst	Removal (Time)	Reference
Buffer, 0.6 mM, pH 9.0	NitEg*	100% (10 min)	This work
Buffer, 4.5 mM, pH 9.0		100% (30 min)	
Buffer, 25 mM, pH 9.0		100% (20 min)	
Buffer, 25 mM, pH 9.5		100% (45 min)	
Buffer, 25 mM, pH 10.0		83% (1 h)	
Buffer, 25 mM, pH 10.5		22% (1 h)	
Buffer, 100 mM, pH 9.0		98% (2 h)	This work
Buffer, 100 mM, pH 8.0	CynH (*N. crassa*)*	100% (1 h)	(Basile et al., 2008)
Buffer, 10 mM, pH 8.0	CynH (*A. niger*)*	100% (5 min)	(Martínková et al., 2016)
Coking effluent, 0.6 mM, pH 9.0	NitEg*	100% (1.5 h)	This work
Mine effluent, 528 mM, pH 11	CynD (*B. pumilus*) immobilized cells	43% (4 h)	(Carmona-Orozco et al., 2019)
Mine effluent, 17.6 mM, -		98% (4 h)	
Petrochemical effluent, simulated, 4.5 mM, pH 9.1	NitEg*	96% (45 min)	This work
Cu-plating effluent, simulated, 100 mM, pH 9.0		96% (2 h)	This work
Ag-plating effluent, simulated, 100 mM, pH 9.0		98 (2 h)	This work
Cu-plating effluent, diluted, 100 mM, pH 8.0	CynH (*N. crassa*)*	≈ 65% (12 h)	(Basile et al., 2008)
Ag-plating effluent, diluted, 100 mM, pH 8.0		≈ 90 (2 h)	(Basile et al., 2008)

*purified

To use the biocatalyst in real industrial conditions, scaling up the production of the enzyme is necessary. Another potential solution to increase the efficiency of the degradation process may be enzyme immobilization, which can increase the stability of the enzyme and make it possible to reuse it.

The main advantage of using biocatalysts for wastewater treatment is environmental safety. Unlike physico-chemical methods, which can cause additional contamination, the products resulting from biocatalysis are relatively benign. The use of the enzyme is possible at high concentrations of cyanide and, most importantly, the enzyme can maintain its activity at an alkaline pH.

The problem of neutralizing cyanide spills, as a result of industrial accidents, is still very relevant, and effective solutions have not been found yet. The solution to this problem may possibly arise in the field of biotechnology. It should be noted, however, that for technical reasons, the application of enzymes for cyanide decontamination for the sake of environmental or population protection would be most feasible for small-scale spills and accidents and for waste-free bioremediation of wastewater in industries where the wastewater amounts are not excessive, e.g., for metal electroplating baths.

The cyanide-transforming enzymes can also serve other purposes, for example, they can be used for detecting cyanide and creating biosensors for analyzing, e.g., samples of industrial effluents and other industrial waste, surface water, groundwater, plant and food samples or soil. Routine test for fCN are based on spectrophotometry or the use of cyanide-selective electrodes, but have several disadvantages (interference and use of toxic reagents in photometric methods, high costs and low stability of electrodes, etc.).

Experimental biosensors for free cyanide were based on the CynD enzymes and the compounds analyzed were formate or ammonia (Mak et al., 2005; Turek et al. 2007). For example, formate was determined by a coupled reaction catalyzed by a NAD-dependent formate dehydrogenase (FDH, EC 1.17.1.9), and the amount of NADH was determined. A sensor of this type consisted of two cartridges with immobilized enzymes – CynD and FDH. The buffer with the sample was passed through the system, while NAD was added, and the NADH formed was determined using an electrode chip (Ketterer et al., 2010). It may also be

possible to determine NADH production photometrically. However, this principle, although used in various other assays, has not been used to determine fCN. In addition, CynD is not optimal for this application as it is sensitive to alkaline media which are typically used to store fCN solutions and wastes.

In this respect, CynHs, such as those studied in this work, outperform CynDs, as they are active even at pH above 10. In addition, their specific activities are usually ten fold higher in comparison with the CynD activities. However, the product of CynH, formamide, is difficult to determine directly. Although there are spectrophotometric methods for formamide (Cluness et al., 1993), they are not sensitive enough. To transform formamide into measurable products such as formate, CynH must be combined with a formamidase. Fortunately, these formamidases are highly active (with specific activities comparable with those of CynHs) and have been produced recombinantly (Skouloubris et al., 2001; Soriano-Maldonado et al., 2011).

Recently, a proof-of-concept for this type of enzymatic assay of fCN (Křístková et al., 2023) was provided. This CynH-formamidase enzyme system, in which FDH is coupled in the last step, is attractive in terms of selectivity, sensitivity, non-toxicity and mildness. Of course, the possible interference of formic acid must be taken into account and the corresponding controls must be performed. The determination of NADH (generated in the last step) at 340 nm is quite sensitive, and the sensitivity can even be increased by replacing this spectrophotometry with fluorimetry. No toxic chemicals are used and, moreover, the fCN in the sample is detoxified during the reaction.

Finally, very small amounts of the enzyme are sufficient, as the specific activities of CynH and formamide are in the order of hundreds to thousands. Therefore, the cost of the enzyme can be managable, especially when the method is performed with microtitre plates.

6. Conclusion

The aim of the work was to evaluate the current status of cyanide wastewater treatment and to assess the feasibility of applying enzymes (NLases, CynHs) in this field, to give insight into novel methods of green detoxification for the sake of protecting population and environment against toxic effects of this hazardous chemical. The literature survey shows that the trend in the cyanide effluent remediation is towards processes combining various principles (physical, chemical, biological) but that the influence of enzymatic processes on these environmental technologies is still limited and rather marginal. In order to contribute to the development of the enzymatic processes, a strategy based on the search for suitable enzymes *in silico*, their production in recombinant hosts and the evaluation of their catalytic properties in model solutions was used in this study.

The first part of the thesis focuses on the search for homologues of plant NLases in fungi and their characterization including the identification of their substrate-specificity subtype. NLases NitTv1 and NitAb, being homologues of NIT4 according to their sequence, were confirmed to act on β-cyano-L-alanine (AlaCN), the key intermediate of fCN metabolism in plants. The results suggest a physiological role of these enzymes: it is likely that these NLases enable fungi to colonize plants, overcoming the high toxicity of AlaCN. In addition, the fungal enzymes exhibited a broader substrate specificity compared to plant NIT4, combining features of the plant NIT1–NIT3 and NIT4 types. Thus, these NLases can increase the resistance of fungi to other natural (plant) nitriles, which are generally toxic. The new fungal NLases produce amides and/or carboxylic acids from these substrates, with one of them, the NitTv1 enzyme, showing activity and stability over a wide pH range. This also suggests a synthetic potential of the enzyme. The presence of NIT4 in higher plants is probably one of the reasons for the important role of plants in the biodegradation of fCN in controlled and passive biosystems. Similarly, NIT4 can be one of the enzymes that contribute to the

degradation of fCN by some fungi, a process that has been observed but not adequately explained.

The second part of the study is dedicated to two fungal CynHs, analyzing their operating conditions, optimum and stability to identify the most promising candidate for cyanide waste processing. The NitSh and NitEg enzymes are the first CynHs described in Basidiomycota, with NitEg emerging as the superior candidate; it shows high specific activity and is resistant to alkaline pH and contaminants, tolerates high concentrations of fCN and other industrial pollutants, and is stable during long-term storage. Besides cyanide decontamination, its potential application as an effective biocatalyst under alkaline conditions may extend to the development of analytical tools – cyanide bioassays and biosensors. This work has created a basis for further research of the enzyme potential in the detoxification of wastewater and in analytics of cyanide as a hazardous chemical for human health and environment.

References

Acha V, Hoang LV, Trapy P-H, Bak A, Duquennoy J, Marion R, Coste C, Pourret O. Simultaneous oxidation of model solutions and polluted waters in an ozonation semi-industrial pilot plant. In Proceedings of the World Congress and Exposition. International Ozone Association, International Ultraviolet Association. 2013 (September 22 – 26)

Akcil A. Managing cyanide: Health, safety and risk management practices at Turkey's Ovacik gold - silver mine. J Clean Prod 2006; 14(8): 727 – 735. doi: 10.1016/j.jclepro.2004.11.006

An X, Cheng Y, Huang M, Sun Y, Wang H, Chen X, Wang J, Li D, Li C. Treating organic cyanide-containing groundwater by immobilization of a nitrile-degrading bacterium with a biofilm-forming bacterium using fluidized bed reactors. Environ Pollut 2018; 237: 908-916. doi: 10.1016/ j.envpol.2018.01.087

Anning C, Wang JX, Chen P, Batmunkh I, Lyu XJ. Determination and detoxification of cyanide in gold mine tailings: A review. Waste Manag Res 2019; 37(11): 1117 – 1126. doi: 10.1177/0734242X19876691

Anning C, Erdenekhuyag BO, Yao G, Li HJ, Zhao JG, Wang LJ, Lyu XJ. Principles and methods of bio detoxification of cyanide contaminants. J Mater Cycles Waste Manag 2020; 22(4): 939 – 954. doi: 10.1007/s10163-020-01013-6

Baeissa ES, Mohamed RM. Enhancement of photocatalytic properties of Ga_2O_3-SiO_2 nanoparticles by Pt deposition. Chinese J Catal 2013; 34(6): 1167 – 1172. doi: 10.1016/S1872-2067(12)60570-1

Bagabas A, Alshammari A, Aboud MFA, Kosslick H. Room-temperature synthesis of zinc oxide nanoparticles in different media and their application in cyanide photodegradation. Nanoscale Res Lett 2013; 8(1): 516. doi: 10.1186/1556-276X-8-516

Ban Q, Zhang L, Li J. Correlating bacterial and archaeal community with efficiency of a coking waste- water treatment plant employing anaerobic-anoxic-oxic process in coal industry. Chemosphere 2022; 286(Pt 2): 131724. doi: 10.1016/j.chemosphere.2021. 131724

Banerjee A, Sharma R, Banerjee UC. The nitrile-degrading enzymes: current status and future prospects. Appl Microbiol Biotechnol 2002; 60(1-2): 33 – 44. doi: 10.1007/s00253-002-1062-0

Barclay M, Tett VA, Knowles CJ. Metabolism and enzymology of cyanide/metallocyanide biodegradation by *Fusarium solani* under neutral and acidic conditions. Enzym Microb Technol 1998; 23(5): 321 – 330. doi: 10.1016/S0141-0229(98)00055-6

Basile LJ, Willson RC, Sewell BT, Benedik MJ. Genome mining of cyanide-degrading nitrilases from filamentous fungi. Appl Microbiol Biotechnol 2008; 80(3): 427 – 435. doi: 10.1007/s00253- 008-1559-2

Benedik MJ, Sewell BT. Cyanide-degrading nitrilases in nature. J Gen Appl Microbiol 2018; 64(2): 90 – 93. doi 10.2323/jgam.2017.06.002

Bhalla TC, Kumar V, Kumar V, Thakur N, Savitri. Nitrile metabolizing enzymes in biocatalysis and biotransformation. Appl Biochem Biotechnol 2018; 185(4): 925 – 946. doi: 10.1007/s12010-018-2705-7

Bini L, Müller C, Vogt D. Mechanistic studies on hydrocyanation reactions. ChemCatChem 2010; 2(6): 590 – 608. doi: 10.1002/cctc.201000034

Bogucki S, Weir S. Pulmonary manifestations of intentionally released chemical and biological agents. Clin Chest Med 2002; 23(4): 777 – 794. doi: 10.1016/s0272-5231(02)00027-8

Bolarinwa IF, Orfila C, Morgan MR. Amygdalin content of seeds, kernels and food products commercially-available in the UK. Food Chem 2014; 152: 133 - 139. doi: 10.1016/j. foodchem.2013.11.002

Bradford MM. A rapid and sensitive method for the quantitation of microgram quantities of protein utilizing the principle of protein-dye binding. Anal Biochem 1976; 72(1): 248 – 254. ISSN 0003-2697

BRENDA. The Comprehensive Enzyme Information System. Available online: https://brenda-enzymes.org (accessed on 2 November 2021).

Brenner C. Catalysis in the nitrilase superfamily. Curr Opin Struc Biol 2002; 12(6): 775 - 782. doi: 10.1016/s0959-440x(02)00387-1

Brunner S, Eppinger E, Fischer S, Groning J, Stolz A. Conversion of aliphatic nitriles by the arylacetonitrilase from *Pseudomonas fluorescens* EBC191. World J Microbiol Biotechnol 2018; 34(7): 91. doi: 10.1007/s11274-018-2477-9

Buonvino S, Arciero I, Melino S. Thiosulfate-cyanide sulfurtransferase a mitochondrial essential enzyme: from cell metabolism to the biotechnological applications. Int J Mol Sci 2022; 23(15): 8452. doi: 10.3390/ijms23158452

Burneo BS., Juárez AS, Nieto-Monteros DA. Un-steady state modeling for free cyanide removal and biofilm growth in a RBC batch process. J Hazard Mater 2020; 388: 120647. doi: 10.1016/j.jhazmat.2019.05.040

Cabello P, Luque-Almagro VM, Olaya-Abril A, Sáez LP, Moreno-Vivian C, Roldán MD. Assimilation of cyanide and cyano-derivatives by *Pseudomonas pseudoalcaligenes* CECT5344: From omic approaches to biotechnological applications. FEMS Microbiol Lett 2018; 365(6): fny032. doi: 10.1093/ femsle/fny032

Carmona-Orozco ML, Panay AJ. Immobilization of *E. coli* expressing *Bacillus pumilus* CynD in three organic polymer matrices. Appl Microbiol Biotechnol 2019; 103(13): 5401 – 5410. doi: 10.1007/s00253-019-09859-z

Chen CY, Chen SC, Fingas M, Kao CM. Biodegradation of propionitrile by *Klebsiella oxytoca* immobilized in alginate and cellulose triacetate gel. J Hazard Mater 2010; 177(1-3): 856-863. doi: 10.1016/j.jhazmat.2009.12.112

Chen Y, Song YH, Chen Y, Zhang XW, Lan XZ. Comparative experimental study on the harm- less treatment of cyanide tailings through slurry electrolysis. Sep Purif Technol 2020; 251: 117314. doi: 10.1016/j.seppur.2020.117314

Chen M, Li S, Jin C, Shao M, Huang Z, Xie X. Removal of metal-cyanide complexes and recovery of Pt(II) and Pd(II) from wastewater using an alkali–tolerant metal-organic resin. J Hazard Mater 2021; 406: 124315. doi: 10.1016/j.jhazmat.2020.124315

Cluness MJ, Turner PD, Clements E, Brown DT, O´Reilly C. Purification and properties of cyanide hydratase from *Fusarium lateritium* and analysis of the corresponding *chy1* gene. J Gen Microbiol 1993; 139: 1807-1815. doi: 10.1099/00221287-139-8-1807

Code of Federal Regulations, 40CFR141, Revised July 1, 2008. Fed. Regist. 2002; Vol 448.

Code of Federal Regulations, 40CFR413, 40CFR131, 40CFR132; Revised July 1, 2008, Fed. Regist. 2008; 214–215, 451–463, 493–494

Council Directive 75/440/EEC of 16 June 1975 concerning the quality required of surface water intended for the abstraction of drinking water in the Member States. https://eur-lex.europa.eu/legalcontent/EN/TXT/PDF/?uri=CELEX:31975L0440

Crum MA, Park JM, Sewell BT, Benedik MJ. C-terminal hybrid mutant of *Bacillus pumilus* cyanide dihydratase dramatically enhances thermal stability and pH tolerance by reinforcing oligomerization. J Appl Microbiol 2015; 118(4): 881 – 889. doi: 10.1111/jam.12754

Crum MA, Sewell BT, Benedik MJ. *Bacillus pumilus* cyanide dihydratase mutants with higher catalytic activity. Front Microbiol 2016; 7: 1264. doi: 10.3389/fmicb.2016.01264

Cuff JA, Clamp ME, Siddiqui AS, Finlay M, Barton GJ. JPred: A consensus secondary structure prediction server. Bioinformatics 1998; 14(10): 892 – 893. doi: 10.1093/bioinformatics/14.10.892

Dennett GV, Blamey JM. A new thermophilic nitrilase from an Antarctic hyperthermophilic microorganism. Front Bioeng Biotechnol 2016; 4: 5. doi: 10.3389/fbioe.2016.00005

Directive 2006/21/EC of the European Parliament and of the Council: of 15 March 2006 on the management of waste from extractive industries and amending Directive 2004/35/EC. In: Official Journal of the European Union. European Parliament, Council of the European Union, 2006, 11.4.2006, 102/15. https://eur-lex.europa.eu/legal-content/EN/TXT/?uri=celex%3A32006L0021

Directive 2000/60/EC of the European Parliament and of the Council of 23 October 2000 establishing a framework for Community action in the field of water policy. Official Journal of the European Communities. https://eur-lex.europa.eu/legal-content/EN/TXT/PDF/?uri=OJ:L:2000:327:FULL

Directive 2012/18/EU of the European Parliament and of the Council of 4 July 2012 on the control of major-accident hazards involving dangerous substances, amending and subsequently repealing Council Directive 96/82/EC. Official Journal of the European Union. Available from: https://eur-lex.europa.eu/legal-content/EN/TXT/PDF/?uri=CELEX:32012L0018

Ebbs S. Biological degradation of cyanide compounds. Curr Opin Biotechnol 2004; 15(3): 231 – 236. doi: 10.1016/j.copbio.2004.03.006

Ebbs SD, Kosma DK, Nielson EH, Machingura M, Baker AJM, Woodrow IE. Nitrogen supply and cyanide concentration influence the enrichment of nitrogen from cyanide in wheat

(*Triticum aestivum L.*) and sorghum (*Sorghum bicolor L.*). Plant Cell Environ 2010; 33(7): 1152 – 1160. doi: 10.1111/j.1365-3040.2010.02136.x

Eisler R, Wiemeyer SN. Cyanide hazards to plants and animals from gold mining and related water issues. Rev Environ Contam Toxicol 2004; 183: 21 - 54. doi: 10.1007/978-1-4419-9100-3_2

Fan L, Yao H, Deng S, Jia F, Cai W, Hu Z, Guo J, Li H. Performance and microbial community dynamics relationship within a step-feed anoxic/oxic/anoxic/oxic process (SF-A/O/A/O) for coking wastewater treatment. Sci Total Environ 2021; 792: 148263. doi: 10.1016/j.scitotenv.2021.148263

Fernandez RF, Kunz DA. Bacterial cyanide oxygenase is a suite of enzymes catalyzing the scavenging and adventitious utilization of cyanide as a nitrogenous growth substrate. J Bacteriol 2005;187(18): 6396 – 6402. doi: 10.1128/JB.187.18.6396-6402.2005

Fernandes BCM, Mateo C, Kiziak C, Chmura A, Wacker J, van Rantwijk F, Stolz A, Sheldon RA. Nitrile hydratase activity of a recombinant nitrilase. Adv Synth Catal 2006; 348(18): 2597 – 2603. doi: 10.1002/adsc.200600269

Fisher FB, Brown JS. Colorimetric determination of cyanide in stack gas and waste water. Anal Chem 1952; 24(9): 1440 – 1444. doi: 10.1021/ac60069a014

Fry WE, Millar RL. Cyanide degradation by an enzyme from *Stemphylium loti*. Arch Biochem Biophys 1972; 151(2): 468 - 474. doi: 10.1016/0003-9861(72)90523-1

García I, Castellano JM, Vioque B, Solano R, Gotor C, Romero LC. Mitochondrial β-cyanoalanine synthase is essential for root hair formation in *Arabidopsis thaliana*. Plant Cell 2010; 22(10): 3268 – 3279. doi: 10.1105/tpc.110.076828

Ghosh TK, Biswas P, Bhunia P, Kadukar S, Banerjee SK, Ghosh R, Sarkar S. Application of coke breeze for removal of colour from coke plant wastewater. J Environ Manag 2022; 302(Pt A): 113800. doi: 10.1016/j.jenvman.2021.113800

Gleadow RM, Møller BL. Cyanogenic glycosides: synthesis, physiology, and phenotypic plasticity. Annu Rev Plant Biol 2014; 65: 155 – 185. doi: 10.1146/annurev-arplant-050213-040027

Global mine production of silver from 2005 to 2020, 2021; https://www.statista.com/statistics/253293/silver-production-volume-worldwide/

Gold mine production worldwide from 2005 to 2020, 2021; https://www.statista.com/statistics/238414/global-goldproduction-since-2005/

Guadalima MPG, Monteros DAN. Evaluation of the rotational speed and carbon source on the biological removal of free cyanide present on gold mine wastewater, using a rotating biological contactor. J Water Process Eng 2018; 23: 84 – 90. doi: 10.1016/j.jwpe.2018.03.008

Gupta N. Balomajumder C, Agarwal VK. Enzymatic mechanism and biochemistry for cyanide degradation: A review. J Hazard Mater 2010; 176(1-3): 1 - 13. doi: 10.1016/j.jhazmat.2009.11.038

Gupta P, Ahammad SZ, Sreekrishnan TR. Improving the cyanide toxicity tolerance of anaerobic reactor: Microbial interactions and toxin reduction. J Hazard Mater 2016; 315: 52 – 60. doi: 10.1016/j.jhazmat.2016.04.028

Howden AJM, Preston GM. Nitrilase enzymes and their role in plant–microbe interactions. Microb Biotechnol 2009; 2(4): 441 – 451. doi: 10.1111/j.1751-7915.2009.00111.x

Howden AJ, Harrison J, Preston GM. A conserved mechanism for nitrile metabolism in bacteria and plants. Plant J 2009; 57(2): 243 - 253. doi: 10.1111/j.1365-313X.2008.03682.x

Ibáñez MI, Cabello P, Luque-Almagro VM, Sáez LP, Olaya A, de Medina VS, de Castro MDL., Moreno-Vivian C, Roldán MD. Quantitative proteomic analysis of *Pseudomonas pseudoalcaligenes* CECT5344 in response to industrial cyanide-

containing wastewaters using Liquid Chromatography-Mass Spectrometry/Mass Spectrometry (LC-MS/MS). PLoS One 2017; 12(3): e0172908. doi: 10.1371/journal. pone. 0172908

Ingvorsen K, Højer-Pedersen B, Godtfredsen SE. Novel cyanide-hydrolyzing enzyme from *Alcaligenes xylosoxidans* subsp. *denitrificans*. Appl Environ Microbiol 1991; 57(6): 1783 – 1789. doi: 10.1128/aem.57.6.1783-1789.1991

Jandhyala D, Berman M, Meyers PR, Sewell BT, Wilson RC, Benedik MJ. CynD, the cyanide dihydratase from *Bacillus pumilus*: Gene cloning and structural studies. Appl Environ Microbiol 2003; 69(8): 4794 - 4805. doi: 10.1128/AEM.69.8.4794-4805.2003

Jandhyala DM, Willson RC, Sewell BT, Benedik MJ. Comparison of cyanide-degrading nitrilases. Appl Microbiol Biotechnol 2005; 68(3): 327 – 335. doi: 10.1007/s00253-005-1903-8

Jarrah N, Mu'azu ND. Simultaneous electro-oxidation of phenol, CN^-, S^{2-} and NH_4^+ in synthetic wastewater using boron doped diamond anode. J Environ Chem Eng 2016; 4: 2656 – 2664. doi: 10.1016/j.jece.2016.04.011

Jenrich R, Trompetter I, Bak S, Olsen CE, Moller BL, Piotrowski M. Evolution of heteromeric nitrilase complexes in Poaceae with new functions in nitrile metabolism. Proc Natl Acad Sci U S A 2007; 104(47): 18848 – 18853. doi:10.1073/pnas.0709315104

Kaplan O, Veselá AB, Petříčková A, Pasquarelli F, Pičmanová M, Rinágelová A, Bhalla TC, Pátek M, Martínková L. A comparative study of nitrilases identified by genome mining. Mol Biotechnol 2013; 54(3): 996 - 1003. doi: 10.1007/s12033-013-9656-6

Ketterer L, Keusgen M, Amperometric sensor for cyanide utilizing cyanidase and formate dehydrogenase. Anal Chim Acta 2010; 673(1): 54-59. doi: 10.1016/j.aca.2010.04.058

Křístková B, Martínková L, Kulik N, Rucká L, Novotný P, Grulich M, Pátek M. Cascade enzymatic reactions for assay of free cyanide, 4th International Conference on Food

Bioactives & Health (FBHC 2023), 18.9.-21.9.2023, Prague (Czech Republic). Book of abstracts: page 228, poster P110

Kumar R, Saha S, Dhaka S, Kurade MB, Kang CU, Baek SH, Jeon BH. Remediation of cyanide-contaminated environments through microbes and plants: a review of current knowledge and future perspectives. Geosystem Eng 2017; 20(1): 28 – 40. doi: 10.1080/ 12269328.2016.1218303

Kumar V, Kumar V, Bhalla TC. Alkaline active cyanide dihydratase of *Flavobacterium indicum* MTCC 6936: Growth optimization, purification, characterization and in silico analysis. Int J Biol Macromol 2018; 116: 591 - 598. doi: 10.1016/j.ijbiomac.2018.05. 075

Kushwaha M, Kumar V, Mahajan R, Bhalla TC, Chatterjee S, Akhter Y. Molecular insights into the activity and mechanism of cyanide hydratase enzyme associated with cyanide biodegradation by *Serratia marcescens*. Arch Microbiol 2018; 200(6): 971 - 977. doi: 10.1007/s0020 3-018-1524-0

Kuyucak N, Akcil A. Cyanide and removal options from effluents in gold mining and metallurgical processes. Miner Eng 2013; 50 – 51: 13 – 29. doi: 10.1016/j.mineng. 2013.05.027

Kwiecińska-Mydlak A, Sajdak M, Rychlewska K, Figa J. The role of a chemical loop in removal of hazardous contaminants from coke oven wastewater during its treatment. Open Chem 2019; 17(1): 1288 – 1300. doi: 10.1515/chem-2019-0142

Laemmli UK. Cleavage of the structural proteins during assembly of the head of bacteriophage T4. Nature 1970; 227(5259): 680–685. doi: 10.1038/227680a0

Li C, Sun Y, Yue Z, Huang M, Wang J, Chen X, An X, Zang H, Li D, Hou N. Combination of a recombinant bacterium with organonitrile-degrading and biofilm-forming

capability and a positively charged carrier for organonitriles removal. J Hazard Mater 2018; 353: 372 – 380. doi: 10.1016/j.jhazmat.2018.03.058

Li Q, Lu H, Yin Y, Qin Y, Tang A, Liu H, Liu Y. Synergic effect of adsorption and biodegradation enhance cyanide removal by immobilized *Alcaligenes sp*. strain DN25. J Hazar Mater 2019; 364: 367 - 375. doi: 10.1016/j.jhazmat.2018.10.007

Li YJ, Yang H, Zhang YC, Hu J, Huang JH, Ning P, Tian SL. Catalytic decomposition of HCN on copper manganese oxide at low temperatures: Performance and mechanism. Chem Eng J 2018; 346: 621 – 629. doi: 10.1016/j.cej.2018.04.055

Liang WS. Drought stress increases both cyanogenesis and beta-cyanoalanine synthase activity in tobacco. Plant Sci 2003; 165(5): 1109 – 1115. doi: 10.1016/S0168-9452(03) 00306-6

Liu YL, Cheng H, He YT. Application and mechanism of sludge-based activated carbon for phenol and cyanide removal from bio-treated effluent of coking wastewater. Processes 2020; 8(1): 82. doi: 10.3390/pr8010082

López ALB, Castro IM. Niobium-titanium-based photocatalysts: Its potential for free cyanide oxidation in residual aqueous effluent. Front Chem 2020; 8: 99. doi: 10.3389/fchem. 2020.00099

Luque-Almagro VM, Moreno-Vivian C, Roldán MD. Biodegradation of cyanide wastes from mining and jewellery industries. Curr Opin Biotechnol 2016; 38: 9 – 13. doi: 10.1016/j. copbio.2015.12.004

Machingura M, Ebbs SD. Increased beta-cyanoalanine synthase and asparaginase activity in nitrogen-deprived wheat exposed to cyanide. J Plant Nutr Soil Sci 2010; 173(6): 808 – 810. doi: 10.1002/jpln.201000164

Mak KKW, Law AWC, Tokuda S, Yanase H, Renneberg R. Application of cyanide hydrolase from *Klebsiella* sp. in a biosensor system for the detection of low-level cyanide. Appl Microbiol Biotechnol 2005; 67(5): 631-636. doi: 10.1007/s00253-004-1825-x

Makumire S, Su SY, Weber BW, Woodward JD, Kimani SW, Hunter R, Sewell BT. The structures of the C146A variant of the amidase from *Pyrococcus horikoshii* bound to glutaramide and acetamide suggest the basis of amide recognition. J Struct Biol 2022; 214(2): 107859. doi: 10.1016/j.jsb.2022.107859

Mamelkina MA, Herraiz-Carbone M, Cotillas S, Lacasa E, Saez C, Tuunila R, Sillanpaa M, Hakkinen A, Rodrigo MA. Treatment of mining wastewater polluted with cyanide by coagulation processes: A mechanistic study. Sep Purif Technol 2020; 237: 116345. doi: 10.1016/j.seppur.2019.116345

Martínková L, Veselá AB, Rinágelová A, Chmátal M. Cyanide hydratases and cyanide dihydratases: Emerging tools in the biodegradation and biodetection of cyanide. Appl Microbiol Biotechnol 2015; 99(21): 8875 – 8882. doi: 10.1007/s00253-015-6899-0

Martínková L, Chmátal M. The integration of cyanide hydratase and tyrosinase catalysts enables effective degradation of cyanide and phenol in coking wastewaters. Water Res 2016; 102: 90 – 95. doi: 10.1016/j.watres.2016.06.016

Martínková L, Křen V. Biocatalytic production of mandelic acid and analogues: A review and comparison with chemical processes. Appl Microbiol Biotechnol 2018; 102(9): 3893 – 3900. doi: 10.1007/s00253-018-8894-8

Mekuto L, Jackson VA, Ntwampe SKO. Biodegradation of free cyanide using *Bacillus sp*. consortium dominated by *Bacillus safensis, lichenformis* and *tequilensis* strains: A bioprocess supported solely with whey. J Bioremed Biodeg 2013; S18: 004. doi: 10.4172/2155-6199.S18-004

Mekuto L, Ntwampe SKO, Jackson VA. Biodegradation of free cyanide and subsequent utilization of biodegradation by-products by *Bacillus* consortia: optimization using response surface methodology. Environ Sci Pollut Res Int 2015; 22(14): 10434 – 10443. doi: 10.1007/s11356-015-4221-4

Mekuto L, Ntwampe SKO, Akcil A. An integrated biological approach for treatment of cyanidation wastewater. Sci Total Environ 2016; 571: 711 – 720. doi: 10.1016/j. scitotenv.2016.07.040

Mekuto L, Ntwampe SKO, Utomi CE, Mobo M, Mudumbi JB, Ngongang MM, Akinpelu EA. Performance of a continuously stirred tank bioreactor system connected in series for the biodegradation of thiocyanate and free cyanide. J Environ Chem Eng 2017; 5(2): 1936 – 1945. doi: 10.1016/j.jece.2017.03.038

Meyers PR, Rawlings DE, Woods DR, Lindsey GG. Isolation and characterization of a cyanide dihydratase from *Bacillus pumilus* C1. J Bacteriol 1993; 175(19): 6105 – 6112. doi: 10.1128/jb.175.19.6105-6112.1993

Mondal A, Sarkar S, Nair UG. Comparative characterization of cyanide-containing steel industrial wastewater. Water Sci Technol 2021; 83(2): 322 – 330. doi: 10.2166/wst. 2020.563

Montalvo Andia JP, Ticona Cayte AE, Illachura Rodriguez JM, López Belón L, Cárdenas Málaga MA, Teixeira L. Combined treatment based on synergism between hydrodynamic cavitation and H_2O_2 for degradation of cyanide in effluents. Miner Eng 2021; 171: 107119. doi: 10.1016/j.mineng.2021.107119

Motegh M, van Ommen JR, Appel PW, Kreutzer MT. Scale-up study of a multiphase photocatalytic reactor-degradation of cyanide in water over TiO_2. Environ Sci Technol 2014; 48(3): 1574 – 1581. doi: 10.1021/es403378e

Mulelu AE, Kirykowicz AM, Woodward JD. Cryo-EM and directed evolution reveal how *Arabidopsis* nitrilase specificity is influenced by its quaternary structure. Commun Biol 2019; 2: 260. doi: 10.1038/s42003-019-0505-4

MyCurveFit. https://mycurvefit.com (accessed on 7 July 2020)

National Primary Drinking Water Regulation. Code of Federal Regulations, Part 141, Title 40, 2008. Fed. Regist. 2008. 22, 448. https://www.ecfr.gov/current/title-40/chapter-I/subchapter-D/part-141

Nolan LM, Harnedy PA, Turner P, Hearne AB, O'Reilly C. The cyanide hydratase enzyme of *Fusarium lateritium* also has nitrilase activity. FEMS Microbiol Lett 2003; 221(2): 161 - 165. doi: 10.1016/S0378-1097(03)00170-8

Olaya-Abril A, Luque-Almagro VM, Pérez MD, López CM, Amil F, Cabello P, Sáez LP, Moreno-Vivian C, Roldán MD. Putative small RNAs controlling detoxification of industrial cyanide-containing wastewaters by *Pseudomonas pseudoalcaligenes* CECT5344. PloS One 2019; 14(2): e0212032. doi: 10.1371/journal.pone.0212032

Olaya-Abril A, Pérez MD, Cabello P, Martignetti D, Sáez LP, Luque-Almagro VM, Moreno-Vivian C, Roldán MD. Role of the dihydrodipicolinate synthase dapa1 on iron homeostasis during cyanide assimilation by the alkaliphilic bacterium *Pseudomonas pseudoalcaligenes* CECT5344. Front Microbiol 2020; 11: 28. doi: 10.3389/fmicb. 2020.00028

O'Reilly C, Turner PD. The nitrilase family of CN hydrolysing enzymes – a comparative study. J Appl Microbiol 2003; 95(6): 1161 - 1174. doi: 10.1046/j.1365-2672.2003. 02123.x

Osswald S, Wajant H, Effenberger F. Characterization and synthetic applications of recombinant AtNIT1 from *Arabidopsis thaliana*. Eur J Biochem 2002; 269(2): 680 - 687. doi: 10.1046/j.0014-2956.2001.02702.x

Oulego P, Laca A, Díaz M. Kinetics and pathways of cyanide degradation at high temperatures and pressures. Environ Sci Technol 2013; 47(3): 1542 – 1549. doi: 10.1021/es304000n

Oulego P, Collado S, Laca A, Díaz M. Simultaneous oxidation of cyanide and thiocyanate at high pressure and temperature. J Hazard Mater 2014; 280: 570 – 578. doi: 10.1016/j.jhazmat.2014.08.051

Pace HC, Brenner C. The nitrilase superfamily: classification, structure and function. Genome Biol 2001; 2(1): REVIEWS0001. doi: 10.1186/gb-2001-2-1-reviews0001

Pala A, Politi RR, Kursun G, Erol M, Bakal F, Öner G, Çelik E. Photocatalytic degradation of cyanide in wastewater using new generated nano-thin film photocatalyst. Surf Coat Technol 2015; 271: 207 – 216. doi: 10.1016/j.surfcoat.2014.12.032

Pan Y, Zhang Y, Huang Y, Jia Y, Chen L, Cui H. Synergistic effect of adsorptive photocatalytic oxidation and degradation mechanism of cyanides and Cu/Zn complexes over TiO_2/ZSM-5 in real wastewater. J Hazard Mater 2021; 416: 125802. doi: 10.1016/j.jhazmat.2021.125802

Papadimitriou CA, Samaras P, Sakellaropoulos GP. Comparative study of phenol and cyanide containing wastewater in CSTR and SBR activated sludge reactors. Bioresour Technol 2009; 100: 31 – 37. doi: 10.1016/j.biortech.2008.06.004

Park JM, Mulelu A, Sewell BT, Benedik MJ. Probing an interfacial surface in the cyanide dihydratase from *Bacillus pumilus*, a spiral forming nitrilase. Front Microbiol 2016; 6: 1479. doi: 10.3389/fmicb.2015.01479

Park JM, Sewell BT, Benedik MJ. Cyanide bioremediation: The potential of engineered nitrilases. Appl Microbiol Biotechnol 2017; 101(8): 3029 – 2042. doi: 10.1007/s00253-017-8204-x

Pattanayak DS, Mishra J, Nanda J, Sahoo PK, Kumar R, Sahoo NK. Photocatalytic degradation of cyanide using polyurethane foam immobilized Fe-TCPP-S-TiO_2-rGO

nano-composite. J Environ Manage 2021; 297: 113312. doi: 10.1016/j.jenvman. 2021.113312

Pérez-Cid B, Calvar S, Moldes AB, Cruz JM. Effective removal of cyanide and heavy metals from an industrial electroplating stream using calcium alginate hydrogels. Molecules 2020; 25(21): 5183. doi: 10.3390/molecules25215183

Petersen AR, Juhl M, Petrovic A, Lee J-W. CO_2-mediated non-destructive cyanide wastewater treatment. Eur J Org Chem 2021; 2021(35): 5003 – 5007. doi: 10.1002/ejoc. 202100997

Pillai IMS, Gupta AK. Potentiostatic electrodeposition of a novel cost effective PbO_2 electrode: Degradation study with emphasis on current efficiency and energy consumption. J Electroanal Chem 2015; 749: 16 – 25. doi: 10.1016/j.jelechem.2015. 04.020

Pillai IMS, Gupta AK. Anodic oxidation of coke oven wastewater: Multiparameter optimization for simultaneous removal of cyanide, COD and phenol. J Environ Manage 2016; 176: 45 – 53. doi: 10.1016/j.jenvman.2016.03.021

Piotrowski M, Schönfelder S, Weiler EW. The *Arabidopsis thaliana* isogene NIT4 and its orthologs in tobacco encode b-cyano-L-alanine hydratase/nitrilase. J Biol Chem 200; 276(4): 2616 – 2621. doi: 10.1074/jbc.M007890200

Piotrowski M, Volmer JJ. Cyanide metabolism in higher plants: cyanoalanine hydratase is a NIT4 homolog. Plant Mol Biol 2006; 61(1-2): 111 – 122. doi: 10.1007/s11103-005-6217-9

Piotrowski M. Primary or secondary? Versatile nitrilases in plant metabolism. Phytochemistry 2008; 69(15): 2655 - 2667. doi: 10.1016/j.phytochem.2008.08.020

Pratiwi NI, Mukimin A, Zen N, Septarina I. Integration of electrocoagulation, adsorption and wetland technology for jewelry industry wastewater treatment. Sep Purif Technol 2021; 279: 119690. doi: 10.1016/j.seppur.2021.119690

Rai A, Chakrabarty J, Dutta S. Phycoremediation of pollutants from coke-oven wastewater using *Tetraspora sp*. NITD 18 and estimation of macromolecules from spent biomass. J Water Process Eng 2021; 39: 101746. doi: 10.1016/j.jwpe.2020.101746

Ranjan B, Pillai S, Permaul K, Singh S. Simultaneous removal of heavy metals and cyanate in a wastewater sample using immobilized cyanate hydratase on magnetic-multiwall carbon nanotubes. J Hazard Mater 2019; 363: 73 – 80. doi: 10.1016/j.jhazmat.2018. 07.116

Rinágelová A, Kaplan O, Veselá AB, Chmátal M, Křenková A, Plíhal O, Pasquarelli F, Cantarella M, Martínková L. Cyanide hydratase from *Aspergillus niger* K10: overproduction in *Escherichia coli*, purification, characterization and use in continuous cyanide degradation. Process Biochem 2014; 49(3): 445 – 450. doi: 10.1016/j.procbio.2013.12.008

Rucká L, Chmátal M, Kulik N, Petrásková L, Pelantová H, Novotný P, Príhodová R, Pátek M, Martínková L. Genetic and functional diversity of nitrilases in Agaricomycotina. Int J Mol Sci 2019; 20(23): 5990. doi.org/10.3390/ijms20235990

Rucká L, Kulik N, Novotný P, Sedova A, Petrásková L, Příhodová R, Křístková B, Halada P, Pátek M, Martínková L. Plant nitrilase homologues in fungi: phylogenetic and functional analysis with focus on nitrilases in *Trametes versicolor* and *Agaricus bisporus.* Molecules 2020; 25(17): 3861. doi: 10.3390/molecules25173861

Rustler S, Motejadded H, Altenbuchner J, Stolz A. Simultaneous expression of an arylacetonitrilase from *Pseudomonas fluorescens* and a (S)-oxynitrilase from Manihot

esculenta in Pichia pastoris for the synthesis of (S)-mandelic acid. Appl Microbiol Biotechnol 2008; 80(1): 87 – 97. doi: 10.1007/s00253-008-1531-1

Sáez LP, Cabello P, Ibáñez MI, Luque-Almagro VM, Roldán MD, Moreno-Vivian C. Cyanate assimilation by the alkaliphilic cyanide-degrading bacterium *Pseudomonas pseudoalcaligenes* CECT5344: Mutational analysis of the *cyn* gene cluster. Int J Mol Sci 2019; 20(12): 3008. doi: 10.3390/ijms20123008

Safe Work Australia 2012; Controlling risks associated with electroplating. https://www.safeworkaustralia.gov.au/system/files/documents/1702/controlling_risks_associated_with_electroplating.pdf

Sedova A, Rucká A, Bojarová P, Glozlová M, Novotný P, Křístková B, Pátek M, Martínková L. Application potential of cyanide hydratase from *Exidia glandulosa*: FCN removal from simulated industrial effluents. Catalysts 2021; 11(11): 1410. doi: 10.3390/catal11111410

Sewell BT, Berman MN, Meyers PR, Jandhyala D, Benedik MJ. The cyanide degrading nitrilase from *Pseudomonas stutzeri* AK61 is a two-fold symmetric, 14-subunit spiral. Structure 2003; 11(11): 1413 – 1422. doi: 10.1016/j.str.2003.10.005

Sharma M, Akhter Y, Chatterjee S. A review on remediation of cyanide containing industrial wastes using biological systems with special reference to enzymatic degradation. World J Microbiol Biotechnol 2019; 35(5): 70. doi: 10.1007/s11274-019-2643-8

Shen J, Zhao H, Cao HB, Zhang Y, Chen YS. Removal of total cyanide in coking wastewater during a coagulation process: Significance of organic polymers. J Environ Sci I(China) 2014; 26(2): 231 – 239. doi: 10.1016/S1001-0742(13)60512-4

Shin D, Park J, Park H, Lee J-C, Kim M-S, Lee J. Key microbes and metabolic potentials contributing to cyanide biodegradation in stirred-tank bioreactors treating gold mining

effluent. Miner Process Extr Metall Rev 2020; 41(2): 85 – 95. doi: 10.1080/08827508.2019.1575213

Singh N, Agarwal B, Balomajumder C. Simultaneous treatment of phenol and cyanide containing aqueous solution by adsorption, biotreatment and simultaneous adsorption and biotreatment (SAB) process. Journal of Environmental Chemical Engineering 2016; 4(1): 564 – 575. doi: 10.1016/j.jece.2015.11.041

Skouloubris S, Labigne A, De Reuse H. The AmiE aliphatic amidase and AmiF formamidase of *Helicobacter pylori*: natural evolution of two enzyme paralogues, Mol Microbiol 2001; 40(3): 596-609. doi: 10.1046/j.1365-2958.2001.02400.x

Soriano-Maldonado P, Martínez-Gómez AI, Andújar-Sánchez M, Neira JL, Clemente-Jiménez JM, Heras-Vázquez FJL, Rodríguez-Vico F, Martínez-Rodríguez S. Biochemical and mutational studies of the *Bacillus cereus* CECT 5050T formamidase support the existence of a c-e-e-k tetrad in several members of the nitrilase superfamily, Appl Environ Microbiol 2011; 77(16): 5761-5769. doi: 10.1128/AEM.00312-11

Thuku RN, Brady D, Benedik MJ, Sewell BT. Microbial nitrilases: versatile, spiral forming, industrial enzymes. J Appl Microbiol 2009; 106(3): 703 – 727. doi: 10.1111/j.1365-2672.2008.03941.x

Turek M, Ketterer L, Classen M, Berndt HK, Elbers G, Krüger, Peter, Keusgen M, Schöning MJ. Development and electrochemical investigations of an EIS(electrolyte-insulator-semiconductor) based biosensor for cyanide detection. Sensors 2007; 7(8): 1415-1426. doi: 10.3390/s7081415

Tyagi M, Kumari N, Jagadevan S. A holistic Fenton oxidation-biodegradation system for treatment of phenol from coke oven wastewater: Optimization, toxicity analysis and

phylogenetic analysis. J Water Process Eng 2020; 37: 101475. doi: 10.1016/j.jwpe. 2020.101475

Valiūnienė A, Baltrūnas G, Keršulytė V, Margarian Z, Valincius G. The degradation of cyanide by anodic electrooxidation using different anode materials. Process Safety and Environmental Protection 2013; 91(4): 269 – 274. doi: 10.1016/j.psep.2012.06.007

Veselá AB, Rucká L, Kaplan O, Pelantová H, Nešvera J, Pátek M, Martínková L. Bringing nitrilase sequences from databases to life: The search for novel substrate specificities with a focus on dinitriles. Appl Microbiol Biotechnol 2016; 100(5): 2193 – 2202. doi:10.1007/s00253-015-7023-1

Vilo CA, Benedik MJ, Kunz DA, Dong QF. Draft genome sequence of the cyanide-utilizing bacterium Pseudomonas fluorescens strain NCIMB 11764. J Bacteriol 2012; 194(23): 6618 – 6619. doi: 10.1128/JB.01670-12

Viña Mediavilla JJ, Perez BF, de Cordoba MCF, Espina JA, Ania CO. Photochemical degradation of cyanides and thiocyanates from an industrial wastewater. Molecules 2019; 24(7): 1373. doi: 10.3390/molecules24071373

Vorwerk S, Biernacki S, Hillebrand H, Janzik I, Müller A, Weiler EW, Piotrowski M. Enzymatic characterization of the recombinant *Arabidopsis thaliana* nitrilase subfamily encoded by the NIT2/NIT1/NIT3-gene cluster. Planta 2001; 212(4): 508 – 516. doi: 10.1007/s004250000420

Wang L, Watermeyer JM, Mulelu AE, Sewell BT, Benedik M.J. Engineering pH-tolerant mutants of a cyanide dihydratase. Appl Microbiol Biotechnol 2012; 94: 131 - 140. doi: 10.1007/s00253-011-3620-9

Wang B. A novel dielectric-barrier-discharge loop reactor for cyanide water treatment. Plasma Chem and Plasma Process 2017; 37(4): 1121 – 1131. doi: 10.1007/s11090-017-9791-0

Watanabe A, Yano K, Ikebukuro K, Karube I. Cyanide hydrolysis in a cyanide-degrading bacterium, *Pseudomonas stutzeri* AK61, by cyanidase. Microbiology 1998; 144(Pt 6): 1677 – 1682. doi: 10.1099/00221287-144-6-1677

Water Framework Directive 2000; https://environment.ec.europa.eu/topics/water/water-framework-directive_en

Weber BW, Kimani SW, Varsani A, Cowan DA, Hunter R, Venter GA, Gumbart JC, Sewell BT. The mechanism of the amidases mutating the glutamate adjacent to the catalytic triad inactivates the enzyme due to substrate mispositioning. J Biol Chem 2013; 288(40): 28514 – 28523. doi: 10.1074/jbc.M113.503284

Xue YP, Wang YP, Xu Z, Liu ZQ, Shu XR, Jia DX, Zheng YG, Shen YC. Chemoenzymatic synthesis of gabapentin by combining nitrilase-mediated hydrolysis with hydrogenation over Raney-nickel. Catal Commun 2015; 66: 121 – 125. doi: 10.1016/j.catcom.2015.03.035

Yanase H, Sakamoto A, Okamoto K, Kita K, Sato Y. Degradation of the metal-cyano complex tetracyanonickelate (II) by *Fusarium oxysporum* N-10. Appl Microbiol Biotechnol 2000; 53(3): 328 – 334. doi: 10.1007/s002530050029

Yang WL, Liu GS, Chen YH, Miao DT, Wei QP, Li HC, Ma L, Zhou KC, Liu LB, Yu ZM Persulfate enhanced electrochemical oxidation of highly toxic cyanide-containing organic wastewater using boron-doped diamond anode. Chemosphere 2020; 252: 126499. doi: 10.1016/j.chemosphere. 2020.126499

Yu X-Z, Lu P-C, Yu Z. On the role of beta-cyanoalanine synthase (CAS) in metabolism of free cyanide and ferri-cyanide by rice seedlings. Ecotoxicology 2012; 21(2): 548 – 556. doi: 10.1007/s10646-011-0815

Yu X.B, Xu RH, Wei CH, Wu HZ. Removal of cyanide compounds from coking wastewater by ferrous sulfate: Improvement of biodegradability. J Hazard Mater 2016; 302: 468 – 474. doi: 10.1016/j.jhazmat.2015.10.013

Zákon č. 224/2015 Sb.: Zákon o prevenci závažných havárií způsobených vybranými nebezpečnými chemickými látkami nebo chemickými směsmi a o změně zákona č. 634/2004 Sb., o správních poplatcích, ve znění pozdějších předpisů. In: Sbírka zákonů. 2015. https://www.zakonyprolidi.cz/cs/2015-224

Zákon č. 254/2001 Sb.: Zákon o vodách a o změně některých zákonů (vodní zákon). In: Sbírka zákonů. 2001. https://www.zakonyprolidi.cz/cs/2001-254

Zhang ZC, Yue XP, Duan YQ, Zhang X, Gao YJ, Zhu R, Cui X. Sulfate radical oxidation combined with iron flocculation for upgrading biological effluent of coking wastewater. RSC Adv 2018; 8(68): 38765 – 38772. doi: 10.1039/C8RA08134D

Zheng Y, Li Z, Wang X, Gao X, Gao C. The treatment of cyanide from gold mine effluent by a novel five-compartment electrodialysis. Electrochim Acta 2015; 169: 150 – 158. doi: 10.1016/j.electacta.2015.04.015

Zou S, Hua D, Jiang Z, Han X, Xue Y, Zheng Y. A integrated process for nitrilase-catalyzed asymmetric hydrolysis and easy biocatalyst recycling by introducing biocompatible biphasic system. Bioresour Technol 2021; 320(Pt B): 124392. doi: 10.1016/j.biortech. 2020.124392

Appendix

Appendix A. HPLC analysis of nitriles used as substrates and the corresponding amides and carboxylic acids – calibration curves.

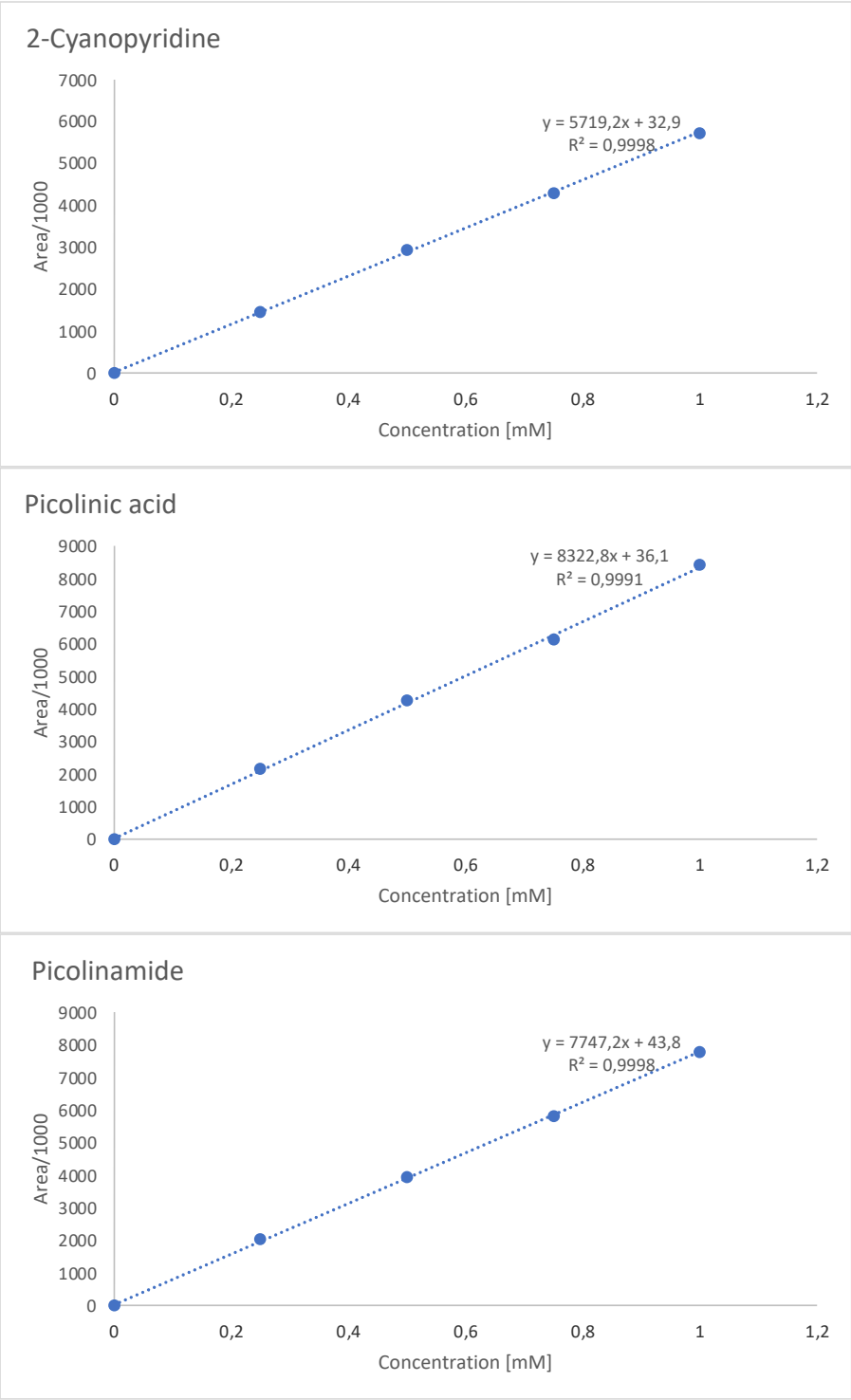

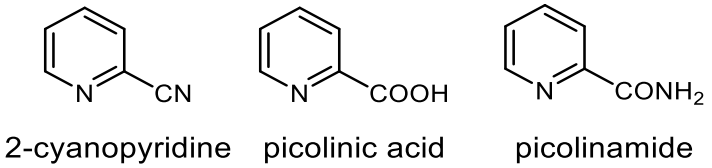

2-cyanopyridine picolinic acid picolinamide

Figure A1. 2-Cyanopyridine, picolinic acid and picolinamide were eluted at retention times of 10.0 min, 2.6 min and 7.3 min, respectively; peak area was determined at 264.0 nm for all three compounds. See section 3.4.1. for the separation conditions.

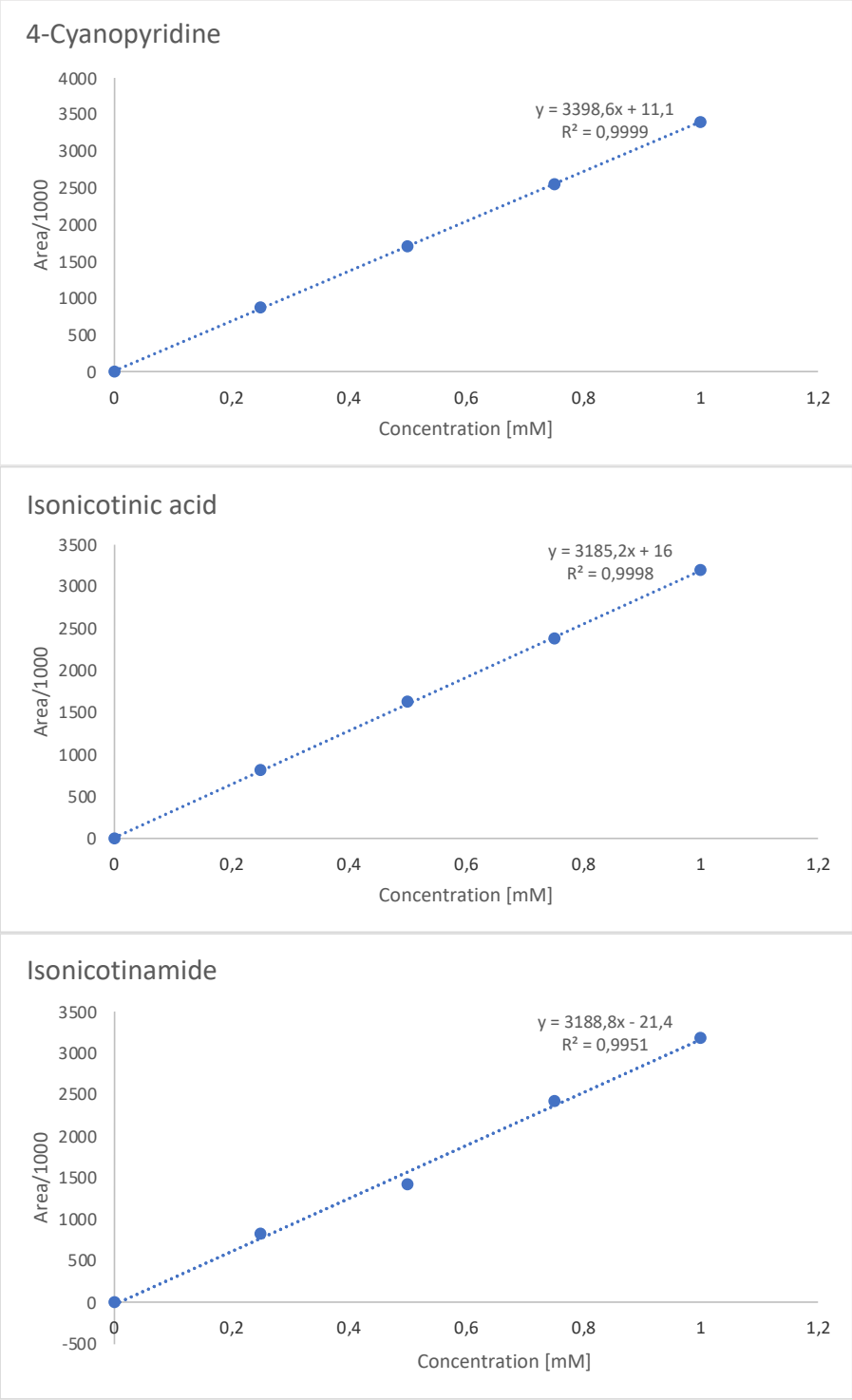

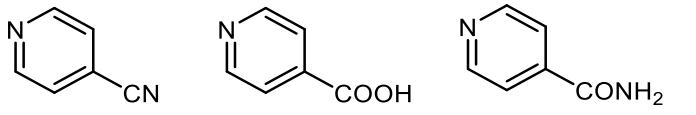

4-cyanopyridine isonicotinic acid isonicotinamide

Figure A2. 4-Cyanopyridine, isonicotinic acid and isonicotinamide were eluted at retention times of 10.3 min, 2.7 min and 4.3 min, respectively; peak area was determined at 274.7 nm, 265.2 nm, and 267.6 nm respectively. See section 3.4.1. for the separation conditions.

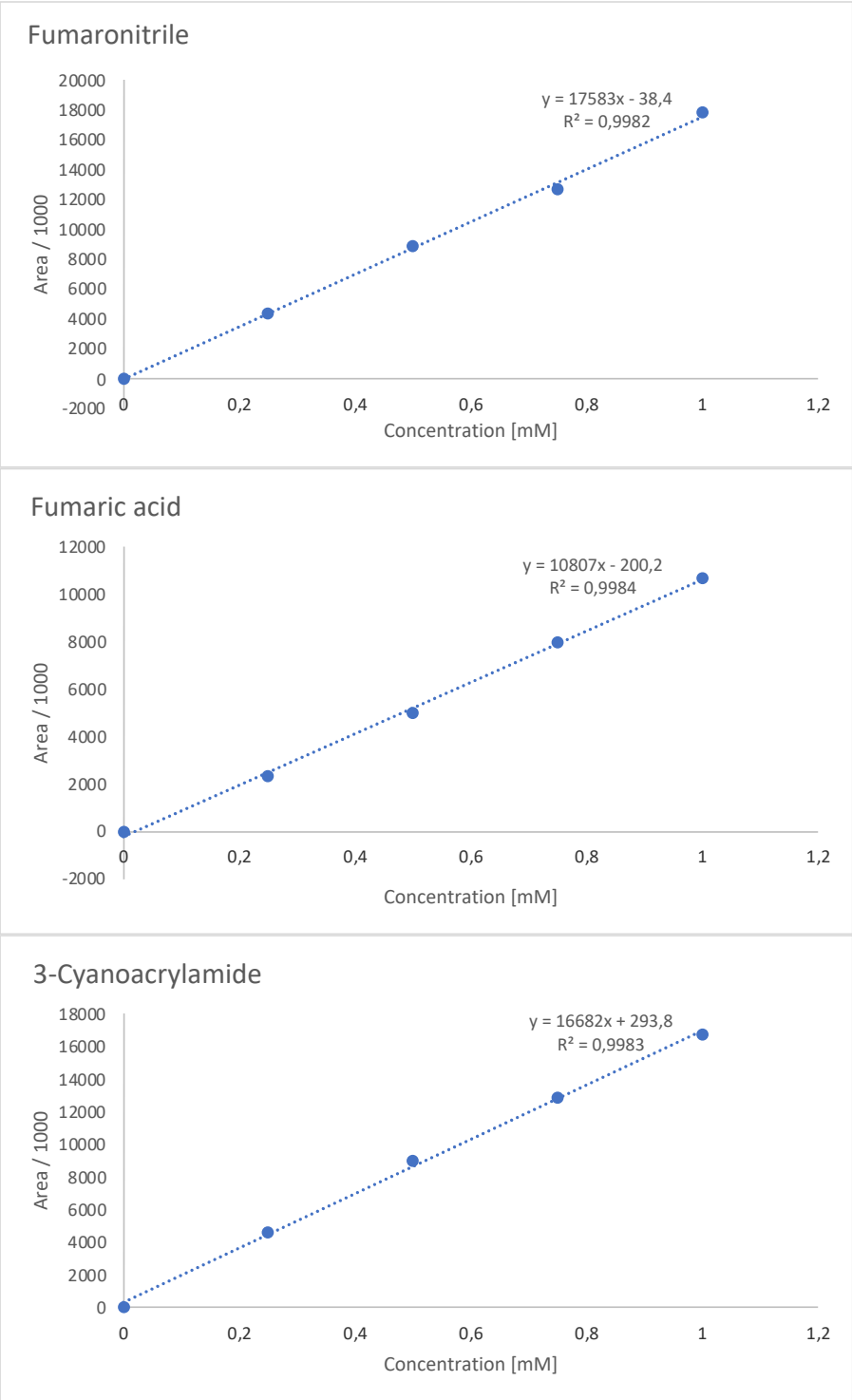

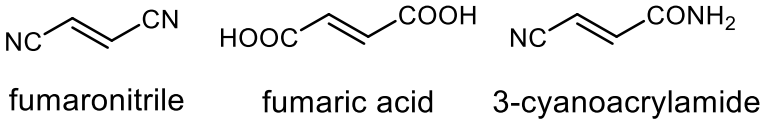

fumaronitrile fumaric acid 3-cyanoacrylamide

Figure A3. Fumaronitrile, fumaric acid and the corresponding cyanoamide (3-cyanoacrylamide) were eluted at retention times of 10.3 min, 2.7 min and 4.3 min, respectively; peak area was determined at 218.1 nm, 210 nm, and 214.6 nm, respectively. See section 3.4.1. for the separation conditions.

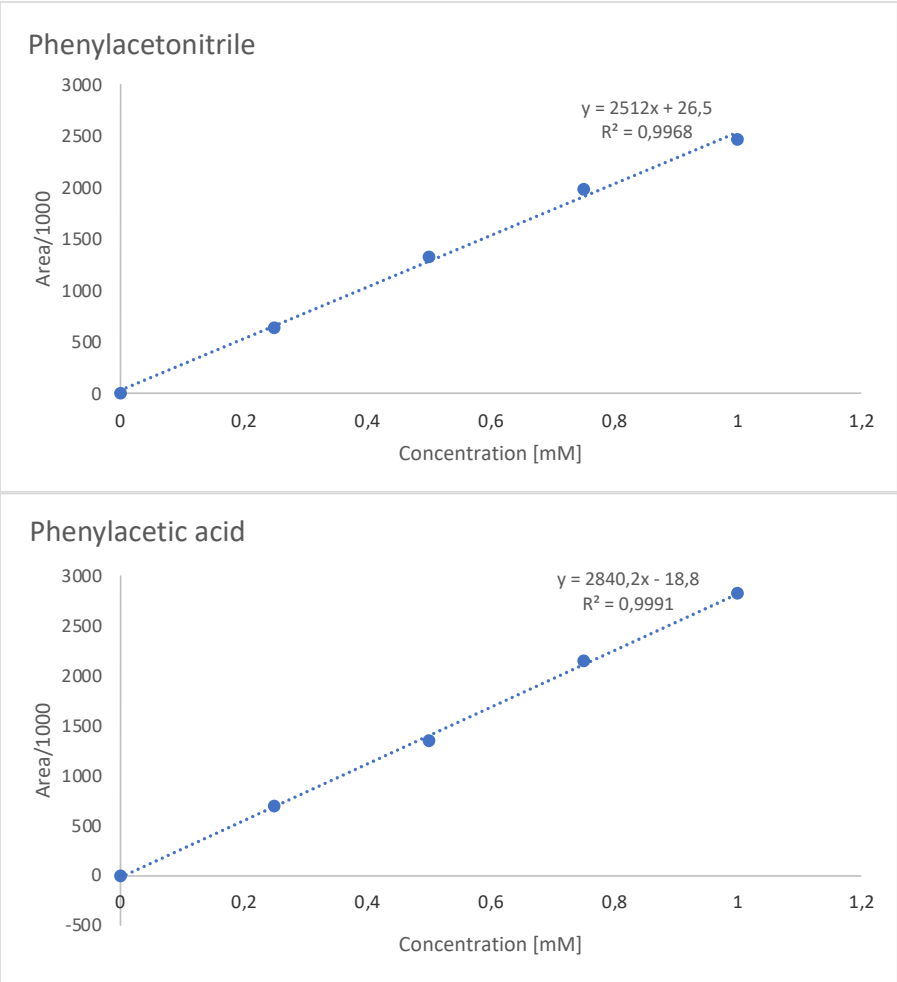

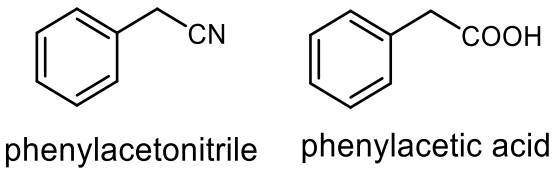

phenylacetonitrile phenylacetic acid

Figure A4. Phenylacetonitrile and phenylacetic acid were eluted at retention times of 2.9 min and 1.6 min, respectively. Peak area was determined at 210 nm (Phenylacetamide was not commercially available). See section 3.4.1. for the separation conditions.

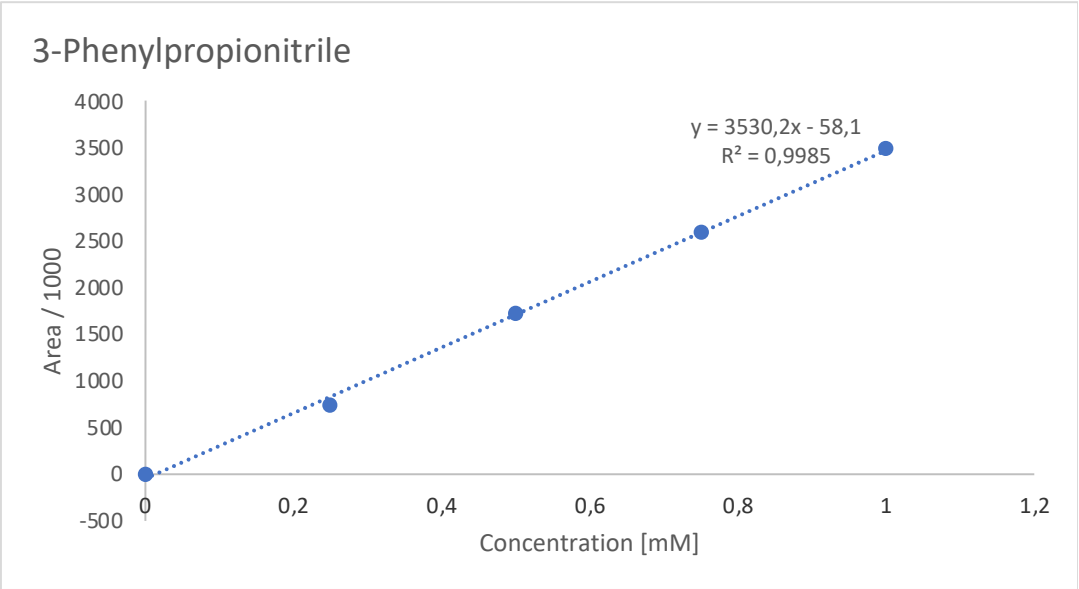

Figure A5. 3-Phenylpropionitrile was eluted at retention times of 2.9 min and 4.2 min, respectively. Peak area was determined at 210 nm (3-Phenylpropionamide was not commercially available). See section 3.4.1. for the separation conditions.

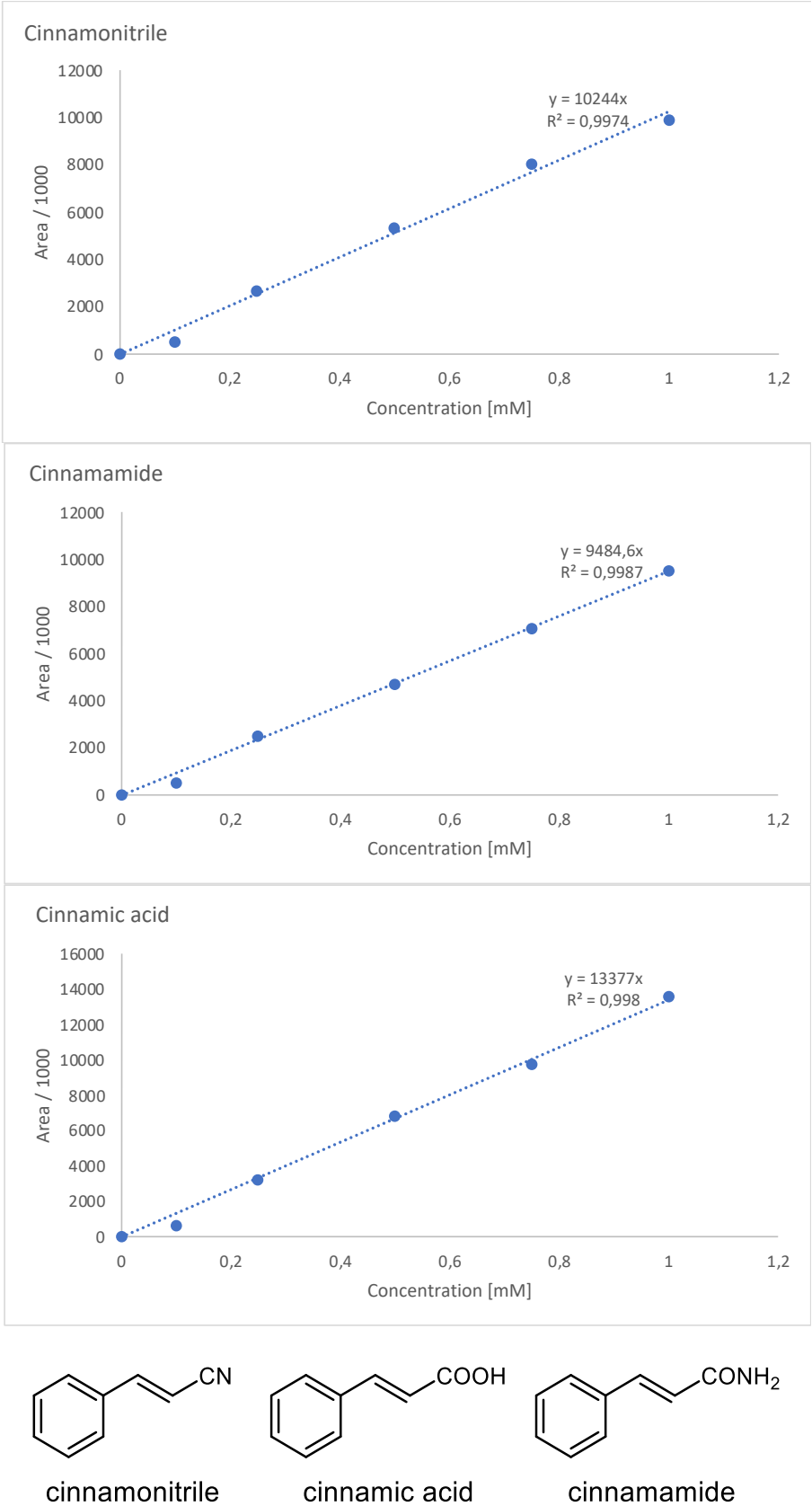

Figure A6. Cinnamonitrile, cinnamic acid and cinnamamide were eluted at retention times of 7.0 min, 3.6 min, and 1.5 min, respectively. Peak area was determined at 273.5 nm, 277 nm and 274.7 nm, respectively. See section 3.4.1. for the separation conditions.

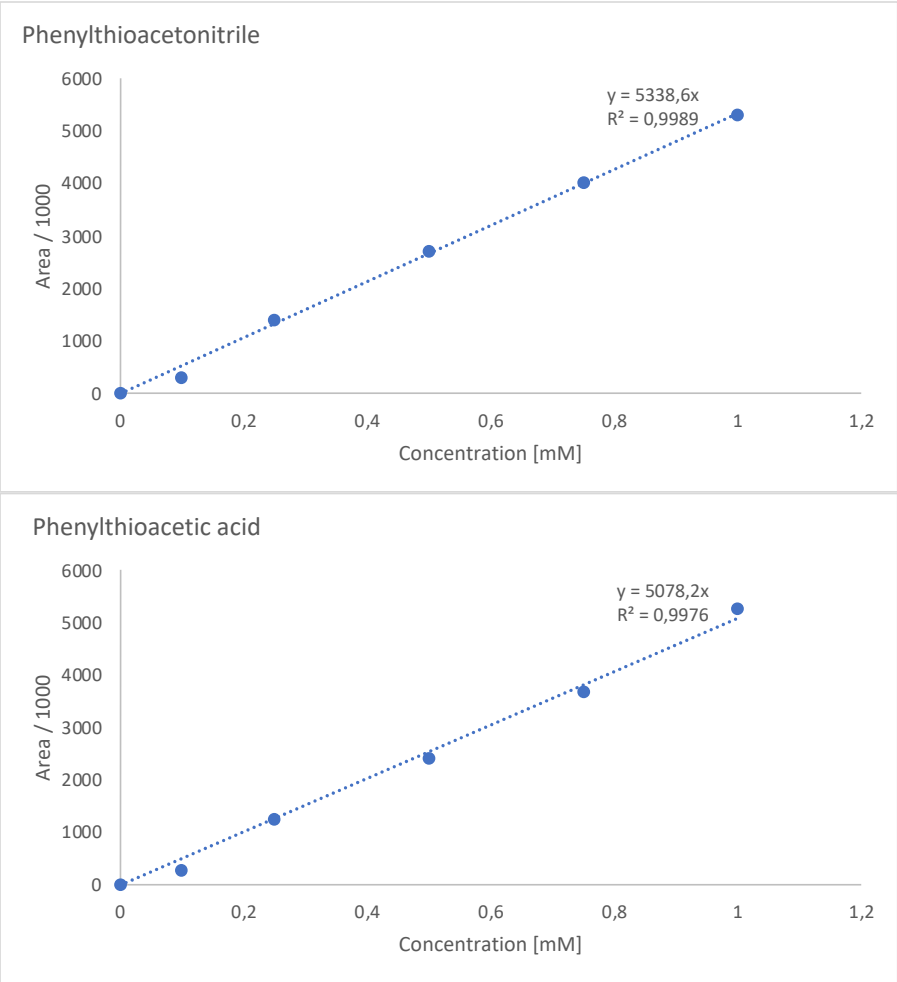

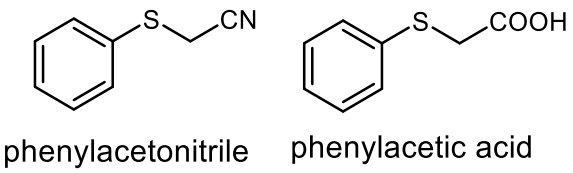

phenylacetonitrile phenylacetic acid

Figure A7. Phenylthioacetonitrile and phenylthioacetic acid were eluted at retention times of 5.7 min and 2.8 min, respectively. Peak area was determined at 210 nm (Phenylthioacetamide was not commercially available). See section 3.4.1. for the separation conditions.

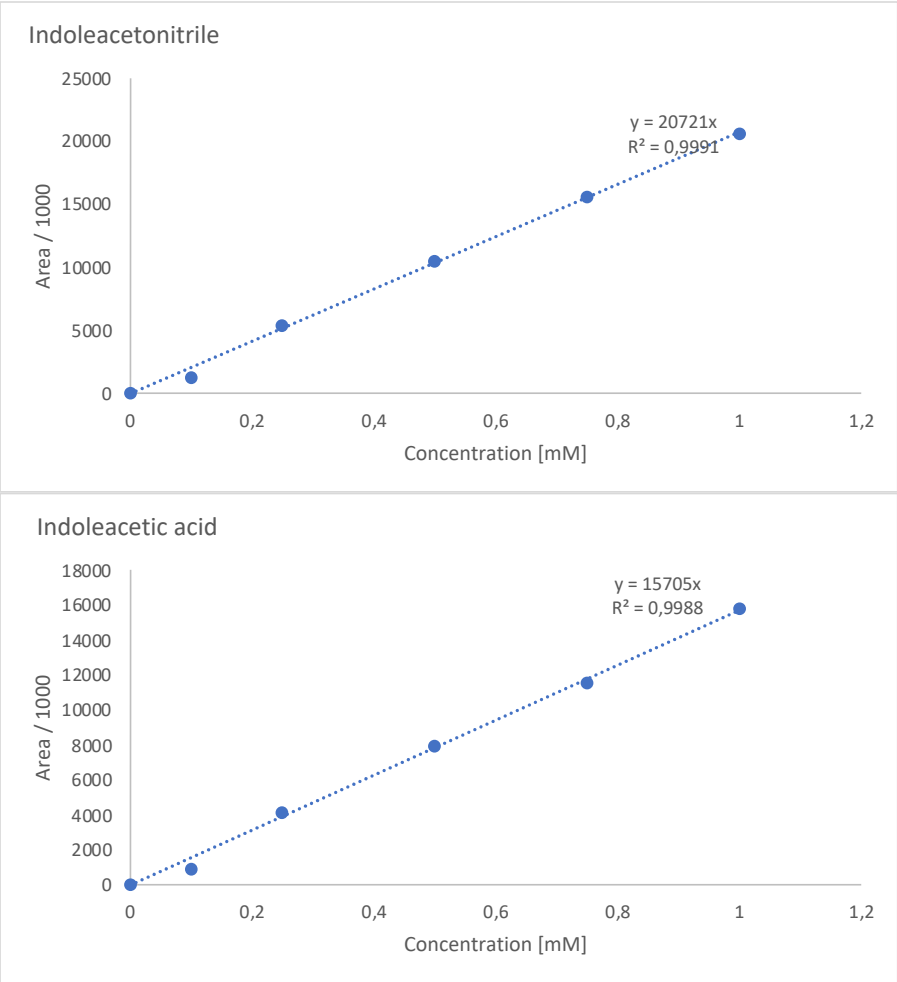

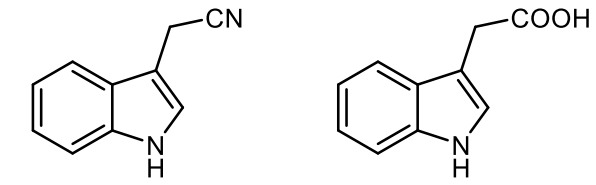

3-indoleacetonitrile 3-indoleacetic acid

Figure A8. 3-Indoleacetonitrile and 3-indoleacetic acid were eluted at retention times of 3.8 min and 1.8 min, respectively. Peak area was determined at 277.0 and 278.2 nm, respectively. (3-Indoleacetamide was not available commercially.) See section 3.4.1. for the separation conditions.

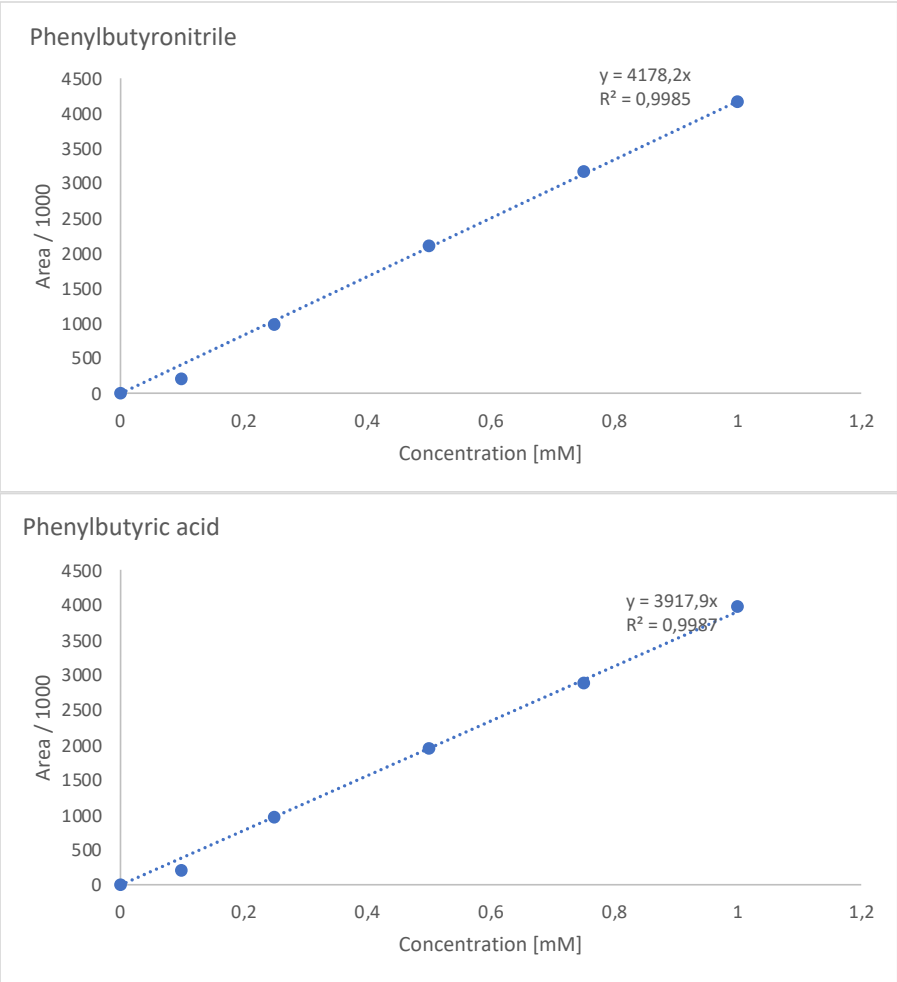

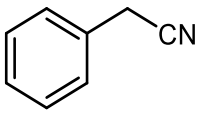

4-phenylbutyronitrile

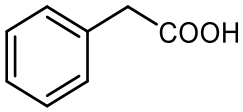

4-phenylbutyric acid

Figure A9. 4-Phenylbutyronitrile and 4-phenylbutyric acid were eluted at retention times of 9.9 min and 6.2 min, respectively. Peak area was determined at 210 nm. (4-Phenylbutyramide was not available commercially). See section 3.4.1. for the separation conditions.

Appendix B. Calibration for spectrophotometric method

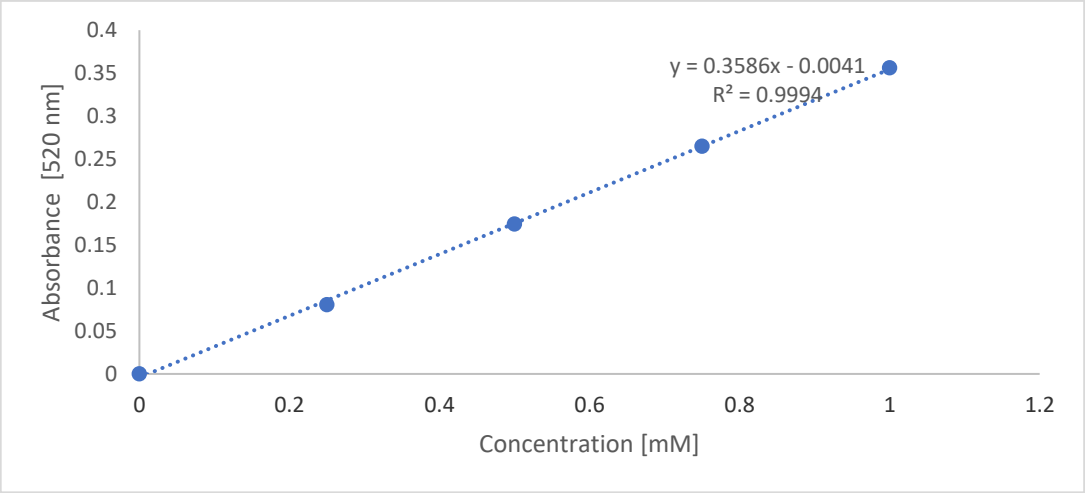

Figure B1. Calibration for free cyanide determined by the picric acid method. See section 3.4.3. for method details.

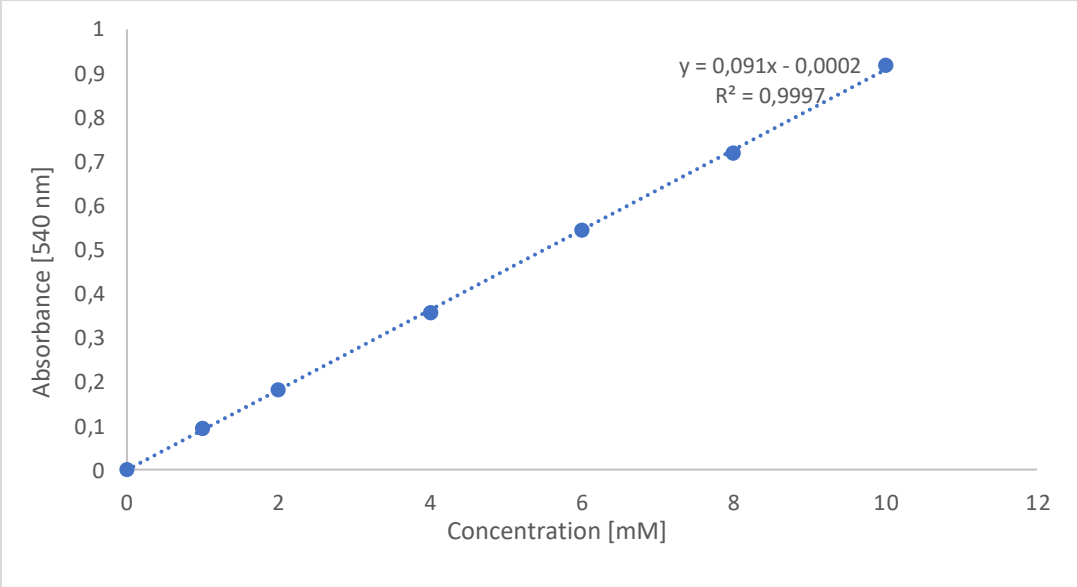

Figure B2. Calibration for formamide determined by the hydroxylamine method. See section 3.4.3. for method details.

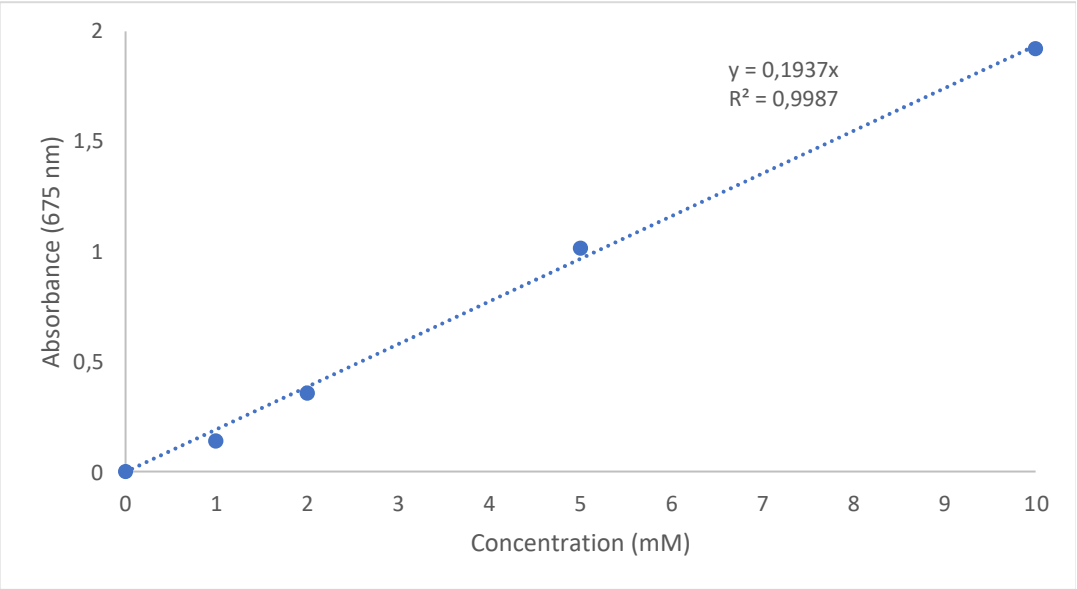

Figure B3. Calibration for ammonia determined by *o*-phthaldehyde (OPA) method. See section 3.4.3. for method details.